

The Application of Digital Filters to Improve Visibility for
People with Maculopathy

by

Ming Mei

A thesis

presented to the University of Waterloo

in fulfillment of the

thesis requirement for the degree of

Doctor of Philosophy

in

Vision Science

Waterloo, Ontario, Canada, 2007

©Ming Mei, 2007

AUTHOR'S DECLARATION

I hereby declare that I am the sole author of this thesis. This is a true copy of the thesis, including any required final revisions, as accepted by my examiners.

I understand that my thesis may be made electronically available to the public.

Abstract

Purpose: Previous studies have shown that some digital filters can enhance picture-image visibility for people with visual impairment. The ultimate purposes of this study are to determine the improvement of picture-image visibility for people with maculopathy using digital image enhancement, and to compare the enhancement effects of generic filters and custom-devised filters. The secondary interests are to investigate the effect of age and maculopathy on supra-threshold contrast matching and to investigate the spatial frequency characteristics of picture-images.

Methods: In order to develop effective custom-devised filters, supra-threshold contrast matching and contrast thresholds for two age groups of subjects with normal vision (14 aged 20-50 years and 15 aged 51+ years) and three groups of people with maculopathy (13 with atrophic ARMD, 14 with exudative ARMD, and 8 with JMD) were measured. Amplitude spectrum at each spatial frequency and the slope of amplitude versus spatial frequency were measured to investigate the spatial frequency characteristics of single face and general scene images. To investigate the preference for filters, 7 generic filters and 4 custom-devised filters were applied to single faces and general scenes. The generic filters were high-pass/unsharp masking, contrast enhancement, Sobel edge enhancement, DoG convolution, DoG FFT, Peli's adaptive enhancement, and a band-pass filter with equi-emphasis of spatial frequencies. The custom-devised filters were band-pass filters based on contrast sensitivity (CS) loss, contrast matching at 3.6% and 27.9%, and emphasis of the peak of the CS curve. Subjects with maculopathy were required to rate the visibility of each image with and

without filtering. Nine subjects with maculopathy participated to assess the enhancement quantitatively during which the recognition of facial expression and details in general scenes was tested with and without filtering.

Results: Contrast constancy was demonstrated in age-matched controls and people with maculopathy. Single faces were found to be of significantly lower average amplitude than the other groups of images. Eight filters were found to be effective in improving perceived visibility; contrast enhancement, Peli's adaptive enhancement, DoG convolution, high-pass/unsharp masking, Sobel edge enhancement, band-pass based on 3.6% and 27.9% contrast matching and equi-emphasis band-pass filters. These filters specifically were found to be effective for one or more combinations of maculopathy type and image category. The most commonly preferred filters were the generic filters, contrast enhancement and Peli's adaptive enhancement. The two highest rated filters for each subject significantly reduced the number of errors of facial expression and errors of recognition of detail within general scene images.

Conclusions: The visual system adjusts to compensate for CS loss with aging and maculopathy. Single faces are unique in spatial frequency characteristics. Some generic and custom-devised filters are effective in enhancing image visibility. The custom-devised filters are not superior to the generic filters. Visibility enhancement can be assessed quantitatively.

Acknowledgements

I give sincere thanks to my supervisor, Dr. Susan J. Leat, for her great guidance and support for my whole study procedure. I am impressed by her profound academic knowledge, brilliant scientific ideas, and hard-working attitude. She contributed richly to my study from course selection at the beginning, to the paper publications and thesis writing in the end. To me, she is not only an excellent supervisor in working but also a good friend in life.

I would like to highlight the help of Dr. Jeffery Hovis and Dr. Trefford Simpson. They are two of my committee. They both contributed their wisdom and time into my project in various areas such as developing methodology, solving difficulties, and meeting me regularly.

I am grateful to Dr. Jernigan and his two former students, Gorden Deng and Fu Jin. They developed the software programme for this project.

I would like to thank Erin Harvey for her assistance with the statistical analysis.

I remember each subject involved in this study. They showed me kindness, patience, and generosity. The data collected from them are precious.

I remember my first vehicle. It worked so hard on driving the subjects without any complaint. It almost contributed its whole life to this project.

I would like to thank the computer technicians (Jim Davidson, Chris Mathers, Andy Lankin) and graduate study officers (Kristin Snell, Krista Parsons) for their assistance.

Thanks to the staff of the Low Vision Clinic, the Ocular Health Clinic and the Primary Health Care Clinic at the school of Optometry and for case files and subject recruitment resources.

Thanks to Norm Benest from CNIB for helping with recruiting subjects.

I would like to thank my former and the current labmates: Jane Qiu, Naveen Yadav, and Krithika Nandakumar, and Fahad Almoqbel for their companionship.

I would like to thank the other graduate students for their kind friendship.

Special thanks to my church siblings for their great support both physically and spiritually.

Dedication

This thesis is dedicated to my heavenly Father and my parents, who have guided and protected me since I existed!

Table of Contents

Author’s Declaration	ii
Abstract.....	iii
Acknowledgements	v
Dedication	vii
Table of Contents	viii
List of Figures.....	xiv
List of Tables	xvii
CHAPTER 1 GENERAL INTRODUCTION	1
1.1 Visual impairment and maculopathy.....	1
1.2 Visual function loss due to maculopathy	3
1.2.1 Visual acuity loss	3
1.2.2 Visual field loss	4
1.2.3 Contrast sensitivity (CS) loss	4
1.2.2 Other visual function loss	4
1.3 Low Vision Rehabilitation (LVR).....	5
1.3.1 Light Modulation	5
1.3.2 Substitution Aids	6
1.3.3 Optical Aids.....	6
1.3.4 Electronic Vision Enhancement Systems (EVES)	7
1.4 Digital Image Enhancement.....	10
1.4.1 Digital Image	10

1.4.2 Digital Image Enhancement Techniques	11
1.4.3 Image processing in low vision	14
CHAPTER 2 PROPOSED STUDY.....	18
2.1 Hypothesis.....	18
2.1 Aims and Purposes.....	18
2.2.1 To obtain age-related supra-threshold contrast matching and investigate the aging effect	19
2.2.2 To investigate the supra-threshold contrast matching in maculopathy Digital	19
2.2.3 To analyze and classify images with spatial frequency	19
2.2.4 To test the perceived visibility improvement with image enhancement	20
2.2.5 To assess the visibility improvement objectively	20
CHAPTER 3 SUPRA-THRESHOLD CONTRAST MATCHING AND THE EFFECTS OF CONTRAST THRESHOLD AND AGE	23
3.1 Introduction	24
3.2 Method and Materials.....	27
3.2.1 Apparatus	27
3.2.2 Stimuli	28
3.2.3 Subjects	29
3.2.3 Procedure	30
3.3 Results	32
3.3.1 Repeatability	32
3.3.2 Contrast Threshold	32

3.3.3 Supra-threshold Contrast Matching	34
3.4 Discussion	41
3.4.1 Contrast Threshold	41
3.4.2 Supra-threshold Contrast Matching	42
3.4.3 Aging and Contrast Matching	49
3.5 Conclusions	50
3.4 Acknowledgement.....	51
CHAPTER 4 SUPRA-THRESHOLD CONTRAST MATCHING IN MACULOPATHY	
.....	54
4.1 Introduction	56
4.2 Methods and Materials	58
4.2.1 Apparatus	58
4.2.2 Stimuli	58
4.2.3 Subjects	59
4.2.4 Procedure	60
4.3 Results	61
4.4 Discussion	69
4.4.1 Contrast Threshold	69
4.4.2 Supra-threshold Contrast Matching.....	70
4.5 Conclusions	73
4.4 Acknowledgement.....	73

CHAPTER 5 CAN SPATIAL FREQUENCY ANALYSIS DISTINGUISH IMAGE

CATEGORIES?	74
5.1 Introduction	74
5.2 Methods	78
5.2.1 Images	78
5.2.2 Software	79
5.2.3 Analysis	79
5.3 Results	82
5.2 Discussion	88
5.2 Coclusions	92

CHAPTER 6 THE PERCEIVED VISIBILITY ENHANCEMENT IN

MACULOPATHY BY IMAGE ENHANCEMENT TECHNIQUE	93
6.1 Introduction	93
6.2 Methods and Materials	95
6.2.1 Subjects	95
6.2.2 Images	97
6.2.3 Apparatus and Filters	98
6.2.4 Procedure	110
6.2.5 Statistical Analysis	114
6.3 Results	115
6.3.1 Within-Filter Rankings - First Phase	115
6.3.2 Within-Filter Rankings - Second Phase	123

6.3.3 Between-Filter Ratings	127
6.4 Discussion	135
6.4.1 Comparison with former studies.....	136
6.4.2 What can be drawn from the current study?	140
6.5 Conclusions	153
CHAPTER 7 QUANTITATIVE ASSESSMENT OF PERCEIVED VISIBILITY	
ENHANCEMENT WITH IMAGE PROCESSING	154
7.1 Introduction	154
7.2 Methods and Materials	157
7.2.1 Images	157
7.2.2 Preliminary study	158
7.2.3 Subjects	164
7.2.4 Digital Filters.....	165
7.2.5 Procedure	165
7.3 Results	168
7.3.1 Repeatability.....	168
7.3.2 The effects of filters with test images	169
7.3.3 The comparison between two best rated filters	171
7.4 Discussion	173
7.5 Conclusions	178
CHAPTER 8 GENERAL DISCUSSION.....	179
8.1 Supra-threshold contrast matching in control groups	180

8.2 Supra-threshold contrast matching in maculopathy	181
8.3 Image analysis and grouping.....	188
8.4 Measurement of perceived visibility improvement.....	189
8.5 Measurement of quantitative visibility improvement	193
8.6 Implementation in the future	195
8.7 Future work	196
CHAPTER 9 GENERAL CONCLUSIONS.....	199
Appendix A Contrast Calibration for Sony Trinitron Monitor and Morphonome Software, used for the Contrast Threshold and Contrast Matching Studies.....	201
Appendix B Spatial Frequency Calibration for Trinitron Monitor and Morphonome Software, used for the Contrast Threshold and Contrast Matching Experiment	202
Appendix C Examples of Filters.....	203
Appendix D Codes of the Generic Filters	208
Bibliography	217

List of Figures

Figure 1-1. Examples of CCTV	8
Figure 1-2. Jordy and NuVision low vision device	9
Figure 3-1. Mean supra-threshold contrast matching results for two age groups.....	33
Figure 3-2. Mean threshold and supra-threshold contrast matching plotted against standard contrast for each spatial frequency	37
Figure 3-3. Mean threshold and normalized supra-threshold contrast matching plotted against standard contrast for each spatial frequency.....	40
Figure 3- 4. Mean supra-threshold contrast matching plotted against standard contrast for three spatial frequencies for four younger subjects	44
Figure 3-5. Contrast matching replotted from Figure 2A of Näsänen (1998).....	48
Figure 4-1. Contrast thresholds for the three diagnostic groups compared with the 95% normal range (1.96 x SD, dashed lines).....	64
Figure 4-2. Contrast threshold and supra-threshold contrast matching curves for three subjects with atrophic ARMD, exudative ARMD, and JMD respectively.....	65
Figure 4-3. Contrast matching at 3.6% and 27.9% for three groups.	66
Figure 4-4. Examples of matched contrast against test contrast in log unit	68
Figure 5-1. An example of image analysis	81
Figure 5-2. Examples of amplitude spectra plots for four images showing the four orientations of 0°, 45°, 90°, and 135°.....	82
Figure 5-3. Plot of average amplitude versus slope for all images.....	85

Figure 6-1. Two half-sized images and one full-sized image showing their relative sizes	98
Figure 6-2. The interface of the Image Processing Tool	99
Figure 6-3. Example of frequency domain plots of the band-pass filter based on CM of 27.9%	104
Figure 6-4. Examples of frequency domain plots of the band-pass filter based on CS loss.	106
Figure 6-5. Examples of frequency domain plots of the band-pass filter based on peak- emphasis of spatial frequencies	108
Figure 6-6. Examples of frequency domain plots of the band-pass filter based on equi- emphasis of spatial frequencies	109
Figure 6-7. Four versions of the half-sized general scenery image processed with different scales of the 3x3 Sobel horizontal and vertical edge enhancement filter	111
Figure 6-8. The average perceived visibility ratings of the control and two un-enhancing filters	130
Figure 6-9. Average ratings for generic filters for two groups of images (general scenes and faces)	131
Figure 6-10. Evaluations of the custom-devised filters	132
Figure 6-11. Demonstrations of Peli's adaptive enhancement	142
Figure 6-12. Face images enhanced with the contrast enhancement filter in two scales (20 and 80) and two modes (HSB and RGB)	145
Figure 6-13. Demonstration of the band-pass filter based on equi-emphasis of spatial frequencies with Gabor and polynomial for the face and the general scene	148

Figure 6-14. Demonstration of the band-pass filter based on equi-emphasis of spatial frequencies of mode of 1-octave and 2-octave with the face and general scene	149
Figure 6-15. Demonstration of the filtering effects of the band-pass filter based on CM at 27.9% with a gain of 2 and band-pass filter based on CS loss with gain of 0.5	151
Figure 7-1. Face expression image display.....	161
Figure 7-2. Examples of the four facial expressions finally chosen from JACFEE.....	161
Figure 7-3. One example of a general scene image for performance measurement.....	164
Figure 8-1. Replotting of Figure 3a from Georgeson (1991).....	186
Figure 8-2. The overlap effects of DoG convolution and DoG FFT.	191
Figure D-1. The scroll bar for the high-pass/unsharp masking and Sobel edge enhancement	209
Figure D-2. Peli's adaptive enhancement filter processing parameters.....	213
Figure D-3. The scroll bar for the contrast enhancement	214
Figure D-4. Examples of DoG FFT filter parameters and filter profile.....	214
Figure D-5. Low pass filter with $f = 100cpi$ (image size is 600x800)	215
Figure D-6. Cutoff frequency of low-pass filter	216

List of Tables

Table 3-1. Settings of the standard and test grating.....	29
Table 3-2. Repeatability of supra-threshold contrast matching	32
Table 3-3. Regression line slopes and the 95% confidence limits of 6 spatial frequencies for data plotted in Figure 3-2 (non-normalized data)	38
Table 3-4. Regression slopes and the 95% confidence limits of 6 spatial frequencies with the normalized values	41
Table 4-1. Means and 95% range for slopes of contrast matching regression lines for subjects with maculopathy and control subjects.....	69
Table 5-1. Average amplitude and slope \pm one standard deviation for the six groups of images in the three orientations and the average of three orientations	86
Table 5-2. Post-hoc Bonferroni analysis of ANOVA for amplitude and slope for separate orientations and averaged across orientations.....	87
Table 6-1. The subjects' diagnosis, ages, and visual acuities	96
Table 6-2. Filter parameters	101
Table 6-3-1. An example of the band-pass filter based on the contrast matching at 27.9%. 103	
Table 6-3-2. An example of the band-pass filter based on the contrast sensitivity loss	105
Table 6-3-3. An example of the band-pass filter based on peak-emphasis of the spatial frequencies	107
Table 6-3-4. An example of the band-pass filter based on equi-emphasis of the spatial frequencies	109
Table 6-4. Latin Square.....	114

Table 6-5-A. First phase rankings of the high-pass/unsharp masking filter	115
Table 6-5-B. First phase rankings of the 3x3 Sobel horizontal and vertical edge enhancement filter.....	116
Table 6-5-C. First phase rankings of the contrast enhancement filter	117
Table 6-5-D. First phase rankings of the DoG Convolution filter.....	117
Table 6-5-E. First phase rankings of the DoG FFT filter	118
Table 6-5-F. First phase rankings of the Peli's Adaptive Enhancement Filter.....	119
Table 6-5-G. First phase rankings of the band-pass filter based on contrast matching at 3.6%	121
Table 6- 5-H. First phase rankings of the band-pass filter based on the contrast matching at 27.9%.....	121
Table 6-5-I. First phase rankings of the band-pass filter based on CS loss.....	122
Table 6-5-J. First phase rankings of the band-pass filter based on peak emphasis of spatial frequency.....	122
Table 6-5-K. First phase rankings of the band-pass filter based on equi-emphasis of spatial frequencies.....	123
Table 6-6. Second phase of within-filter rankings between kernels/modes for each generic filter.....	125
Table 6-7-A. Second phase of within-filter rankings for the custom-devised filter with the function of Gabor and polynomial.....	127
Table 6-7-B. Second phase of within-filter rankings for the custom-devised filter according to 1-octave and 2-octave band-width.....	127

Table 6-8. Bonferroni adjustment for all the significant p values	134
Table 6-9. The filters that gave significant improvement in perceived visibility	136
Table 7-1. Number of mistakes of facial expression recognition with face expression image display duration of 0.73 second	162
Table 7-2. Results of the performance measure of visibility enhancement.....	170
Table 7-3. Qualitative ratings of the 1 st and 2 nd filters for the 9 subjects for the single faces and the general scenes.....	172
Table 7-4. The comparison of quantitative assessment of performance between the 1 st filter and 2 nd filter	173

Chapter 1

General Introduction

1.1 Visual Impairment and Maculopathy

Visual impairment is defined by the World Health Organization (WHO) as a measurable loss of visual function compared to the normal range of healthy eyes, a psychophysical measurement which is outside the normal range (World Health Organization, 1980). There are two levels of visual impairment – low vision and legal blindness. Low vision is defined by WHO as “inability to reach near normal performance with visual aids”. Leat et al. (1999) reconsidered various definitions and suggested that low vision be defined as visual impairment which is sufficient to cause a disability, which would be visual acuity $< 6/12$, contrast sensitivity < 1.05 (Pelli-Robson), and visual field of 120° with the III – 3e target (60° with Humphry). Legal blindness was defined by WHO as “the inability to perform tasks which normally require gross vision without increased reliance on other senses” (World Health Organization, 1980). The definition of legal blindness in the US and Canada is best corrected visual acuity $\leq 6/60$ or a visual field $\leq 20^\circ$ in any meridian (Kirchner, 1988).

With the increased aging of the population in industrialized nations, age-related vision problems need more and more attention. Prevent Blindness America reported that about 2.5 million Americans over the age of 40 have moderate visual impairment and an additional 1 million have severe impairment, including blindness (about 300, 000). These

numbers are expected to continually grow in the next two decades (Prevent Blindness America, 1994). Age-related macular degeneration (ARMD) is the primary cause of blindness in industrialized countries (Attebo et al., 1996; Bressler et al., 1988; Haymes et al., 2001; Klaver et al., 1998). Its prevalence increases with age. For example, the Blue Mountain Eye Study found that exudative ARMD or geographic ARMD affected 0.2% of people from 55 to 64 years of age, while it went up to 5.7% of the population aged 75 to 84 years (Mitchell et al., 1995). With the rapid increase of the elderly population (Olshansky et al., 1993), there will be more people experiencing ARMD.

ARMD is a degenerative and progressive condition involving the retinal pigment epithelium (RPE), Bruch's membrane, and choriocapillaris (Green & Enger, 1993; Green, 1999; Schneider et al., 1998; Zarbin., 1998). Clinical symptoms include degraded or distorted central vision and central visual field loss. The early stage is accompanied by hypo- or hyper-pigment and formation of drusen (Bressler et al., 1994; Sarks, 1994), and is called age-related maculopathy (ARM) (Bird et al., 1995). The later stage involves geographic atrophy or neovascular complications (Green & Enger, 1993), which are called "atrophic" and "exudative" ARMD respectively. Much more rarely, younger people, including infants and young children, develop macular dystrophies, and they do so in clusters within families, their disorders being more directly inherited. These types of macular degeneration that affect young people are collectively called juvenile macular degeneration or dystrophy (JMD) and include diseases such as Stargardt's disease, Best's disease, cone dystrophy.

Numerical and functional reduction in photoreceptors in all stages of ARMD has been shown with a variety of techniques (Curcio, 1990, 1996, 2000; Li et al., 2001). Some studies

show that the other layers of retina are also damaged by maculopathy. An early study by Enoch (1978) used special psychophysical methods to isolate the function of the outer retinal layer (bipolars and outer plexiform layers) from the inner retina (ganglion cells and inner plexiform layers). The results showed that around 1/3 of ARM cases demonstrated outer retina involvement and 2/3 demonstrated both inner and outer retina involvement. Dunaief et al. (2002) studied apoptosis in ARMD and reported that RPE, photoreceptors, and inner nuclear layer cells died by apoptosis (cell death). Kim et al. (2002) evaluated the extent of neural cell death in eyes with geographic atrophy and exudative ARMD. They found the outer nuclear layers were most severely affected while the inner nuclear layers were relatively preserved for both types of ARMD. However ganglion cell reduction was found to be significant in geographic atrophy but not in exudative ARMD.

A “preferred retinal locus” (PRL) is formed in maculopathy to compensate for the central vision loss (Cummings et al., 1985; Schuchard & Fletcher, 1994). Studies have shown that 72% -84% of eyes with central scotoma due to ARMD or JMD adopt a PRL (Cummings et al., 1985; Fletcher & Schuchard, 1997). Because of the dysfunction of retinal cells and the use of PRL, various visual function losses have been observed in maculopathy.

1.2 Visual Function Loss due to Maculopathy

1.2.1 Visual acuity loss is obvious in maculopathy. When visual acuity reaches 6 / 15 or worse, performance of daily tasks will be more difficult (Sultan et al., 1997). Leat et al. (1999) suggested an adoption of visual acuity < 6/12 as a standard criterion for disability caused by visual impairment. In some western countries, people with maculopathy with

visual acuity loss to poorer than 6/15 would restrict the eligibility of driving. There is a big span of visual acuity exhibited for advanced maculopathy (MPS Group, 1994). It is generally found that visual acuity is not the best indicator of some abilities such as face recognition and mobility (Rubin et al., 2000).

1.2.2 Visual field loss happens within the central visual field, i.e., there is a central scotoma. ARMD primarily affects the central 5 degrees of the retina (Folk, 1985; Leibowitz et al., 1980).

1.2.3 Contrast sensitivity (CS) loss shows the reduced capacity limit of the visual system to detect gratings with respect to spatial frequency for people with maculopathy. Increases of contrast threshold in early ARM mainly happen at high and intermediate frequencies whereas in ARMD, the impairment happens across the whole frequency range (Sjostrand & Frisen, 1977; Loshin & White, 1984). Supra-threshold contrast perception in maculopathy is another consideration. Little is known about supra-threshold contrast perception in maculopathy. Leat and Millodot (1991) showed that supra-threshold contrast perception was also influenced by maculopathy, however, not as much as the threshold contrast loss would indicate.

1.2.4 Other visual function loss also occurs. For example, some studies tested dark adaptation in early stages of ARM, revealing a scotopic dysfunction (scotopic sensitivity loss more than photopic sensitivity loss) and delays in rod-mediated dark adaptation (Owsley et al., 2000; Owsley et al., 2001; Steinmetz et al., 1993). Some researchers tested cone-mediated visual functional changes. Delayed visual adaptation of cones was observed (Cheng & Vingrys,

1993; Eisner, Stoumbos et al., 1991). Phipps et al. (2003) also found delayed cone recovery. Mayer et al. (1994) demonstrated a loss of flicker sensitivity.

1.3 Low Vision Rehabilitation (LVR)

Medical treatment of maculopathy, such as laser and radiation therapies, retinal transplants, gene therapies, ozone and hyperbaric therapies (Seddon, Ajani, Sperduto et al., 1994; Eger, 1998) is limited. Therefore low vision rehabilitation (LVR) plays an important part to enhance the quality of life for low vision patients. “LVR involves the assessment of visual impairment and the evaluation of functional performance, such as reading, writing, and mobility, within the context of lifestyle (e.g., employment, family activities), attitude, and psychological well-being. Rehabilitation goals are defined in terms of what matters most in a person’s life, and attempts are made to solve functional problems through adaptive options (e.g., vision enhancement and substitution devices, environmental modification) and coping strategies” (Elliott, Glasser, & Rubin, 2001).

Maculopathy causes the loss of high resolution, contrast perception, and central visual field loss compared to normal vision. Most of LVR strategies are aimed at compensating for these three main visual function losses.

1.3.1 Light Modulation

For outdoor activities, a dark filter to reduce the light transmission into the eye is beneficial to patients with advanced maculopathy. Indoor activities such as reading require increased illumination because this results in more light reaching transitional areas of scotoma and produces increased contrast sensitivity (Markowitz, 2006). Generally it is

suggested that the lighting source is positioned either behind the patient or on top of the target (such as a book or an image). Besides, reducing glare by suppressing the short wavelength light is also helpful. This can improve contrast sensitivity and visual acuity (Markowitz, 2006).

1.3.2 Substitution Aids

Larger-size materials such as large print books, large print watches, large print clocks, large print microwave buttons etc., can compensate for the loss of resolution. Materials with better contrast compensate for the contrast threshold increase. Voice output devices or instruments are a totally different approach from compensation for the loss of resolution. They translate text into voice information. Obviously this strategy cannot improve image viewing.

1.3.3 Optical Aids

Optical magnification devices provide enlarged images of text or images to compensate for the loss of resolution, but generally sacrifice the field of view. To date, these optical magnifiers are more commonly used by the visually impaired due to the advantage of being small and light, easy to carry and simple to use. Optical aids are available for distance and near tasks.

For distance vision

Telescopes are made of two or more lenses. They can be monocular or binocular, spectacle-mounted or handheld, focal or afocal. With increased magnification, the field of view is reduced. Generally, these devices are useful only for tasks performed while stationary or for spotting during mobility and orientation.

For near vision

There are four categories of optical magnifiers used for near tasks: microscopes, hand magnifiers, stand magnifiers, and telemicroscopes. All these magnifiers limit the field of view. They cannot increase the contrast, which will be the same or decreased after the image has been magnified.

1.3.4 Electronic Vision Enhancement Systems (EVES)

In the 1950's electronic visual enhancement systems (EVES) began to be used for the visually impaired (Lund & Watson, 1997). Not only is the object enlarged through the device, but other compensations can be made such as increased contrast or reversed contrast. These devices may be called high-tech devices. Basically they are categorized into two groups.

Electro-optical Magnifiers

A closed-circuit television (CCTV) is a device with a direct cable link between the camera imaging system and monitor viewing system (in contrast to broadcast television). The magnified image is displayed on the monitor. CCTV systems are available either as desktop, or handheld devices (see examples in Figure 1-1). They usually provide varying magnification, variable contrast and contrast reversal, variable brightness, and are available with or without color. They permit binocular vision. Compared with optical aids, CCTVs generally enable the use of a more comfortable posture, longer reading duration, and faster reading speed (Stelmack et al., 1991).

Desktop CCTV (ClearView)



Half-compact CCTV (Tieman Traveller)



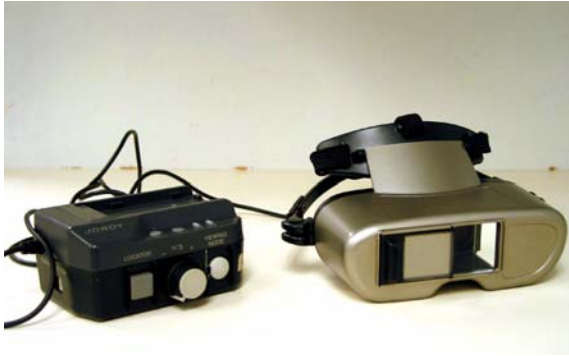
Compact CCTV (Tieman Traveller)



Figure 1-1. Examples of CCTV

The Jordy is a head-mounted video display unit incorporating magnification and image processing (shown in figure 1-2). The first generation was called V-Max. According to Enhanced Vision the features of Jordy include magnification up to 30x, auto-focus which keeps images in focus, extremely lightweight and portable, wide field-of-view, four viewing modes (full-color, black and white, high-contrast positive and negative) and a digital zoom which provides the ability to magnify and view faces, objects, or any image instantly. The NuVision is a similar device made by Keeler, UK..

Jordy



NuVision



Figure 1-2. Jordy and NuVision low vision device

Computers

Adaptive computer software improves accessibility to electronic and printed text and images for low vision patients. Hardware such as modified keyboards, large monitor screens, and attached scanners increase usefulness (Markowitz, 2006). There are two main electronic methods that adapt computers for low vision patients, magnification of text or images with or without more contrast and translation to auditory or tactile sensorial perception. There are several available softwares which provide magnification such as MAGic (Freesom Scientific, St. Petersburg, Fla), ZoomText (www.AISuared.com), and LunarPlus (www.DolphinUSA.com). The translation to auditory or tactile sensorial perception can be used for text information.

Text information is very important in daily life. A large body of research on reading shows that both optical and electronic magnifiers can provide dramatic enhancement in reading (Cheong et al., 2005; Leat et al., 1994; Legge et al., 1985; Stelmack et al., 1991). The audio substitutes can offer a good solution for patients with more severe visual loss.

However, we gain a lot of information about the world from color images. Due to the complexity of image structure, merely enlarging an image with optical or electronic magnifiers may not be sufficient. Audio output would not help in viewing images. Therefore, digital image enhancement has been investigated and applied to images for the visually impaired.

1.4 Digital Image enhancement

1.4.1 Digital images

To form a digital image, an optical image is digitized through two processes—sampling and quantization (Baxes, 1994). “The sampling process samples the intensity of the continuous-tone image at specific locations into a rectangular array of pixels” (Baxes, 1994). The first pixel of a digital image is located at the top and left and is represented by (0, 0). Then a pixel (x,y) represents a pixel located x pixels to the right of and y lines down from the pixel (0,0) of the image. The quantization process determines the digital brightness value (for example 0 to 255) of each pixel, ranging from black to white (Baxes, 1994). Therefore, a digital image exists as a large array of numbers, which correspond to different brightness. There are two common ways to deal with color. One is to create color with the primary colors of red, green, and blue (RGB). The other one is to create color with the hue, saturation, and brightness (HSB).

1.4.2 Digital image enhancement techniques

Digital image processing is a technique of mathematical manipulation of pixel values in digital images. This process can emphasize details, sharpen the picture, remove anomalies, or detect differences between pictures. For the visually impaired, the perceived images are degraded. Digital processing may aim to compensate for the degradation by increasing overall contrast, amplitude of specific spatial frequencies, or enhancing the edges of the original image. If the processed images are more visible compared to the original images, the visually impaired might perceive the processed image better, as being more close to “normal” (Peli et al, 1984; Peli, 1991; Lawton, 1989; Lawton, 1992). This image processing is called image enhancement and it could be used to improve the visibility of video images displayed on a screen or printed out in hardcopy.

The image enhancement used in most studies for the visually impaired does not increase the inherent information in an image but merely increases the dynamic range of the chosen features so that the observer can detect them more easily. During processing, some new pixel values fall outside of the dynamic range. Two methods can solve this problem, clipping and rescaling. Clipping allows the increased contrast in the middle ranges of pixel values to be maintained while the low and high ranges are chopped. The values that are outside of the range are set to the lowest or the highest value. Rescaling sets the maximum pixel value after processing to the highest value (such as 255 if the range is 0-255) and the minimum to the lowest value (such as 0 if the range is 0-255) and the intermediate values are rescaled proportionally to fit in between.

There are two main categories of digital image processing technique that will be discussed here. One is in the spatial domain and the other in the frequency domain.

1.4.2.1 Spatial domain processing

The spatial domain processing works on the pixels of a digital image directly. The primary value of a pixel is replaced with a new value. Digital filters based on spatial domain processing are the generic filters in this study. There are three basic techniques to generate this group of filters:

A) Pixel Point Processing On an individual basis, each pixel is dealt with independently of its neighbors. The gray level of each pixel in the original image is modified, by a mathematical or logical manipulation, to a new value and placed in the processed image at the same spatial location (Baxes, 1994). With this processing, the contrast could be reversed, that is the black changed to white, and white to black. Many CCTVs and computer programs include basic functions of this type, e.g. contrast reversal.

B) Pixel Group Processing This operates on a group of pixels surrounding a center pixel. One group of these pixels is called a kernel. The brightness trends of a kernel can be reflected by the values of the pixels in the kernel. The minimum kernel size (above 1x1, which is the same as point processing) is 3× 3 pixels. “The bigger the kernel size is, the larger the flexibility of the filter will be because there are more pixels involved in the calculation” (Baxes, 1984). All the output pixels are assigned a new value of brightness based on the values of the surrounding pixels. This technique is known as spatial convolution.

Image processing was introduced as an aid to enhance visual perception for the visual impaired by Peli and Peli at 1984. Later, Peli and his colleagues have done a considerable

amount of research in this area. Two filters based on pixel group processing were created to enhance image visibility for the visually impaired: Peli's adaptive thresholding filter and Peli's adaptive enhancement filter (Peli & Lim, 1982; Peli & Peli, 1984, Peli et al., 1991).

Peli's adaptive thresholding filter This is a kind of binary contrast enhancement. Using a mask or kernel, the value of a centered pixel is determined by the average luminance of the pixels around. All pixels of brightness less than a selected threshold brightness are set to black (0), and those equal or above are set to white (255). The threshold value varies as a function of the average pixel under the mask, so that varying the mask size produces differently enhanced images.

Peli's adaptive enhancement filter With a local averaging technique, the image is separated into low and high spatial frequency components. The high spatial frequency component is enhanced while the low spatial frequency is reduced. The average brightness of a mask and the size of the mask are two parameters for this filter. A slope determines the degree of attenuation of the low spatial frequency component. It was found that the change of slope and the intercept of this filter did not have a strong effect (Leat et al, 2005); therefore these two parameters could be set at certain values.

1.4.2.2 Frequency Domain Processing

A transform such as a fast Fourier transform (FFT) decomposes an image from its spatial domain to the frequency domain. Particular frequency components are reduced or enhanced from the frequency image. The frequency image is then transformed back to spatial domain with the changed frequency information.

1.4.3 Image processing in Low Vision

The image processing technique has been applied to both text and images for the visually impaired. Lawton (Lawton, 1989, 1992; Lawton, et al., 1998) applied individualized contrast sensitivity loss compensation filters to text for ARM patients. The filter was based on the ratio of the observer's contrast sensitivity function divided by the contrast sensitivity function of an age-matched normal observer. So the contrast was enhanced dependant on the contrast sensitivity loss. A gain factor was applied to determine the maximum amount of enhancement. The filtering was done in the frequency domain and a re-scaling method was used to solve the problem of saturation of dynamic range. The results showed that reading speed was improved and the magnification required could be reduced with filtered text. The reading speed improvement was demonstrated both with static and drifting texts.

Peli developed two filters (adaptive thresholding and adaptive enhancement) that he applied to images viewed by the visually impaired (Peli & Lim, 1982; Peli & Peli, 1984; Peli, et al., 1991). The images they used included faces (Peli & Peli, 1984; Peli et al., 1991) and video scenes (Peli et al., 1994). First, high spatial frequencies in all the images that exceed the observers' resolution limit were eliminated to save dynamic range for increases of the amplitude of frequencies which were within the resolution limit. Then either adaptive thresholding or adaptive enhancement was applied. The visual impairment they investigated was central visual loss, mostly age-related maculopathy (ARM). Their results showed that both filters significantly enhanced visibility of images for 40% of subjects (Peli et al., 1991) although the adaptive enhancement filter seemed to give more frequent improvement than the adaptive thresholding (9 out of 21 subjects with enhancement, and 6 out of 17 with

thresholding). A series of DigiVision devices have been developed to implement the adaptive enhancement algorithm in real time (Fullerton, & Peli, 2006; Hier, et al., 1993).

In addition to the two adaptive filters, Peli's group also investigated other filters. For example, they implemented wideband enhancement by detecting visually relevant edge and bar features in an image to produce a bipolar contour map. Then these contours were added to the original image resulting in an enhanced image (Peli, et al., 2004). However, only 22% of 35 visually impaired patients showed improved perceived visibility with these filters. In another study (Tang, et al., 2004), an algorithm to increase the contrast at all spatial frequencies by a certain factor was applied to images for visually impaired patients. The results showed a moderate improvement in image perception.

Most of these image enhancement techniques enhance high spatial frequency information. But studies show that it is not necessarily the high spatial frequencies that are most important for image recognition. For example, single faces, as a unique image category, seem to have critical frequencies for recognition. Early studies showed some discrepancy on this issue. Ginsburg (1985) argued that the low spatial frequencies (1-4 cycles/face) were sufficient. However Fiorentini et al. (1983) found that face recognition performance benefited from information at spatial frequencies higher than 5 cycles/face rather than only information of below 5 cycles/face. Rubin and Siegel (1984), using only one pose of each face, showed that discrimination was possible even when the faces were low-pass-filtered to 1.12 cycles/face. However, accurate recognition of numerous poses of the same face, including changes in expression, required information above 4.12 cycles/face. Sergent (1986) found that the identification of faces benefits from the presence of high frequencies. Hubner

et al (1985) derived high-frequency content from one face and low frequency content from another face and found that the high spatial frequency content dominates recognition. To verify the existence of critical spatial frequencies for face recognition, which could then be enhanced to improve performance in that task, Peli (1994) measured the degradation in recognition of familiar faces by older observers. His results showed that the band of spatial frequencies between 4 and 8 cycles/face is critical for face recognition. In that study, by enhancing spatial frequency information at 4 to 8 cycles/face, the recognition of faces was increased.

As well as the filters that Peli's group has investigated, there are other categories of digital filters which improve image visibility. Leat et al. (2005) compared custom-devised filters based on contrast sensitivity loss at each spatial frequency, some generic filters, plus Peli's two adaptive filters on 28 subjects with low vision. In that study, the eye pathology included many different disorders such as ARMD, glaucoma, diabetic retinopathy and retinitis pigmentosa. Fourteen images were selected in each of four classes: single full face, multiple faces (head and shoulders), outdoor scenes (street scenes with activity) and sports events. The filters were implemented with ImageLab software (Kennedy, Leat, & Jernigan, 1998), which ran on the NeXStep platform. The custom-devised filters used were based on contrast sensitivity loss. A gain was determined according to the ratio of the subject's contrast threshold and average normal CS in the same age group. Most generic filters were applied with a limited range of parameters. Subjects made within filter rankings followed by between filter ratings. The results showed that generally lower gains were more preferred than higher gains. Unsharp masking significantly increased perceived visibility for some

image types. Three filters showed borderline enhancement. They were Peli's adaptive enhancement, edge enhancement, and histogram equalization. Adaptive thresholding and the custom-devised filters, based on CS loss, did not result in improvement. Leat et al also showed that the optimum filters were dependent on the type of image and the type of visual disorder.

If digital image processing can improve the perceived visibility of digital images for people with maculopathy, then the next question would be how to assess the visibility improvement quantitatively. Peli's lab team reported several studies which attempted this. The earliest ones were based on the use of receiver operating curves (ROC's) by measuring the recognition of familiar and un-familiar faces (Peli et al., 1991; Peli, 1994; Peli, 2005). This method may be limited by the subjects' familiarity with the celebrities. Peli's group (Peli, 2005; Peli, 1999) also developed questions about video images to quantitatively measure enhancement. However, the results demonstrated a ceiling effect which may have reduced the sensitivity of the method.

Chapter 2

PROPOSED STUDY

2.1 Hypothesis

The hypothesis of this study is that the application of image enhancement to digital images will improve visibility for people with maculopathy, and that this can be measured both qualitatively and quantitatively.

The current study is a continuation of Leat et al.'s study (2005). There are several modifications in the approach of the current study. Firstly, the visual impairment will be restricted to three groups of maculopathy (atrophic ARMD, exudative ARMD, and JMD). Secondly, all the filters will be applied on a Windows system using Matlab. Thirdly, the “strength” of generic filters will be variable. Fourthly, custom-devised filters will be based on supra-threshold contrast matching as well as CS loss. Fifthly, in addition to the Gabor envelope, a polynomial envelope will be utilized for the band-pass filters. Sixthly, for spatial frequency filters, a band-width of two-octaves will be added in addition to one-octave band-width.

2.2 Aims and Purposes

The ultimate aim of this study is to continue investigating the application of digital image enhancement techniques to improve visibility of digital images for three groups of subjects with maculopathy (atrophic ARMD, exudative ARMD, and JMD). To reach this goal, there are five separate steps or goals:

2.2.1 Obtain age-related contrast matching data and investigate the aging effect

In order to develop the custom-devised filters derived from supra-threshold contrast loss for people with maculopathy, two age groups of control data of supra-threshold contrast matching will be collected. The main purpose is to develop a control data set against which the subjects with maculopathy will be compared to calculate the gain for the various custom-devised filters. The effects of age and contrast threshold on supra-threshold will be investigated at this stage.

2.2.2 Investigate supra-threshold contrast matching in maculopathy

To investigate the supra-threshold contrast loss in maculopathy and as a basis for the custom-devised filters, the supra-threshold contrast matching was tested for the three groups of subjects with maculopathy (atrophic ARMD, exudative ARMD, and JMD). The results will be compared to the older control group for statistical analysis.

2.2.3 Analyze and classify images with spatial frequency

The effective digital filters were found to be not only specific to type of maculopathy but also specific to the category of image (Leat et al., 2005). However, in their study the image grouping was according to the subject content in the images. There was no objective evidence to support their grouping. The purpose of this stage is to group images in a more objective way. The two parameters of amplitude spectrum and slope of the amplitude against spatial frequency will be considered, measured at three orientations (horizontal, vertical, and

oblique). Then the amplitude spectra and slopes will be analyzed statistically to show which groups are distinctive from other groups.

2.2.4 Test the perceived visibility improvement of with image enhancement

The purpose of this stage is to investigate the perceived improvement in visibility using some effective generic filters from Leat et al. (2005) in three groups of subjects with maculopathy and to investigate custom-devised filters based on supra-threshold contrast matching. There will be three phases to approach this goal. Firstly, the optimal “strength” of each version of a filter would be determined. Next, with the optimal “strength” each specific version of a filter type will be compared to each other so that the optimal version of the filter type will be determined. Then, with the optimal strength and version of each filter, all the filters will be rated. The effects of the generic filters and the custom-devised filters will be compared.

2.2.5 Assess the improvement of visibility objectively

The purpose of this stage is to measure how much improvement was generated by digital image enhancement. This section will be done in two steps. The first step is to develop effective methods in a preliminary study. The second step is to apply these methods to the nine subjects to attempt to demonstrate the improved visibility quantitatively.

Chapter 3 of this thesis is a paper published in Clinical and Experimental Optometry.

Title: Supra-threshold Contrast Matching and the Effects of Contrast Threshold and Age

Authors: Ming Mei, Susan J. Leat, and Jeffery Hovis

Contributions of each author:

Ming Mei – worked on methodology development, instrument set up, subjects' recruitment, being a driver for some of the subjects, data collection, data analysis, the first draft of the paper, and further revision of the draft.

Susan J. Leat – worked on methodology development, instrument set up and draft revision.

Jeffery Hovis – helped with calibration of instruments and data analysis.

The coauthors, Susan J. Leat and Jeffery Hovis, permit the microfilming of this thesis.

Permission is granted for you to use the material you specify below subject to the usual acknowledgements (author, title of material, title of book/journal, ourselves as publisher) and on the understanding that nowhere in the original text do we acknowledge another source for the requested material. Non-exclusive World English Language, one edition, print and electronic version of publication only.

This permission is granted on the condition that you contact the author for consent should you wish to adapt/modify the material. This is not the responsibility of Blackwell Publishing.

Ash Rahmani (Mr.)

Permissions Assistant

Wiley-Blackwell

9600 Garsington Road

Oxford OX4 2DQ, UK

Tel: +44 1865 476158

Fax: +44 1865 471158

Email: ash.rahmani@oxon.blackwellpublishing.com

Chapter 3

Supra-threshold Contrast Matching and the Effects of Contrast Threshold and Age

Ming Mei, Susan J. Leat, and Jeffery Hovis

University of Waterloo

Abstract

Background: The effects of age on contrast threshold are well known, however little is known about its effect on supra-threshold contrast perception. This study examines supra-threshold contrast matching and the effects of age in naïve observers.

Methods: Two age groups (20 – 50 years and 51+ years) with 14 and 15 subjects in each group participated. Contrast threshold and supra-threshold contrast matching up to 8.53 cycles per degree were measured.

Results: Both age groups demonstrated some degree of contrast constancy at medium and higher contrasts, but this was not perfect even at the highest contrast tested (55.9%). There was no overall effect of age on supra-threshold contrast matching ($p=0.086$) but there was an interaction between age and spatial frequency ($p<0.001$). The plots of matched contrast against standard contrast showed that, for some spatial frequencies, the slope was significantly different from unity, indicating a gain in the visual system for supra-threshold perception. This was still true when corrected for threshold differences.

Conclusion: Contrast constancy exists in a larger group of naïve subjects of different ages, but does not perfectly compensate for the differences in thresholds. The results are discussed in terms of the currently proposed models of contrast perception and are best explained by the model proposed by Näsänen et al (1998).

Keywords: Contrast matching, Contrast constancy, Contrast threshold, contrast sensitivity, Age groups

3.1 Introduction

The use of achromatic sine-wave gratings with varying spatial frequencies is an efficient tool to study contrast perception. It is known that contrast perception behaves differently at threshold and supra-threshold levels (Georgeson & Sullivan, 1975). Research on contrast threshold with varying spatial frequencies has shown that the maximum contrast sensitivity is at 2-5 cycles per deg (cpd) (Cannon, 1985; Owsley, Sekuler, and Siemsen, 1983; Pointer, and Hess, 1989; Watson, 1987; Peli, Yang, Goldstein, and Reeves, 1991). Factors such as grating area, duration time, mean luminance, and retinal location have a significant effect on contrast threshold (Peli et al., 1991; Patel, 1966; Tolhurst, 1975; Howell, 1978; Legge, 1978; Swanson & Wilson, 1985; Luntinen, et al., 1995; Owsley, et al., 1995). However, it could be argued that studies of supra-threshold contrast perception give us more information about our day to day visual perception.

With the method of contrast matching it has been shown that supra-threshold contrast matching functions (CMFs) have decreasing spatial frequency dependency with increasing

contrast. At higher contrast they take the shape of a wide band-pass or become flat (Georgeson & Sullivan, 1975; Peli et al., 1991; Blakemore & Muncey, 1973; Kulikowski, 1976; Swanson, Wilson, & Giese, 1984; Nasanen, Tiippana, & Rovamo, 1998). This phenomenon was termed “contrast constancy” (Georgeson & Sullivan, 1975) and holds for a wide range of spatial frequencies and retinal eccentricities. Because of this contrast constancy, we perceive objects at a constant contrast regardless of the size and distance. However, several studies have demonstrated conditions under which contrast constancy breaks down. Peli et al (1991) tested CMFs under natural viewing conditions, showing that contrast matching was dependent on luminance below 8cd/m^2 . Legge & Foley (1980) agree that contrast processing above 10% contrast is invariant with number of grating cycles. Hess’s study (1990) with dichoptic presentation and a long duration of light adaptation showed that at very low luminance (less than 0.02cd/m^2) and higher spatial frequencies (10cycles/degree) there were substantial deviations from contrast constancy. Peli (1997) reported that increasing stimulus size had no effect on CMFs but that adaptation was another factor that affected contrast constancy. A later study from Peli’s group (Peli, Arend, & Labianca, 1996), regarding the effect of luminance and spatial frequency on contrast perception, demonstrated contrast constancy for 1-4 cpd across a luminance range of 0.5-50 cd/m^2 . However, perceived contrast was reduced for gratings of 8 cpd when the luminance was less than 2cd/m^2 and perceived contrast was reduced for 16 cpd gratings across the entire luminance range. Thus at low spatial frequencies the supra-threshold contrast perception was less affected by decreased luminance than at high spatial frequencies.

Researchers have tried to use modeling to explain contrast constancy. Georgeson and Sullivan (1975) suggested that the gain of spatial frequency channels in the visual cortex was adjusted to compensate for earlier multiplicative attenuations that limit CSF. Kulikowski (1976) proposed a “subtractive factor” model, that is, if perceived contrast is a function of $(C-C_0)$, where C is the test grating contrast and C_0 the corresponding spatial frequency threshold, then the form of the CMF curves is well predicted. Georgeson (1991) provided a model combining both compensation and subtraction. Some other models are based on matched filters, signal-to-noise ratio, visual transfer functions and spatial integration window (Burgess & Colborne, 1988; Rovamo, Luntinen, & Nasanen, 1993). Näsänen et al. (1998) proposed a new model assuming that perceived contrast is related to the signal-to-noise ratio at low contrast levels, while at higher contrast levels perceived contrast is based on estimated local contrast obtained by using the reciprocals of the optical and neural filters.

Aging causes optical, anatomical, and physiological changes of the vision system, causing a decrease of contrast sensitivity which starts at age 50 (Owsley et al., 1985; Tulunay-Keesey, et al., 1988). However, studies are conflicting with regard to which spatial frequencies are affected. Some studies reported that contrast sensitivity decreased with aging mainly at the medium and high spatial frequencies (Owsley et al., 1985; Arundale, 1978; Derefeldt, Lennerstrand, & Lundh, 1979), one found decreases at low and medium spatial frequencies (Sekuler, Hutman, & Owsley, 1980), while others found a decrease at all spatial frequencies (Skalka, 1980; McGrath & Morrison, 1981; Ross, Clarke, & Bron, 1985; Nomura, et al., 2003). There are few studies on the effect of aging on supra-threshold contrast perception. Bead et al. (1994) used a contrast discrimination method to show that,

once normalized for contrast detection thresholds, contrast discrimination functions have the same shape in young and older adults. Tulunary-Keesey et al. (1988) measured contrast matching at one contrast level (1 log unit above the individual's threshold) and showed no age-related effect.

All of these studies of CMFs share similarities. Either contrast matching was tested only at one contrast level per spatial frequency, or only with a few subjects (mostly experienced experts). The present study aims to analyze CM more thoroughly by measuring CMFs on a larger sample of naïve subjects with normal vision and at a greater number of contrast levels [7 supra-threshold contrast levels (1.7- 55.9%)]. The subjects were separated into two groups, above and below 50 years. CSFs were also measured to determine the influence of CSFs on CMFs with respect to age. The results are compared with some current models of perceived contrast.

3.2 Method and Materials

3.2.1 Apparatus

A MacIntosh 6100/66 computer was used to generate stimuli with Morphonome 3.5 software (Tyler & McBride, 1997). The stimuli were displayed on a grey-scale 21" Sony Trinitron monitor with mean luminance of 60cd/m² and a resolution of 1152 × 864. A hardboard surround with peripheral luminance of 60cd/m² was placed around the monitor to provide a constant level of light adaptation. The luminance was measured with a Minolta LS-100 photometer. The display area measured 30.3° horizontally and 28.5° vertically at a viewing distance of 57 cm.

3.2.2 Stimuli

Vertical cosine gratings with a circular vignette envelope were used. The "vignette" is a computed blurring of the edge of the grating, not a physical window. The edge blur is the integral of a Gaussian with a standard deviation of 10 pixels, invariant with field size or the spatial frequency of the modulation. It results in a less gradual blur than a Gaussian, so that more cycles are visible at threshold, but it still gives an indistinct edge to reduce spatial transients. This is different from some of the recent studies which used a Gaussian envelope (Peli et al., 1991; Peli, 1997; Peli et al., 1996; Brady & Field, 1995). Gaussian-windowed stimuli have a more limited number of cycles, which may influence contrast threshold measurement (Savoy & McCann, 1975) and supra-threshold contrast matching of lower spatial frequencies at lower contrast levels (Legge & Foley, 1980). Contrast thresholds were measured for spatial frequencies of 0.26, 0.58, 1.11, 2.17, 4.29, 8.53 cpd. The highest frequency measured was 8.53 cycles/degree because this data was also to be used as control data in a subsequent study of age-related maculopathy (ARM). The viewing distance for 4.29 cpd and lower was 57 cm, and for 8.53 cpd was 114 cm. To guarantee at least 4 cycles in width (Savoy & McCann, 1975; Hoekstra, et al., 1974), the 0.26 cpd grating had a width of 16.6° , and higher spatial frequencies had a width of 10° . The duration of the stimulus for threshold measurement was 1.053 seconds, and the inter-stimulus interval was 583ms.

For the supra-threshold contrast matching, similar to Georgeson and Sullivan's work in 1975, two gratings (Table 3-1A) were presented side by side. The standard grating with a fixed spatial frequency of 0.58 cpd was on the right of the display screen and was presented at seven contrast levels (Michelson contrast): 1.7, 3.6, 7.2, 13.7, 27.9, 41.5, and 55.9%. The

spatial frequency of 0.58 cpd was chosen to be the standard grating because these normal data would be used as control of a subsequent study of low vision in ARM and it is appropriate to those subjects. The test grating with varying spatial frequency of 0.26, 0.58, 1.11, 2.17, 4.29, 8.53 cpd was on the left.

Table 3-1. Settings of the standard and test grating.

Viewing Distance	Standard Grating Settings		Test Grating Settings	
	Spatial frequency	Diameter	Spatial frequency	Diameter
A: Contrast matching stimuli for two age groups				
57cm	0.58cpd	10°	0.26cpd	16.6°
57cm	0.58cpd	10°	0.58-4.29cpd	10°
114cm	0.58cpd	6.65°	8.53cpd	5°
B: Contrast matching stimuli for 4.29 and 8.53cpd for 4 subjects				
57cm	1.11cpd	10°	2.17cpd	10°
114cm	1.11cpd	5°	4.29cpd	5°
228cm	1.11cpd	3.3°	8.53cpd	2.5 °

3.2.3 Subjects

Naive subjects with normal vision were recruited from the Optometry Clinic at the School of Optometry, University of Waterloo. There were two age groups (20 – 50 years and 51+ years) with 14 and 15 subjects in each. The average age of younger group was 32 ± 9 years, and the older group was 70 ± 11 years. All subjects gave written informed consent for

participating in the study, which was approved by the Office of Research Ethics at the University of Waterloo. The following were the exclusion criteria:

- a) Corrected VA worse than 6/7.5.
- b) Refractive error greater than ± 6.00 DS or 2.50DC.
- c) Any history of amblyopia, strabismus, or anisometropia.
- d) Opacities on the cornea, lenticular opacities in the undilated pupil area, or within the vitreous along the visual axis.
- e) Any retinal pigmentary changes or more than 4 drusen in an area of 1 disc diameter around the fovea.
- f) Intraocular pressure greater than 21 mmHg.
- g) Systemic disease (hypertension, diabetes or vascular disease) or medication with known ocular effects (such as chloroquine, oxazepan, melperon or oral contraceptive).

3.2.4 Procedure

Subjects wore their habitual spectacles plus a working distance correction. Monocular visual acuity was measured with the University of Waterloo logMAR chart (Strong & Woo, 1985) and all subjects had visual acuity of 6/6 or better. Five minutes of light adaptation was allowed beforehand. For contrast threshold measurement, a temporal two-alternative forced choice (2-AFC) staircase method was used. The staircase went up three steps for each wrong response and down one step for each correct response. The minimum number of

presentations was 14. Each step value was 0.05 log unit. There were two stopping rules, a) number of presentations = 30, b) the ending sample count, $n = 14$. For stopping rule b) a regression line is fitted to the last n presentations and when the slope of this regression line is less than $=1/n$, in this case less than $1/14$, the staircase stops. This assumes that when the slope of the last n presentations is zero or close to zero, the staircase is no longer ascending or descending and the threshold has been reached. The threshold value is calculated as the moving average of the last set of this number, n , of trials. At each spatial frequency the threshold was measured once for each subject.

For supra-threshold contrast matching, a method of adjustment but under experimenter control was used. The minimum step size was 0.05 log units across the whole contrast span. Subjects, looking freely between the standard and the test gratings, compared the contrasts between the standard grating (0.58 cpd) and the test grating (with varying spatial frequency), then told the experimenter to increase or decrease the contrast level of the test grating to match the contrast of the standard grating. Subjects were instructed to make judgements based on apparent contrast, not visibility. To minimize any pattern adaptation (Blakemore et al., 1975), subjects were instructed not to look at the standard grating for too long. Three matches were done at each combination of spatial frequency and contrast and the average calculated.

Nine younger subjects and five older subjects from the two age groups took part in a test-retest repeatability study, which was done by determining the contrast match with test gratings of 0.26 cpd and 2.17 cpd at contrast levels of 3.6% and 41.5% on two separate visits.

For statistical analysis, Systat was used for ANOVA and curve fitting (single degree-of-freedom polynomial contrasts) and Excel was used to calculate the slopes of the regression lines.

3.3 Results

3.3.1 Repeatability

The result of repeatability measurement is shown in Table 3-2. Generally speaking, the older subjects showed better repeatability except with 2.17 cpd at 41.5%, where the coefficients of repeatability for the two age groups were close. The coefficients of repeatability ($1.96 \times \text{SD of test minus re-test}$) (Bland & Altman, 1986) were in the region of 0.05 which is similar to the step sizes used for the contrast matching and indicates that subjects could make consistent matches.

Table 3-2. Repeatability of supra-threshold contrast matching

Contrast Level		3.6%		41.5%	
Spatial Frequency		0.26cpd	2.17cpd	0.26cpd	2.17cpd
Coefficient of Repeatability (\log) ⁴²	Younger Group	0.094	0.147	0.061	0.051
	Older Group	0.045	0.070	0.018	0.061

3.3.2 Contrast Threshold

Contrast thresholds with respect to spatial frequency are shown in Figure 3-1 (the highest two curves). For the younger group, 2.17 cpd was the most sensitive spatial frequency, while for the older group, it was 1.11 cpd. Generally, the older group showed higher contrast thresholds than the younger group across this spatial frequency range. The

two curves appear parallel from 0.26 to 1.11 cpd where there is a smaller discrepancy between the age groups, then they split further at higher frequencies. Repeated measures ANOVA (2 groups \times 6 spatial frequencies) calculated in log values showed a main effect of age ($p = 0.011$) and spatial frequency ($p < 0.001$) but no interaction between age and spatial frequency ($p = 0.273$).

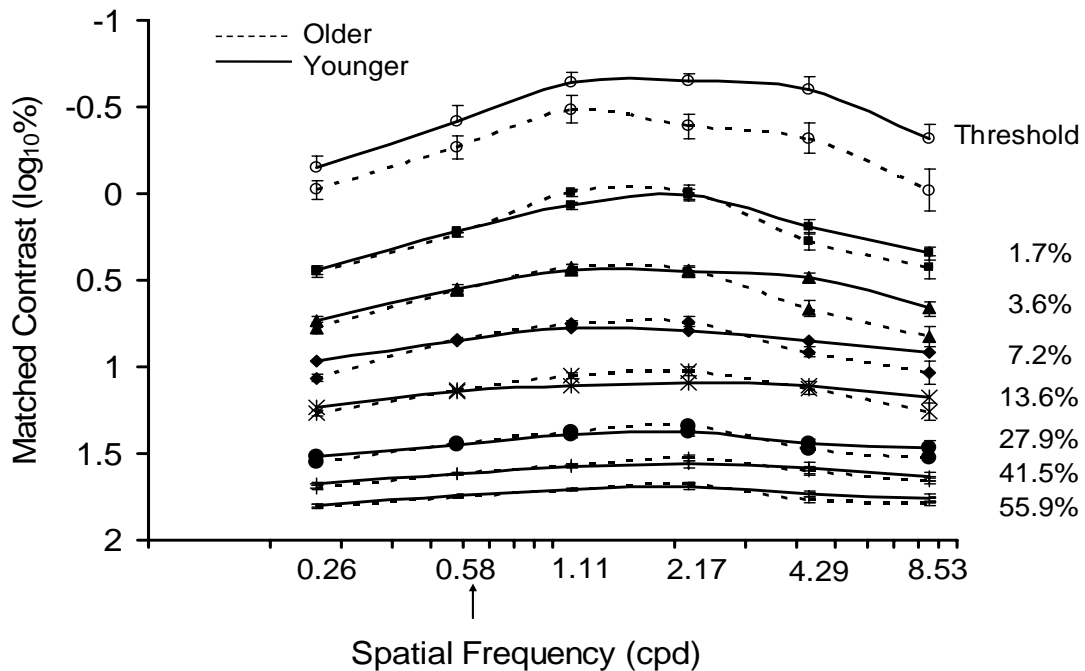


Figure 3-1. Mean supra-threshold contrast matching results for two age groups. The dashed-lines represent the older group, and the solid-ones represent the younger group. The top line of each data set represents the thresholds. The lower lines represent the matched contrasts against each contrast of the standard grating as shown on the right. The error bars show ± 1 standard error. The arrows indicate the spatial frequency of the standard grating.

3.3.3 Supra-threshold Contrast Matching

Supra-threshold contrast matching as a function of spatial frequency is also shown in Figure 3-1. Generally, the matching curves for lower contrast levels resemble the threshold curve showing apparent spatial frequency dependence, with the peak (matched with less contrast than the standard grating) at either 1.11 or 2.17 cpd. The matching curves of medium and higher contrast levels show increasing flatness demonstrating contrast constancy, but there is still an apparent peak at 2.17 cpd. To explore the effect of age as a factor in contrast perception more thoroughly, repeated-measures ANOVA (2 groups x 6 spatial frequencies x 7 contrast levels [excluding contrast threshold]) calculated in log values were applied. The results showed no main effect of age ($p = 0.086$) but there were main effects for contrast ($p < 0.001$) and spatial frequency ($p < 0.001$). There was no interaction between contrast and age group ($p = 0.149$), but there were interactions between spatial frequency and age group ($p = 0.005$) and contrast and spatial frequency ($p < 0.001$) but no interaction between age, contrast and spatial frequency ($p = 0.12$).

The interaction between age and spatial frequency can be seen in Figure 3-1. There is a trend that the matched contrast curves of the older group show narrower band-pass functions compared to that of the younger group - that is, the older group tended to match the standard grating with higher contrast at both low and high spatial frequencies (0.26, 4.29, and 8.53 cpd) than the younger group, while at the middle spatial frequencies (0.58, 1.11, and 2.17 cpd), the older group tended to match with similar or lower contrast.

To explore whether contrast constancy is complete at the highest contrast, repeated measures ANOVAs were undertaken at each contrast level with respect to spatial frequency (2 groups x 6 spatial frequencies) This showed an effect of spatial frequency at all contrast levels, even at the highest contrast of 55.9% ($p < 0.001$) i.e. contrast matching is still dependant on spatial frequency at high contrasts. Curve fitting was undertaken of contrast matches with respect to spatial frequency. At all contrasts, the contrast matching functions were best fit with a quadratic function rather than a straight line. At 55.9% contrast the best fit straight line gave a $p = 0.175$ and the quadratic fit gave a $p < 0.001$.

To analyze the gain of matched contrasts against reference contrast the data were plotted at each spatial frequency (Georgeson & Sullivan, 1975) as shown in Figure 3-2, and regression lines were calculated. If contrast matching was perfect, all of the contrast matching lines should lie along the diagonal line for equal contrast. Generally speaking, the lower the contrast, the more distant the data points are from the diagonal. The regression line slopes and corresponding 95% confidence limits are shown in Table 3-3. At 0.58 and 4.29 cpd, the slopes of the contrast matching regression lines were close to the diagonal. At 0.26 and 8.53 cpd, the slopes were shallower than that of the diagonal, while at 1.11 and 2.17 cpd they were steeper. However, although the slope of these lines was not always significantly different from unity (based on the 95% confidence limits), the magnitude of the slope was in the correct direction (either above or below unity) as would be predicted from the thresholds in all cases i.e. assuming that there is a “gain” that compensates for differences in contrast threshold. When the test grating had a higher threshold than the reference grating the line was positioned above the line for equal matches, and has a slope which is shallower than 1 and

vice versa when the threshold was lower. For example, 0.26 and 8.53 cpd show lower thresholds than 0.58 cpd and the contrast matching lines are significantly above the diagonal. Conversely, 1.11 and 2.17 cpd show higher thresholds, the matching lines are significantly below the diagonal. Contrast matching at 0.58 cpd is at the same spatial frequency as the standard and is along the perfect match diagonal line. The slopes of the regression lines were similar for the two age groups (two sample t-test, $p > 0.05$ in all cases).

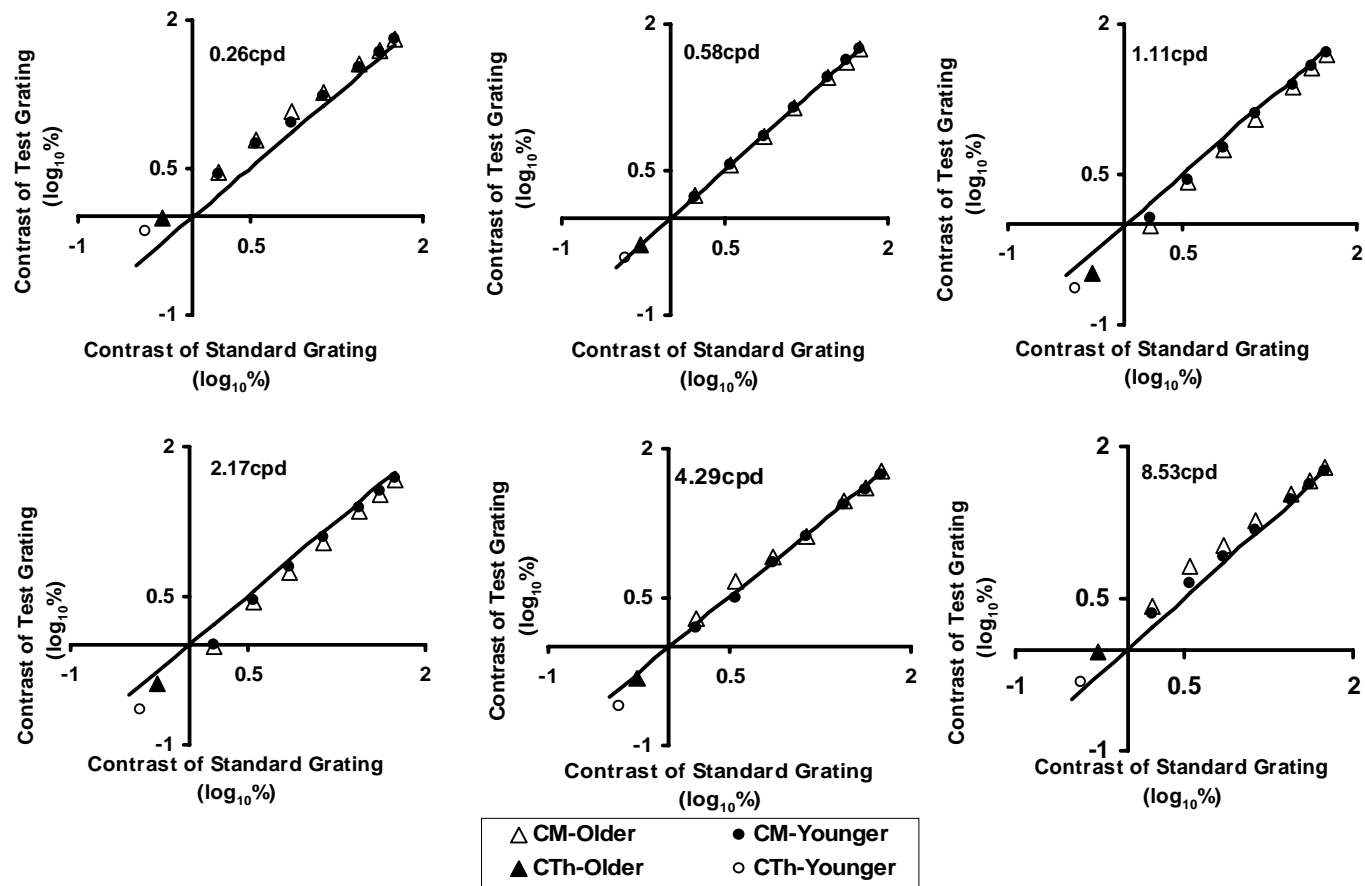


Figure 3-2. Mean threshold and supra-threshold contrast matching plotted against standard contrast for each spatial frequency. The standard grating was 0.58 cpd. The perfect contrast match is shown by the diagonal straight line. CTh = contrast threshold. CM = contrast matching.

Table 3-3. Regression line slopes and the 95% confidence limits of 6 spatial frequencies for data plotted in Figure 3-2 (non-normalized data). Confidence limits are based on ± 1 standard error. Those in bold indicate where the slope is significantly different from 1.

		0.26cpd	0.58cpd	1.11cpd	2.17cpd	4.29cpd	8.53cpd
Older	Slope	0.877	0.993	1.104	1.071	0.946	0.852
	Confidence limits	0.839 to 0.915	0.982 to 1.003	1.074 to 1.134	1.027 to 1.116	0.885 to 1.008	0.774 to 0.929
Younger	Slope	0.892	1.002	1.071	1.068	1.004	0.909
	Confidence limits	0.865 to 0.92	0.989 to 1.015	1.038 to 1.103	1.015 to 1.12	0.943 to 1.065	0.842 to 0.976

To test whether contrast matching can be accounted for by subtracting the thresholds (Kulikowski, 1976), and to examine the differences of contrast matching with respect to age, the data were normalized by subtracting the linear threshold for 0.58 cpd from the standard contrast and the threshold at each matched frequency from the matched contrast (McIlhagga, 2004) and then taking the logarithm. The resultant plots and the regression analysis are shown in Figure 3-3 and Table 3- 4. With this transformation, the matching functions should fall on a line of slope 1 passing through the origin if the subtractive theory is correct. Similar to the non-normalized data, the regression lines are still affected by their corresponding thresholds. At 0.58 and 4.29 cpd, the slopes of the contrast matching regression lines were close to the diagonal. At 0.26 and 8.53 cpd, the slopes were still significantly shallower than that of the diagonal, while at 1.11 and 2.17 cpd the slopes of younger group were close to the diagonal but those of the older group were still significantly steeper. Thus the normalized contrast matching lines still show similar trends even though the thresholds have been

subtracted. Additionally, in some cases (1.11 and 2.17 cpd for the older group) the slope is more different from unity after normalization.

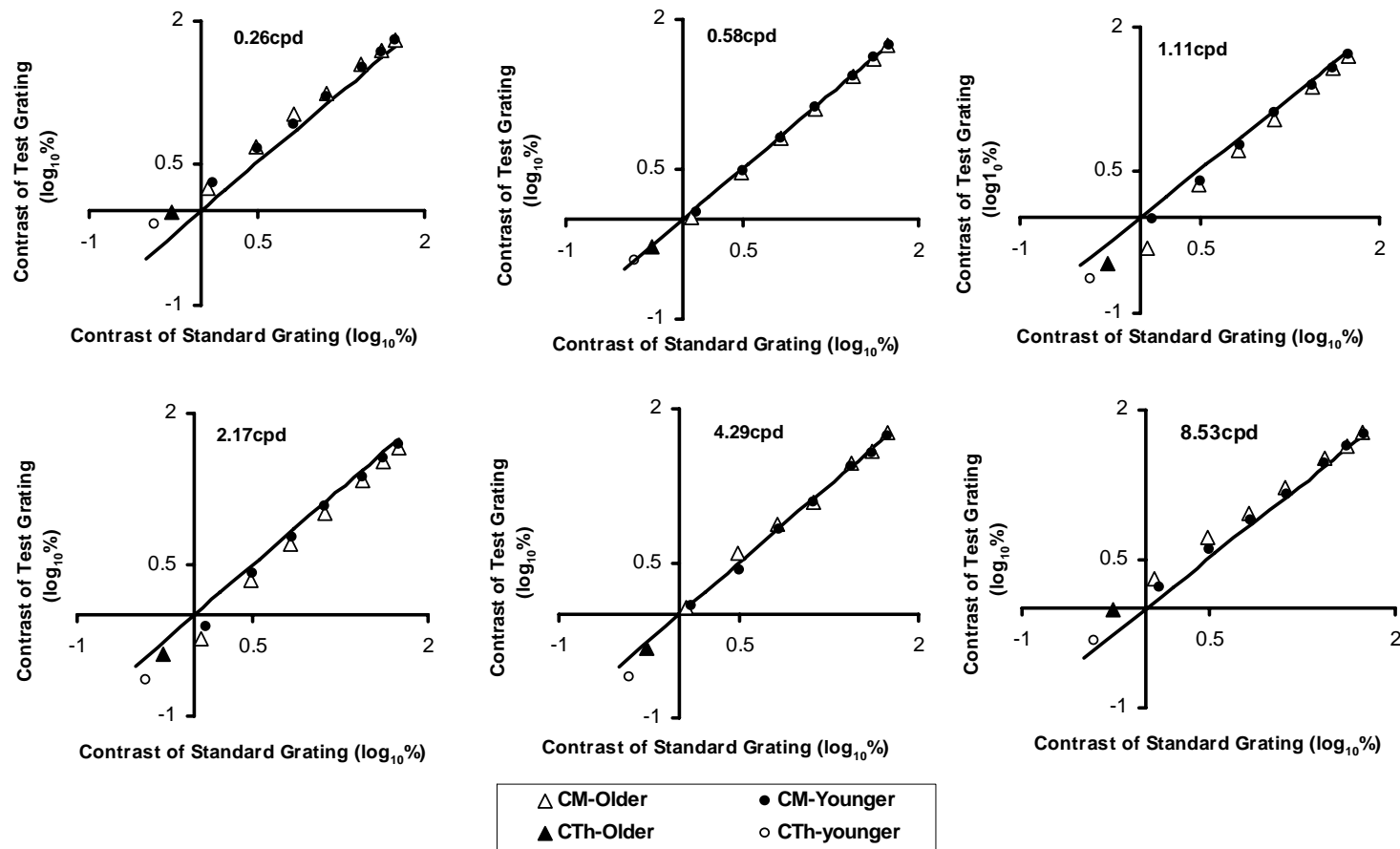


Figure 3-3. Mean threshold and normalized supra-threshold contrast matching plotted against standard contrast for each spatial frequency. The standard grating was 0.58 cpd. The perfect contrast match is shown by the diagonal straight line. CTh = contrast threshold. CM = contrast matching.

Table 3-4. Regression slopes and the 95% confidence limits of 6 spatial frequencies with the normalized values. Confidence limits are based on +/- 1 standard error. Those in bold indicate where the slope is significantly different from 1.

		0.26cpd	0.58cpd	1.11cpd	2.17cpd	4.29cpd	8.53cpd
Older	Slope	0.894	0.989	1.134	1.074	0.936	0.863
	Confidence limits	0.838 to 0.950	0.972 to 1.007	1.046 to 1.222	1.030 to 1.118	0.87 to 1.003	0.776 to 0.949
Younger	Slope	0.917	1.004	1.043	1.039	0.983	0.906
	Confidence limits	0.861 to 0.973	0.984 to 1.024	0.989 to 1.097	0.98 to 1.097	0.92 to 1.047	0.828 to 0.984

3.4 Discussion

3.4.1 Contrast Threshold

The peaks of the two contrast threshold curves for both age groups were at 1.11-2.17 cpd. When we take into account the fact that the present study measured CS down to a lower spatial frequency (0.25 cpd), this is in agreement with the results of Peli et al.'s study (Peli et al., 1991). As for the effects of age, the younger group showed overall lower contrast thresholds across all spatial frequencies tested, which is in agreement with those studies that showed CS loss at all spatial frequencies with age (Skalka, 1980; McGrath & Morrison, 1981; Ross et al., 1985; Nomura et al., 2003). The peak of the contrast threshold curve shifted to lower spatial frequencies with age. The younger group was most sensitive at 2.17 cpd and the older group at 1.11 cpd. This shift of the peak to lower spatial frequencies supports Owsley et al.'s study (1983). As for the explanation of the effect of age on contrast threshold,

there is no consensus as to whether optical or retinal factors are the primary cause (Elliott, 1987; Elliott, Whitaker, & MacVeigh, 1990), but that discussion is beyond the scope of the present paper.

3.4.2 Supra-threshold contrast matching

Our supra-threshold contrast matching results plotted across contrast levels (Figure 3-1) are quite similar to Georgeson and Sullivan's findings (1975). At low contrast, the matching curves resemble the threshold curve, while at medium and higher levels, the curves become flatter, described as contrast constancy. Other studies also have shown similar results (Blakemore & Muncney, 1973; Kulikowski, 1976; Swanson, Wilson et al., 1984; Nasanen et al., 1998). However, all these studies were mainly based on the data obtained from a few subjects who were experienced observers. Our study extends their data to show that contrast constancy exists in a larger group of naïve subjects of different ages.

There are a few differences between the study of Georgeson & Sullivan (1975) and the current study. In their study, using gratings of constant spatial extent, the reference spatial frequency was 5 cpd and a wider range of spatial frequencies (0.25-25 cpd) was tested. The current study used gratings of variable spatial extent, took 0.58 cpd as the reference and the tested spatial frequencies ranged from 0.26 to 8.53 cpd - a narrower span. Another difference is that their subjects were two experienced observers, and ours were 29 naïve subjects. They do not describe their psychophysical technique for threshold measurement and the peak of their SC functions appears around 2-5 cpd which is similar to the current findings for the younger age group. When it came to the supra-threshold contrast matching curves, the two subjects in their study behaved differently from each other. If we only consider their results

for 0.25 to 10 cpd, one subject (GDS) mostly peaked at around 1 cpd or 10 cpd until 30%. The other subject (MAG) peaked at around 5 cpd. For the current data, the supra-threshold contrast matching curves of both age groups peak at around 2.17 cpd. By observation, both these studies show that contrast thresholds affect supra-threshold contrast perception until at least around 30-60% contrast although this influence declines with increasing contrast. This observation is supported by some of Kulikowski's (1976) data (his Figure 3). The current data showed that at 55.9% contrast, the matching functions were best fit with a quadratic function, rather than a straight line ($p < 0.001$) and the matching was still spatial frequency dependant, with a peak at 1.11 to 2.17 cpd. This indicates that contrast constancy is still not perfect up to 55.9%.

We should discuss the possible influence of sampling artefacts at the higher frequencies of 4.29 and 8.53 cpd. The screen had a horizontal resolution of 1152, which means that, at the testing distances of 57 and 114 cm respectively, one cycle would have been represented by 9 pixels. Thus the contrast actually displayed may have been less than that intended, so that the subject would have to set it higher to gain perceptual equality. To check that the results were not affected by this artefact, we repeated the contrast matches at a greater testing distance so that the higher spatial frequencies of 4.29 and 8.53 were each represented by twice this number of pixels (see Table 3-1B) with 4 younger subjects. The ages of these younger subjects were between 23 to 32 years. In order to maintain the at least 4 cycles, a standard spatial frequency of 1.11 cpd was used for these matches. The results are shown in Figure 3-4. Since we used 1.11 cpd as reference instead of 0.58 cpd, the relative positions of the three regression fitting lines for 2.17, 4.29, and 8.53 cpd to the diagonal line

are different from previous data shown in Figure 3-2. However, the most obvious result here is for the 8.53 cpd matches, since the threshold for 8.53 cpd is significantly higher than for 1.11 cpd. The contrast matches for 8.53 cpd were consistently set at a higher contrast than the standard. This validates the previous finding that contrast constancy is not perfect up to 55.9% contrast.

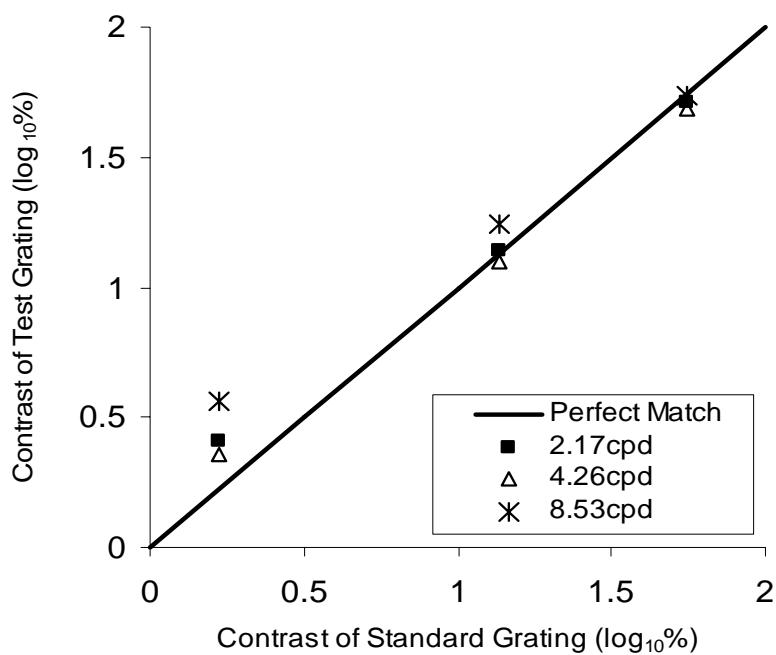


Figure 3- 4. Mean supra-threshold contrast matching plotted against standard contrast for three spatial frequencies for four younger subjects. The standard grating was 1.11 cpd. The perfect contrast match is shown by the diagonal straight line.

In order to explain contrast constancy, different models have been suggested. Kulikowski (1976) used a linear “subtractive factor” theory. He suggested that perceived contrasts in linear terms would match if $C_F - T_F = C_{0.58} - T_{0.58}$, where C_F is the test grating

contrast, T_F the corresponding contrast threshold, $C_{0.58}$ the reference contrast, and $T_{0.58}$ the threshold of reference grating. This model would assume equal gain in all channels. Our findings, once corrected for threshold, showed that some slopes were still significantly different from unity (Figure 3-3) which implies that Kulikowski's model is not an adequate explanation.

McIlhagga (2004) re-evaluated Kulikowski's threshold model and postulated that threshold subtraction is a method of noise suppression. They replotted the data from Näsänen et al. (1998) with linear (C-T) values (see their Figure 1). They suggested that from 0.5 to 8 cpd the contrast matching values were close to the diagonal line. However careful observation of the graph indicates that the slopes at different spatial frequencies do not appear equal to unity. For example, the regression line of 8 cpd appears above the diagonal as does that for 2 cpd. Thus their data are in agreement with the present study. In our study, slopes for 0.26, 1.11, 2.17, and 8.53 cpd show statistically significant differences from a slope of 1. So, again, the supra-threshold contrast perception does not function in this simple linear threshold subtractive way.

Georgeson and Sullivan (1975) proposed that the visual system adjusts its gain in inverse proportion to the attenuation due to optical and neural processes. According to Brady and Field (1995), this model is effective only at high contrasts while at low contrasts both signal and noise would be exaggerated due to the large gain of inverse filtering so that variability of perceived contrast is increased. Brady and Field suggested that threshold sensitivity is a function of the signal to noise ratio, whereas perceived contrast is assumed to be a function of the signal alone and to be independent of the noise. According to their

model, there is no need to propose different gains in different channels and that the contrast matching curves (as plotted in our Figure 3-2) should have a slope of 1. Their study reports that there was no transitional region between contrast threshold and supra-threshold contrast matching and that contrast constancy was observed immediately above threshold even at low contrasts such as 3%. They did discuss that, at the higher spatial frequencies, this might be due to the method (whether the high frequency is adjusted to match the lower or vice versa), but this did not seem to be the explanation for medium frequencies such as 4 cpd. However if this model is accurate, the supra-threshold contrast matching curves for low contrast should be close to a straight line when plotted against spatial frequency, which is not the case in the current study. Even in their results (their Figure 5B and 6B) departures from constancy at both low and high spatial frequencies are obvious and their other matching data (their Figure 7) does not include data for contrast matches close to threshold. Our quadratic curve fitting analysis with respect to spatial frequency further excludes the possibility that contrast matching is as accurate as they claim at higher contrasts. Additionally, the current data do not show a sudden transition to contrast constancy, but rather a more gradual change towards accurate matches at higher contrasts, and we do show departures from a slope of 1, even when corrected for thresholds.

Näsänen et al. (1998) proposed a contrast restoration model. In this model, at low contrast the perceived contrast is assumed to be related to the signal-to-noise ratio of the mechanism that is responsible for contrast detection. At high contrast, perceived contrast is based on estimated local contrast obtained by using the reciprocals of the gain due to the optical and neural filters (inverse filtering). Their data has been replotted in terms of matched

contrast against standard contrast before and after normalizing by subtracting the corresponding thresholds (Figure 3-5). In their experiment 4 cpd was the reference spatial frequency which showed the lowest contrast threshold among the tested spatial frequencies of 0.5, 1, 2, 4, 8, and 16 cpd. At supra-threshold contrast levels, the matched contrasts of other spatial frequencies were under-estimated and therefore matched with higher contrasts. Thus the regression lines were above the diagonal line for unity while that of 4 cpd was along the diagonal. These trends were similar after correction for thresholds. Note that we did not use a spatial frequency as high as 16 cpd in the current study, nor fit the models statistically. Thus, of the models currently proposed, Näsänen's model is qualitatively the better description of the current data.

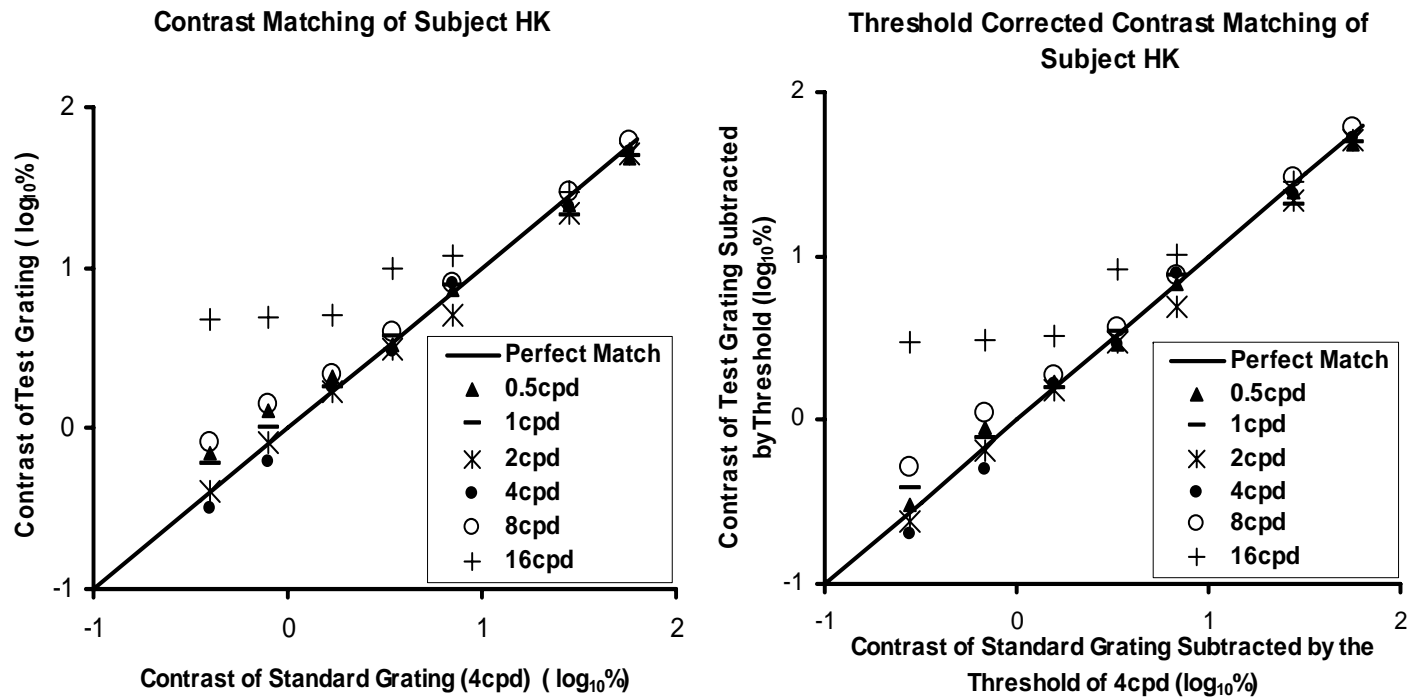


Figure 3-5. Contrast matching re-plotted from Figure 2A of Näsänen et al. (1998) in terms of matched contrast against standard contrast before and after normalized by subtracting the corresponding thresholds. (A) Before normalization. (B) After normalization. The standard grating was 4 cpd. The perfect contrast match is shown by the diagonal straight line.

3.4.3 Aging and contrast matching

The current study has shown that aging increases contrast thresholds from 0.26 to 8.53 cpd, and has also shown that supra-threshold contrast perception is related to threshold. So, what is the effect of aging on supra-threshold perception? Are any differences simply the result of threshold differences caused by aging? Repeated ANOVA and regression analysis show there are interactions between spatial frequency and aging. Leat and Millodot (1990) found an age effect on supra-threshold contrast perception using the method of contrast discrimination, measured at standard levels above threshold. Beard et al. (1994) found an age effect with contrast discrimination. However they concluded that this effect disappeared after normalizing the data for thresholds. Tulunay-Keesey et al. (1988) using contrast matching showed no age-related effects. The two age groups of their study were 20-29 years and 60-69 years, while those of the current study were 21-50 years and 51- 86 years. In their study, one contrast level was tested which was 10 times the corresponding threshold at each spatial frequency, so the two age groups matched contrast at different absolute levels. They analyzed the ratios between log threshold and log match contrast, again different from the current study in which absolute values of contrast were used. These differences make these two studies difficult to compare.

The effects of age were border-line for the present supra-threshold data (showing as an interaction with spatial frequency, but not with contrast). The interesting question here is, whether, as thresholds change with age, there is a change in the supra-threshold gain of the system to compensate.

However, whether age-related supra-threshold differences would be found would depend on the relative thresholds of the standard and the test grating. If these differences in threshold are similar between the age groups (although both might be elevated for the older subjects) no differences in the supra-threshold slopes would be found. If the threshold curves in Figure 3-1 are examined, it can be seen that the relative thresholds 0.58 cpd and other spatial frequencies for the two age groups are similar. Since the older subjects showed a decrease of contrast sensitivity at all spatial frequencies, there is little change in the relative thresholds. Also, as it happened, there was no example where the data point for the relative thresholds in Figure 3-2 or 3 was above the line for unity for one group and below it for the other. Thus the present data cannot answer the question of whether there are changes in the gain to compensate for thresholds changes.

3.5 Conclusion

Our data supports the work of Georgeson and Sullivan (1975), but extends their data to show that contrast constancy exists in a larger group of naïve subjects of different ages. But contrast constancy was not found to be perfect up to 55.9%. Of the currently proposed models, the current data are best explained with the model proposed by Näsänen et al. (1998) in which at low contrast the perceived contrast is related to the signal-to-noise ratio. Alternatively at high contrast, perceived contrast is based on estimated local contrast obtained by using the reciprocals of the gain due to the optical and neural filters (inverse filtering). Thus the mechanisms of contrast threshold and low contrast perception are distinct from contrast perception at intermediate and higher contrasts. Our data show only subtle

changes of contrast matching with age (note that this is at absolute contrast levels) but were not able to indicate if there are adaptations in the gain of the supra-threshold system because of the changes in threshold due to optical and neural changes with age.

3.6 Acknowledgements

This research was supported by the Macular Disease Society, UK. We would like to extend thanks to Trefford Simpson for help in the use of Morphonome.

Chapter 4 of this thesis is a paper accepted for publication (in press) in Investigative Ophthalmology and Vision Science.

Title: Supra-threshold Contrast Matching in Maculopathy

Authors: Ming Mei and Susan J. Leat

Contributions of each author:

Ming Mei – worked on methodology development, instrument set up, subjects' recruitment, being a driver for some of the subjects, data collection, data analysis, the first draft of paper, and further revision of the draft.

Susan J. Leat – worked on methodology development, instrument set up and draft revision.

The coauthor, Susan J. Leat, permits the microfilming of this thesis.

IOVS

Investigative Ophthalmology & Visual Science

March 30, 2007

Ming Mei
School of Optometry
University of Waterloo
Ontario
Canada

Dear Ming Mei:

Permission is hereby granted to include the following article in your thesis:

Mei M, Leat SJ. Supra-threshold contrast matching in maculopathy. *Invest Ophthalmol Vis Sci.* in press.

A reprint of this material must include a full article citation (if known at the time the thesis is published) and acknowledgment of the Association for Research in Vision and Ophthalmology as the copyright holder.

Regards,



Debra L. Chin
Editorial Specialist
Tel: 240-221-2920
Fax: 240-221-0355
E-mail: dchin@arvo.org

ROBERT N. FRANK, MD, EDITOR-IN-CHIEF
KAREN COLSON, DIRECTOR OF PUBLISHING AND COMMUNICATIONS

IOVS IS THE OFFICIAL PUBLICATION OF THE ASSOCIATION
FOR RESEARCH IN VISION AND OPHTHALMOLOGY

IOVS EDITORIAL OFFICE ■ 12300 TWINBROOK PARKWAY ■ SUITE 250 ■ ROCKVILLE, MD 20852-1606
TEL: 240-221-2920 ■ FAX: 240-221-0355 ■ E-MAIL: iovs@arvo.org ■ WEBSITE: www.iovs.org

Chapter 4

Supra-threshold Contrast Matching in Maculopathy

Ming Mei and Susan J. Leat

From the School of Optometry, University of Waterloo, Waterloo, Ontario, Canada.

Abstract

PURPOSE. To compare suprathreshold contrast perception among three groups of participants with maculopathy (atrophic age-related macular degeneration [ARMD], exudative ARMD, and juvenile macular dystrophy [JMD]) and to compare suprathreshold contrast matching between controls and subjects with maculopathy.

METHODS. Three groups of subjects with macular disorders (13 atrophic ARMD, 14 exudative ARMD, and 8 JMD) and one group of control subjects (15 subjects 50 years and older) participated. Contrast sensitivity (CS) up to 8.53 cycles per degree (cpd) was measured with a temporal two-alternative forced-choice staircase procedure. Suprathreshold contrast matching was measured using a method of limits. A 0.58 cpd sine-wave grating was the standard; the subject was asked to match the contrast of gratings of different spatial frequencies.

RESULTS. Subjects with maculopathy showed marked deficits of contrast threshold. Suprathreshold contrast constancy was shown, though deficits were observed in absolute matches compared with control subjects. The slopes of matched contrast against standard

contrast for the subjects with maculopathy were significantly different from those for the controls, and these differences were in the direction that implies compensation for differences in thresholds. There were no significant differences among the three groups of subjects with maculopathy.

CONCLUSIONS. In this study, the authors observed a degree of contrast constancy in subjects with maculopathy, though there were still deficits compared with control subjects. This is discussed in terms of gain of the visual system adjusting to compensate for CS losses (though incompletely) or contrast overconstancy, present in normal peripheral vision, which helps to compensate for CS loss.

4.1 Introduction

Age-related macular degeneration (ARMD) is the leading cause of visual impairment in Western developed countries. The later stages of ARMD are categorized into atrophic ARMD and exudative ARMD (Bird, et al, 1995). Both conditions involve loss of central vision, including loss of contrast sensitivity and visual acuity. In juvenile macular dystrophy (JMD), such as Stargardt disease and Best disease, a similar loss of visual function occurs. Studies have shown that contrast threshold measurement is a better predictor of functions such as reading speed, mobility performance, and recognition of targets (e.g., faces) than visual acuity (Evans & Ginsburg, 1985; Hazel, et al., 2000; Leat & Woodhouse, 1993; Rubin & Legge, 1989; West, et al., 2002). However, most of our daily visual function happens at suprathreshold contrast levels. Little is known about how suprathreshold contrast perception is affected by maculopathy and whether suprathreshold perception might have a greater or lesser influence on visual disability than threshold measurements.

Studies on normal vision have suggested that suprathreshold contrast perception is different from threshold detection in that it is less dependent on spatial frequency and exhibits constancy at higher contrasts (Georgeson & Sullivan, 1975; Peli et al., 1991; Nasanen et al., 1998). Thus, at higher contrasts, gratings of equal contrast but different spatial frequency are perceived as having similar contrast despite large differences in contrast threshold. Several studies have investigated contrast matching between the fovea and eccentric retinal areas (Georgeson & Sullivan, 1975; Cannon, 1985; Swanson & Wilson, 1985). This is of interest in studies of maculopathy, because an eccentric location {the preferred retinal locus [PRL]} (Georgeson & Sullivan, 1975; Cannon, 1985; Swanson &

Wilson, 1985)}, rather than the nonfunctional anatomic fovea, is used for fixation. These studies showed that subjects could make fairly accurate matches between the two retinal locations despite large differences in threshold. They suggested that the gain functions of peripheral channels are adjusted to compensate for the neural blur at each retinal locus. However, there was a consistent tendency to perceive an eccentric grating to be of higher contrast than the standard grating at the fovea (Georgeson & Sullivan, 1975). This was called contrast overconstancy (Georgeson, 1991). Overconstancy also seemed to occur when gratings of different spatial frequencies, presented at the same retinal eccentricity, were matched—higher spatial frequencies appeared to have more contrast than lower spatial frequencies (Georgeson, 1991).

A few studies have examined contrast matching in people with visual impairment caused by a variety of disorders, namely nystagmus (Dickinson & Abadi, 1992), amblyopia (Hess & Bradley, 1980), and demyelinating disease (Medjbeur & Tulunay-Keesey, 1986). All these studies showed normal or lower deficit in suprathreshold contrast perception compared with contrast sensitivity. Maculopathy is different from these eye diseases in that a PRL is developed and used instead of the anatomic fovea. A study by Leat and Millodot (1990), using contrast discrimination (CD) in four subjects with maculopathy, found that CD was significantly poorer for the maculopathy group than for the group with normal vision at all spatial frequencies (0.25–3.0 cycles per degree [cpd]). However, this measure of suprathreshold contrast perception was less affected by maculopathy than were contrast thresholds.

This study aimed to compare suprathreshold contrast perception studied with contrast matching among three groups of subjects with maculopathy—atrohic ARMD, exudative ARMD, and JMD—and to compare suprathreshold contrast matching between controls and subjects with maculopathy. Our hypothesis was that suprathreshold function in maculopathy is less affected than contrast thresholds. Additionally, we sought to determine whether there is evidence of contrast overconstancy in maculopathy.

4.2 Method and Materials

4.2.1 Apparatus

A computer (MacIntosh 6100/66; Apple, Cupertino, CA) was used to generate stimuli with Morphonome 3.5 software (Tyler & McBride, 1997). Stimuli were displayed on a high-resolution 21-inch monitor (Trinitron; Sony, Tokyo, Japan) with a mean luminance of 60 cd/m². A hardboard surround with luminance of 60 cd/m² was placed around the monitor to provide a constant level of light adaptation. The luminance was measured with a photometer (LS-100; Minolta, Tokyo, Japan). The display area measured 30.3° horizontally and 28.5° vertically at a viewing distance of 57 cm.

4.2.2 Stimuli

The stimuli were vertical cosine gratings of at least four cycles in width with a circular vignette envelope. Contrast thresholds were measured for spatial frequencies of 0.26, 0.58, 1.11, 2.17, 4.29, and 8.53 cpd. The viewing distance for 4.29 cpd and lower was 57 cm,

and for 8.53 cpd it was 114 cm. The duration of the stimulus was 1.053 seconds, and the interstimulus interval was 583 ms.

For suprathreshold contrast matching, two horizontally separated gratings were presented. The standard grating, with a fixed spatial frequency of 0.58 cpd, was on the right of the display screen and was presented at seven contrast levels: 1.7%, 3.6%, 7.2%, 13.7%, 27.9%, 41.5%, and 55.9%. The test grating, with varying spatial frequency of 0.26, 0.58, 1.11, 2.17, 4.29, or 8.53 cpd, was presented on the left.

4.2.3 Subjects

Subjects with normal vision or maculopathy were recruited from the Optometry Clinic at the School of Optometry, University of Waterloo, and the Canadian National Institute for the Blind (CNIB). Given that our previous findings (Mei & Leat, 2007a) showed no main effect of age for suprathreshold contrast matching and most of the maculopathy subjects (30 of 36) were older than 50 years, one control group was used in this study (15 subjects aged 50 and older). There were three groups of subjects with maculopathy (13 subjects with atrophic ARMD, 14 with exudative ARMD, and 8 with JMD). Average ages of the groups were as follows: control group, 70 ± 11 years; atrophic ARMD group, 81 ± 5 years; exudative ARMD group, 81 ± 8 years; and JMD group, 47 ± 14 years. All subjects gave written informed consent for participation in the study, which was approved by the Office of Research Ethics at the University of Waterloo. All subjects were treated in accordance with the Declaration of Helsinki.

4.2.4 Procedure

Subjects' refractive errors were checked by subjective refraction. If there was no improvement in visual acuity, they wore their spectacles plus a working distance correction. If there was a significant change, the refractive correction, plus a working distance lens, was worn in a trial frame. Monocular visual acuity of the preferred eye was measured with the University of Waterloo logMAR chart (Strong & Woo, 1985). Five minutes of light adaptation was allowed beforehand. For contrast threshold measurement, a temporal two-alternative forced-choice (2-AFC) staircase method was used.

For suprathreshold contrast matching, a method of adjustment, under experimenter control, was used. Subjects, looking freely between the standard and the test grating with the preferred eye, compared the contrast between the standard grating (0.58 cpd) and the test grating (with varying spatial frequency) and told the experimenter to increase or decrease the contrast of the test grating to match the contrast of the standard grating. To minimize any pattern adaptation, subjects were instructed not to look at the standard grating for too long (Blakemore, Muncey, & Ridley, 1971). Subjects with maculopathy were allowed to use their natural PRL.

The number of contrast matches each subject could make was limited because of fatigue and level of vision; for instance, some subjects could not detect the lowest contrasts at some spatial frequencies to make a match. Therefore, the aim was to complete matching across all spatial frequencies at 3.6% and 27.9% contrast so as to get as full a data set as possible for these parameters and to undertake as many other contrast matches as possible for

the other contrast levels, including the highest spatial frequency and the lowest contrast that each subject could detect. Only a few subjects could undertake matches for 8.53 cpd (1 at 3.6%, and 5 at 27.9%); therefore, 8.53 cpd was not included in the ANOVA statistical analysis for the contrast matching.

Statistical Analysis

ANOVA in Systat was used to analyze the contrast thresholds for 0.26 to 8.53 cpd and the contrast matching (3.6% and 27.9%) for 0.26 to 4.29 cpd. Given that some data were missing for both contrast thresholds and contrast matches, we assumed sphericity and repeated the ANOVAs according to Winer (1962), a method that uses all the data. To analyze the slopes of the contrast-matching curves, all data that were available for each subject were included.

4.3 Results

ANOVA showed an age difference between the ARMD group and the control group ($F = 19.53$; $P < 0.01$). This occurred because it was difficult to recruit subjects with normal vision according to our criteria (no age-related maculopathy [ARM], no cataract within the pupil area, no diabetes, good general health) of the same age as some of the older subjects with ARMD. Average VAs were logMAR -0.03 ± 0.10 for control subjects, 0.88 ± 0.09 for atrophic ARMD, 1.06 ± 0.04 for exudative ARMD, and 1.06 ± 0.05 for JMD. ANOVA showed there was no significant difference in VA among the three maculopathy groups ($F = 2.05$; $P = 0.146$).

First, the contrast threshold results are considered. Figure 4-1 shows the individual contrast thresholds of the three groups and the 95% range of the control subjects. As expected, most subjects with maculopathy showed some deficit of contrast sensitivity, especially at high spatial frequencies. To compare the performance of the three maculopathy groups, mixed ANOVA (three maculopathy groups/six spatial frequencies) was applied. There was no effect of diagnosis ($F = 0.43$; $P = 0.658$) and no interaction between spatial frequency and diagnosis ($F = 2.074$; $P = 0.102$). Because the three groups showed similar contrast sensitivity, they were pooled for comparison with the normal control data. Mixed ANOVA (two groups/six spatial frequencies) confirmed a difference between the normal control and the group with maculopathy ($F = 182.26$; $P < 0.001$).

Examples of contrast thresholds and full suprathreshold contrast matching for three subjects (one each with atrophic ARMD, exudative ARMD, and JMD) who finished all contrast matches with a full range of contrasts and spatial frequencies are shown in Figure 4-2. Matching curves for medium and higher contrast levels show increasing flatness demonstrating contrast constancy.

Contrast matching of 3.6% and 27.9% for all subjects is shown in Figure 4-3, together with the 95% range of normal. Fifty of 175 data points were missing at 3.6%, and 10 of 175 at 27.9%. To compare the performance of the three maculopathy groups, mixed ANOVA (three groups/five spatial frequencies/two contrast levels [excluding contrast threshold]) was undertaken but showed no main effect of diagnosis ($F = 0.891$; $P = 0.431$) and no higher interactions based on diagnosis.

Given that no effect of diagnosis was found, the three groups were pooled into one larger maculopathy group for final analysis. Mixed ANOVA (two groups/five spatial frequencies/two contrast levels [excluding contrast threshold]) showed a main effect of the presence of maculopathy ($F = 49.34$; $P < 0.001$) and main effects of contrast ($F = 4500$; $P < 0.001$) and spatial frequency ($F = 76.30$; $P < 0.001$). Interactions occurred between contrast and group ($F = 16.81$; $P < 0.001$), spatial frequency and group ($F = 23.15$; $P < 0.001$), contrast and spatial frequency ($F = 23.7$; $P < 0.001$), and group, contrast, and spatial frequency ($F = 11.70$; $P < 0.001$).

Interactions occurred between macular health and spatial frequency and between macular health and contrast that were explored further by post hoc mixed ANOVAs with respect to spatial frequency and contrast. Mixed ANOVA at each contrast level showed effects of macular health at both 3.6% ($F = 45.64$; $P < 0.001$) and 27.9% ($F = 17.86$; $P < 0.001$), which indicates that maculopathy affects suprathreshold contrast perception at low and medium contrast levels. Interactions occurred between macular health and spatial frequency at both contrast levels (both $P < 0.001$). All our ANOVA results were confirmed with those determined by the method according to Winer (1962).

Post hoc *t*-tests with Bonferroni correction (the new *P* value for significance is $0.05/5 = 0.01$, treating each ANOVA as a separate group of *t*-tests) showed an effect of macular health at 3.6% and 27.9% at spatial frequencies of 1.11 cpd and higher ($P < 0.01$). Thus, at higher spatial frequencies, subjects with maculopathy needed higher contrast than did controls to make a match. At higher contrasts, however, contrast-matching curves become flatter and more data points were within the normal range (Fig. 4-3).

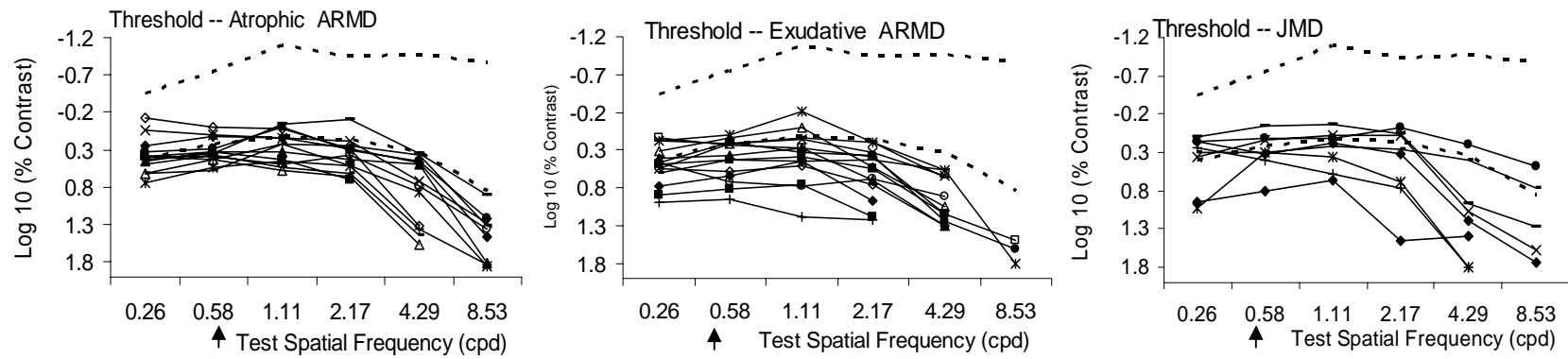


Figure 4-1. Contrast thresholds for the three diagnostic groups compared with the 95% normal range ($1.96 \times SD$, dashed lines). The solid curves represent the contrast thresholds of individual subjects with maculopathy. The arrows show the spatial frequency of the standard grating.

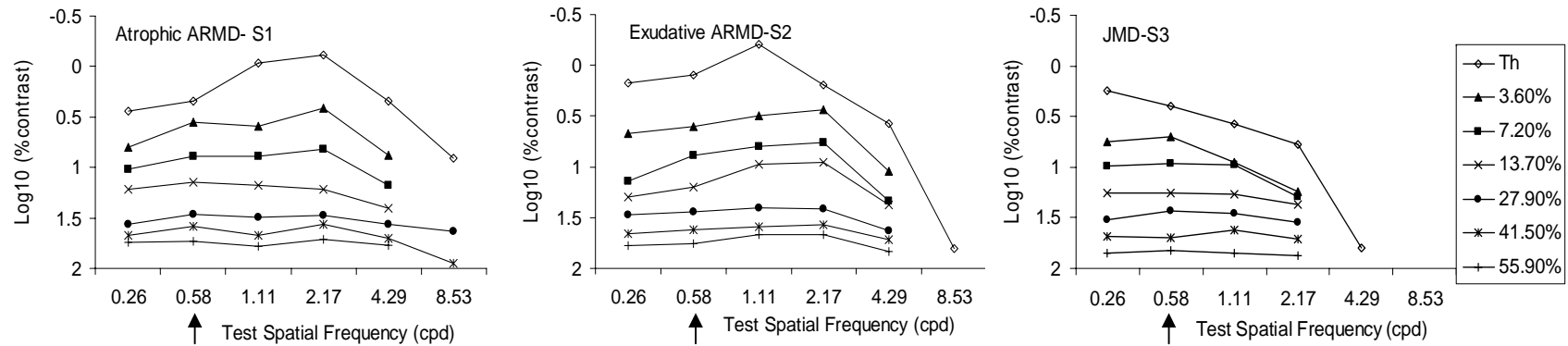


Figure 4-2. Contrast threshold and supra-threshold contrast matching curves for three subjects with atrophic ARMD, exudative ARMD, and JMD respectively. The top curve represents the contrast threshold. The lower curves represent the contrast matching curves at six contrast levels. All of them could not match 1.7% contrast and S2 and S3 could not match certain contrast levels at 4 and 8 cpd. The arrows show the spatial frequency of the standard grating.

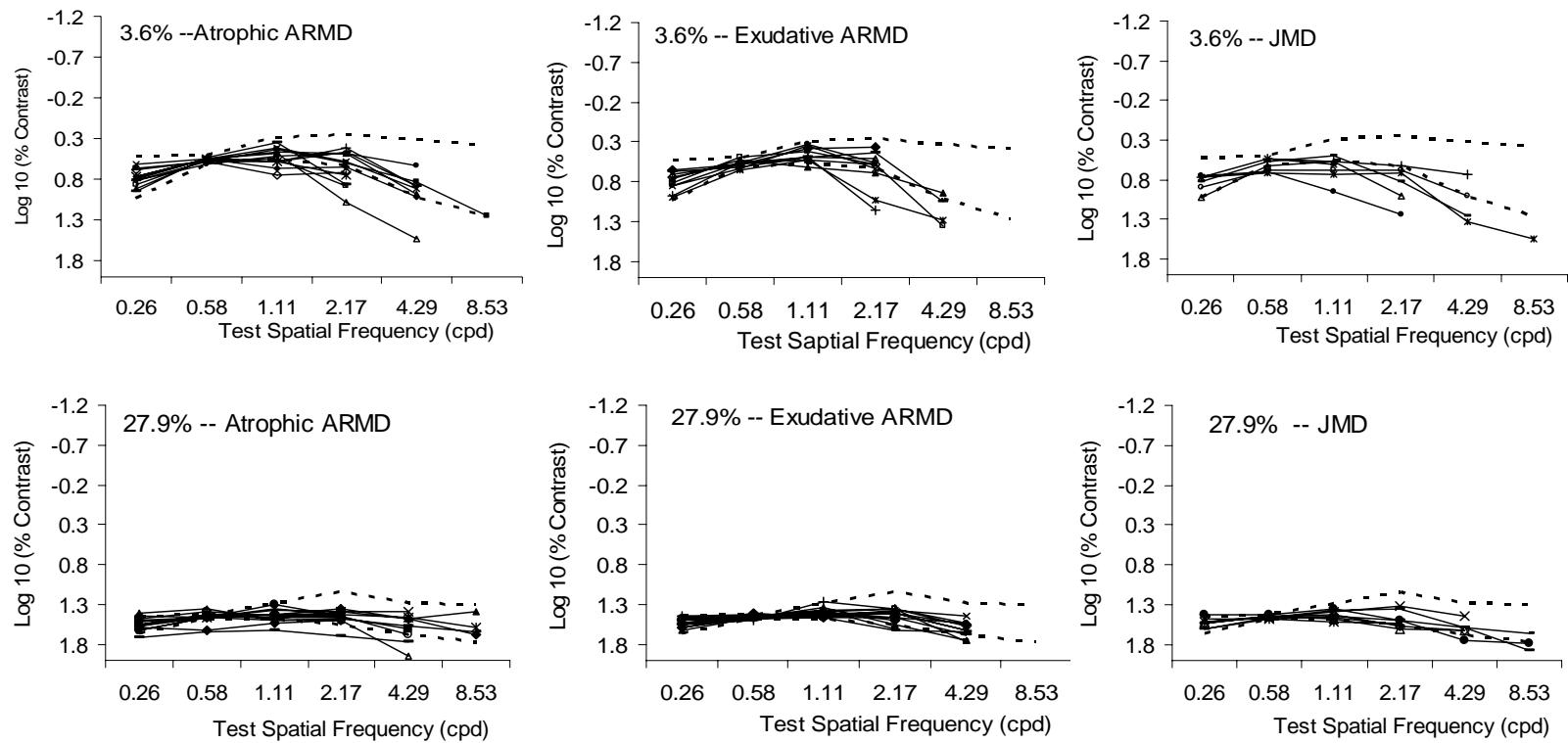


Figure 4-3. Contrast matching at 3.6% and 27.9% for three groups. The dashed line curves represent the 95% confidence limits of normal older control subjects (1.96 x SD). The solid curves represent the contrast matches of individual subjects with maculopathy. The arrows show the spatial frequency of the standard grating.

To analyze the gain of matched contrasts against reference contrast, the data were plotted as the matched contrast against the test contrast at each spatial frequency (Georgeson & Sullivan, 1975) for subjects who were able to complete the contrast matching at a range of contrasts (four or more) at each spatial frequency. The numbers of these subjects for each spatial frequency are shown in Table 4-1. If contrast matching were perfect, all the contrast-matching data points would lie along the diagonal line for equal contrast. Figure 4-4 shows some examples of this analysis. Generally speaking, the regression slopes of subjects with maculopathy showed larger variability than did those of the control subjects. Some of the contrast-matching points fell out of the 95% confidence limits of control group. At the higher spatial frequencies, there were more contrast matches outside the normal range. Regression lines were calculated for each subject, and the average slopes of each spatial frequency and the 95% confidence limits are shown in Table 4-1. Regression lines for 0.58 and 1.11 cpd were along the diagonal line; those for 0.26, 2.17 and 4.29 cpd were above the diagonal, with a tendency to flatter slopes. Between the slopes of the control and the maculopathy group, *t*-tests showed significant differences at 1.11 cpd ($P = 0.001$), 2.17 cpd ($P = 0.001$), and 4.29 cpd ($P < 0.001$). It was not possible to analyze the 8.53 cpd data in this way because data were missing for many subjects.

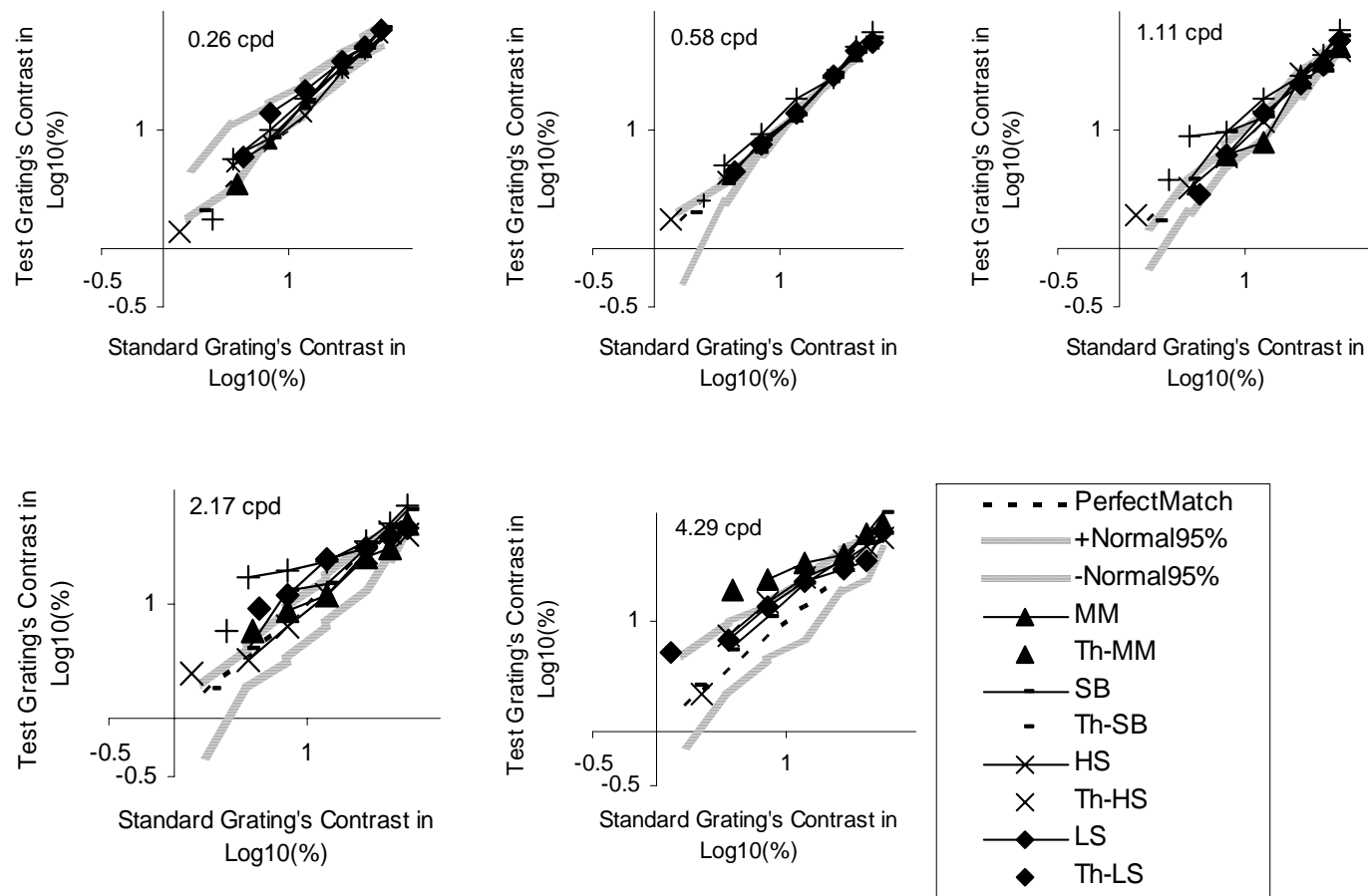


Figure 4-4. Examples of matched contrast against test contrast in log unit. The dashed diagonal line represents perfect matching with a slope of 1. The two heavy shadowed lines represent the 95% range of normal. Lines connecting different symbols represent the contrast matching of different subjects. The isolated symbols represent thresholds of those subjects.

Table 4-1. Means and 95% range for slopes of contrast matching regression lines for subjects with maculopathy and control subjects.

Spatial Frequency(cpd)		Mean Slope	95% -	95% +
0.26 cpd	Maculopathy (n = 18)	0.837	0.795	0.880
	Control (n = 15)	0.877	0.839	0.915
0.58 cpd	Maculopathy (n = 17)	0.986	0.966	1.005
	Control (n = 15)	0.993	0.982	1.003
1.11 cpd	Maculopathy (n = 17)	1.012	0.978	1.046
	Control (n = 15)	1.104	1.074	1.134
2.17 cpd	Maculopathy (n = 17)	0.900	0.821	0.978
	Control (n = 15)	1.071	1.027	1.116
4.29 cpd	Maculopathy (n = 10)	0.739	0.658	0.820
	Control (n = 15)	0.946	0.885	1.008

4.4 Discussion

4.4.1 Contrast threshold

Our results showed that contrast thresholds in subjects with maculopathy were significantly higher than in the 95% range of age-matched control subjects, which is in agreement with previous findings (Bellmann et al., 2003; Brown & Lovie-Kitchin, 1989; Loshin & White, 1984; Owsley, et al., 2001), and that this deficit of contrast sensitivity increased with increasing spatial frequency. Our results also showed that the average contrast threshold was abnormal at all spatial frequencies tested, which is also in agreement with former studies (Loshin & White, 1984; Sjostrand & Frisen, 1977; Wolkstein, Atkin, & Bodis-Wollner, 1980). In all three groups of subjects with maculopathy, the peak of the CSF

shifts to lower spatial frequencies, to around 0.58 cpd, compared with 1.11 cpd in control subjects. This shift can probably be attributed to two causes: eccentric fixation and photoreceptor dysfunction.

4.4.2 Supra-threshold contrast matching

The first finding of this study is that, for subjects with maculopathy who were able to undertake contrast matching at all contrast levels (examples shown in Figure 4-2), the suprathreshold contrast-matching results plotted across contrast levels appear similar to previous findings in subjects with normal vision (Georgeson & Sullivan, 1975; Peli et al., 1991; Nasanen et al., 1998). At low contrasts, the matching curves resembled the threshold curve, whereas at medium and higher levels, the curves became flatter, demonstrating contrast constancy. All the maculopathy subjects performed contrast matching at 3.6% and 27.9% (shown in Figure 4-3), and the matching curves at higher contrast were flatter than those at lower contrast, again demonstrating some degree of contrast constancy. Thus, observers with maculopathy performed similarly to subjects with other visual disorders (Dickinson & Abadi, 1992; Hess & Bradley, 1980; Medjbeur & Tulunay-Keesey, 1986). This is particularly interesting because these studies included subjects in whom the disorder was located at the retinal level (maculopathy and albinism), the optic nerve (demyelinating disease), the cortical level (amblyopia), and the motor centers of the brain (congenital nystagmus).

However, there were differences between the control and the maculopathy groups at both levels of contrast. Thus, our results are also in agreement with those of a previous study

(Leat & Millodot, 1990), showing deficits of suprathreshold contrast perception in subjects with maculopathy. As in this previous study, these deficits were not as great as the deficits in contrast threshold; there is some compensation for contrast sensitivity loss. As with contrast threshold, the peaks of the contrast-matching curves shifted to lower spatial frequencies compared with those of the control group. As with the contrast threshold differences, this shift could be attributed to two factors: the attenuation of medium and high spatial frequencies resulting from normal neural changes with eccentricity and the dysfunction of photoreceptors resulting from maculopathy (Swanson & Wilson, 1985; Rempt, Hoogerheide, & Hoogenboom, 1976). A few studies have compared visual function at a given eccentricity between people with ARMD and normal vision and show a loss of function compared with healthy eccentric retina (Brown & Lovie-Kitchin, 1989; Sunness et al., 1985).

As in normal vision, there is a connection between contrast threshold and suprathreshold contrast perception, though these two mechanisms are probably different. Figure 4-4 and Table 4-1 show the regression slopes of contrast matching at each spatial frequency compared with the 95% normal ranges, indicating that the threshold differences between the test and the standard spatial frequency determined the position of the regression line relative to the diagonal line. Most subjects with maculopathy had highest contrast sensitivity for spatial frequencies of 0.58 and 1.11 cpd. Correspondingly, the regression line slopes of 0.58 and 1.11 cpd were close to the diagonal, and the other spatial frequencies of 0.26, 2.17, and 4.29 cpd were above the diagonal line and had flatter slopes. These slopes were also significantly different from those of the controls, and these differences were in the direction expected to compensate for differences in thresholds. These findings are in

agreement with previous studies suggesting neural compensation by means of a change in gain (Dickinson & Abadi, 1992; Hess & Bradley, 1980; Leat & Millodot, 1990).

Alternatively, the results may be explained according to the model of Brady and Field (1995).

Accordingly, maculopathy would result in an increase in noise that would result in an increase in threshold, but suprathreshold performance, which depends on average signals rather than the signal-to-noise ratio, would be affected to a lesser extent or not at all. With this model there would be no need to suggest a change in gain. In fact, the partial-contrast constancy might indicate some deficit in gain.

Given that observers with advanced maculopathy use a PRL for fixation, some discussion of the performance of eccentric retina is in order. At eccentric retinal locations, visually normal observers show overconstancy (Georgeson & Sullivan, 1975), a trend to overestimate the test gratings' contrast at higher spatial frequencies (>3 cpd), especially at low contrasts. Observers with maculopathy, matching with a PRL (shown in Figure 4-3), did not show this trend but, rather, underestimated test grating contrast at higher spatial frequencies (>0.58 cpd). In other words, they have partial-contrast constancy. There are two possible ways to explain this. First, the PRL functions as a new "fovea," losing the normal overconstancy of eccentric vision but utilizing adjustment of the gain to compensate for the loss of CS caused by the disease process. Second, the PRL still functions as eccentric retina with contrast overconstancy, which in itself partially tends to compensate for loss of CS resulting from the disease process. The present data are not able to distinguish between these two situations.

Studies of suprathreshold contrast perception may give information that is more relevant to daily function than contrast sensitivity. This study has shown a suprathreshold contrast perception defect in maculopathy compared with normal, though this deficit is not as great as that for CS. Thus, we would conclude that the actual performance of people with ARMD may not be as poor as CS predicts. Whether this is found to be true is a matter for future research.

4.5 Conclusions

We have shown that a degree of contrast constancy is apparent in subjects with maculopathy, though deficits persist compared with control subjects. No significant difference was observed among three groups of subjects with maculopathy in suprathreshold contrast matching. Evidence indicates that either the gain of the visual system adjusts to compensate for CS losses (though incompletely) or that contrast overconstancy, as in normal peripheral vision, helps to compensate for the CS loss. A third possibility is that maculopathy results in an increase of noise in the visual system that affects threshold, but not suprathreshold, performance.

4.6 Acknowledgement

This research was supported by The Macular Disease Society (Andover, Hampshire, UK).

Chapter 5

Can Spatial Frequency Analysis Distinguish Image Categories?

5.1 Introduction

In order to understand how the human brain performs complex cognitive tasks it is necessary to understand the neural activities triggered by various visual stimuli. In recent years, recognition of single faces, one of the most important skills in daily life, has aroused interest among visual scientists. Neuroimaging studies in humans have found that the fusiform gyrus and the superior temporal sulcus selectively respond to face images (Allison, et al., 1999; Grill-Spector, & Malach, 2004; Haxby, et al., 1994; Kanwisher, et al., 1997; Loffler, et al., 2005; Puce, et al., 1995; Sergent, et al., 1992). Further studies suggest that the superior temporal sulcus is more concerned with the details of facial structure than the fusiform gyrus (Allison, et al., 2000; Andrews, Schluppeck, et al., 2002; Haxby, et al., 2000). Studies of the visual cortex have found areas selective for objects other than faces in the parahippocampal gyrus (Epstein & Kanwisher, 1998; Ishai, et al, 1999; Kanwisher et al., 1997) and the lateral occipital lobe (Grill-Spector, et al., 1999; Malach, et al., 1995). It is suggested that the visual cortex analyzes non-face objects in a more parts-based way than it does for face objects (Ishai, et al., 2000). This is possibly because there are more variable parts in spatial arrangements for non-face objects, while each single face only has five organs located in various spatial ratios. Thus, several lines of research have suggested that face recognition is unique in humans and have stressed the importance of global configuration of

faces compared to other kinds of objects (Farah, et al., 1998; Wang, et al., 1998, Hasson, et al., 2001).

Neuroimaging studies have also described a different activation pattern associated with specific images other than faces. These images include scenes/buildings (Haxby, et al., 1999; Kanwisher et al., 1997), chairs (Ishai et al., 1999; Aguirre, et al., 1998; Epstein & Kanwisher, 1998), letters (Polk & Farah, 1998; Puce, et al., 1996), animals and tools (Chao, et al., 1999; Martin, et al., 1996), and hands (Puce, et al., 1999). These findings have led to the interpretation that the ventral temporal cortex contains anatomically segregated modules that are category-specific although not as specific as the regions responsive to faces (Puce et al., 1999; Aguirre et al., 1998; Kanwisher et al., 1997; Allison, et al., 1994). Alternatively, Ishai et al. (2000) proposed that the visual cortex areas responding to non-face objects are not highly selective to a certain object (such as a red iron chair) but to object form category (such as the shape of chair no matter what specific kind of chair it is). Besides, each cortical region mainly responds to one category of non-face object, but will give weaker responses to other categories of non-face objects (Chao, et al., 1999; Haxby, et al., 2001).

Since it appears that some different regions of the visual cortex respond to specific images, it is interesting to determine whether there are differences in the characteristics of these stimuli that trigger these different visual responses. Additionally, if image processing is to be applied to images which will be viewed by human observers, it is useful to be able to classify images according to their characteristics. Spatial frequency amplitude spectra and the corresponding slope of amplitude versus spatial frequency are two parameters which may describe image physical characteristics. To date, most of the studies of amplitude spectra and

slopes have concentrated on natural scenes, i.e. scenes with no human-made content (Burton, et al., 1986; Field, 1987; van Hateren & van der Schaaf, 1998; Ruderman & Bialek, 1994; Tolhurst, et al., 1992; van der Schaaf & van Hateren, 1996). The visual system is believed to have evolved and developed to adapt to the natural environment. It has been known for some time that although the apparent complexity of natural images is high, natural images have a characteristic Fourier spectrum: Amplitude (f) = $cf^{-\beta}$, where c is a constant and f is spatial frequency. The average β value of all orientations varies from 0.7 to 1.5 in achromatic images (Burton, et al., 1986; Field, 1987; van Hateren & van der Schaaf, 1998; Ruderman & Bialek, 1994; Tolhurst, et al., 1992; van der Schaaf & van Hateren, 1996). Billock, et al., (2001) applied correlation analysis to the human contrast sensitivity function and found that cortical spatial frequency channels are well suited to analyzing the exponent of $f^{-\beta}$ images. Therefore, the characteristics of different images represented by $f^{-\beta}$ could be reflected in visual perception processing.

The amplitude spectrum of an image varies with orientation. Fourier analyses of natural scenes have shown that horizontal and vertical orientations contain more contrast than do the oblique orientations (Baddeley & Hancock, 1991; Coppola, et al., 1998; Keil & Cristobal, 2000; Switkes, et al., 1978; van der Schaaf & van Hateren, 1996). Using orientation-sensitive filters to process three groups of digital images (indoor scenes, outdoor scenes, and natural scenes), Coppola et al. (1998) also found a greater prevalence of contours near the cardinal axes. Contrary to the anisotropy (different sensitivities in different orientations) in perceiving simple stimuli (e.g. isolated grating patterns), Essock et al. (2003),

using images consisting of broadband spatial content (such as noise patch), showed that visual performance is best for image components at oblique orientations, worst for horizontal, and intermediate for vertical orientations. Several studies have shown that there are most neurons responding to the horizontal components of an image, fewer at the vertical, and fewest at oblique orientations (Essock et al, 2003, Hansen et al., 2003; Furmanski & Engel, 2000; Li, Peterson, & Freeman, 2003; Mansfield & Ronner, 1978). Essock et al. (2003) suggested that the visual cortex has the the largest perceptual response (gain) in oblique orientations and a smaller perceptual response (gain) in the horizontal and vertical orientations. In this paper they speculated that the consequence of this anisotropy would be to perceptually decrease the horizontal and vertical structure in a natural scene, thereby increasing the relative salience of other orientations. Torralba and Oliva (2003) studied the relationship between amplitude spectra and natural image categories. They found that simple image statistics such as amplitude spectra could be used to predict if one kind of object exists in a scene or not. We would deduce that images with similar content would show similar response characteristics in various orientations. We would also deduce that there might be different amplitude spectra and slopes among images of different objects and that there might be similarities in these two parameters within a category of images of similar objects, such as different styles of chairs or hands viewed from different angles. All of the neuroimaging studies described above were done with photographs of faces or objects presented either in blocks or as single images. However, in real life, usually the received images are much more varied than those used in these studies which tended to be either natural images or single

objects. Nevertheless, it is still anticipated that similar scenes share similarities in physical characteristics.

The current study was devised to answer two questions: First, can amplitude spectra and slope show differences in a wide range of image types to support the differentiated image perception in the visual cortex; i.e. can images be classified according to spatial frequency content? Second, where are the differences of amplitude spectrum and slope in orientations between image groups?

The ultimate application for this analysis is an attempt to categorise images into groups according to spatial frequency content for future study of digital image enhancement to improve visibility of images for people with visual impairment. Since the image processing is spatial frequency based, we would anticipate that images with similar spatial frequency content may be increased in visibility with similar processing.

5.2 Methods

5.2.1 Images

132 digital images were obtained either by a Cannon G2 4.0 mega pixel or by a Nikon 4300 4.0 mega pixel digital camera. The image size was 990×1250 pixels (height x width). All were filtered with a low-pass filter with a maximum half-height of 15 cycles per degree (cpd) based on a viewing distance of 57 cms (equivalent to 427.5 cycles per image). This was to optimize the images for the future study of people with visual impairment, so as to avoid unnecessarily enhancing high frequencies beyond the subject's acuity limit which would further compromise the dynamic range of an enhanced image (Peli, 1992; Leat, et al.,

2005). Fifteen cpd (equivalent to 6/12 Snellen acuity) is the maximum spatial frequency that would be perceived by this population if we define low vision as visual acuity $< 6/12$ (Leat et al., 1999). The images were categorized into six groups according to the apparent subject matter of the images: single face (21 images), one whole person (15 images), two or more whole persons (21 images), indoor scenes (17 images), natural scenes (20 images), and miscellaneous (38 images). The face images showed one single whole face in the center covering more than 4/5 of the vertical dimension of the image, with varying backgrounds. The one-person images showed a single whole person in the center with varying backgrounds. The two or more-person images showed at least two persons in whole or in part in the center with varying backgrounds. The indoor images showed typical house or office interiors i.e., mainly furniture, floor, staircases, walls and pictures etc. The natural scenes were all outdoor scenes without any human-made content. The miscellaneous group includes animals, plants, outdoor scenes which include human-made content e.g. street scenes.

5.2.2 Software

A MatLab image analysis tool programmed by the Systems Design Engineering Department, University of Waterloo was used. The MatLab 6P51 Work software was available in the lab of Dr. Susan Leat.

5.2.3 Analysis

The low-passed images were subjected to a 2-dimensional Fourier transform in Matlab and the amplitude spectrum was obtained in a logarithmic scale for the four orientations of 0° , 45° , 90° , and 135° (shown in Figure 5-1A) with respect to spatial frequency in a linear scale. Zero degrees correspond to the horizontal meridian and the others

are measured counter-clockwise from there. Note that spatial frequency components along the horizontal correspond to vertical contours or edges. The spatial frequency was in units of cycles per image relative to the image height. These amplitude spectra were retrieved to Excel files (shown in Figure 5-1B). Then the amplitude spectra for the four orientations versus spatial frequency were plotted as shown in Figure 5-1C. Plotting the log of the amplitude spectrum against the log of the spatial frequency turned the amplitude spectrum plot into straight lines (Burton et al., 1987; Field, 1987; van Hateren and van der Schaaf, 1998; Ruderman and Bialek, 1994; Tolhurst et al., 1992; van der Schaaf and van Hateren, 1996). The slopes of the corresponding regression lines were calculated.

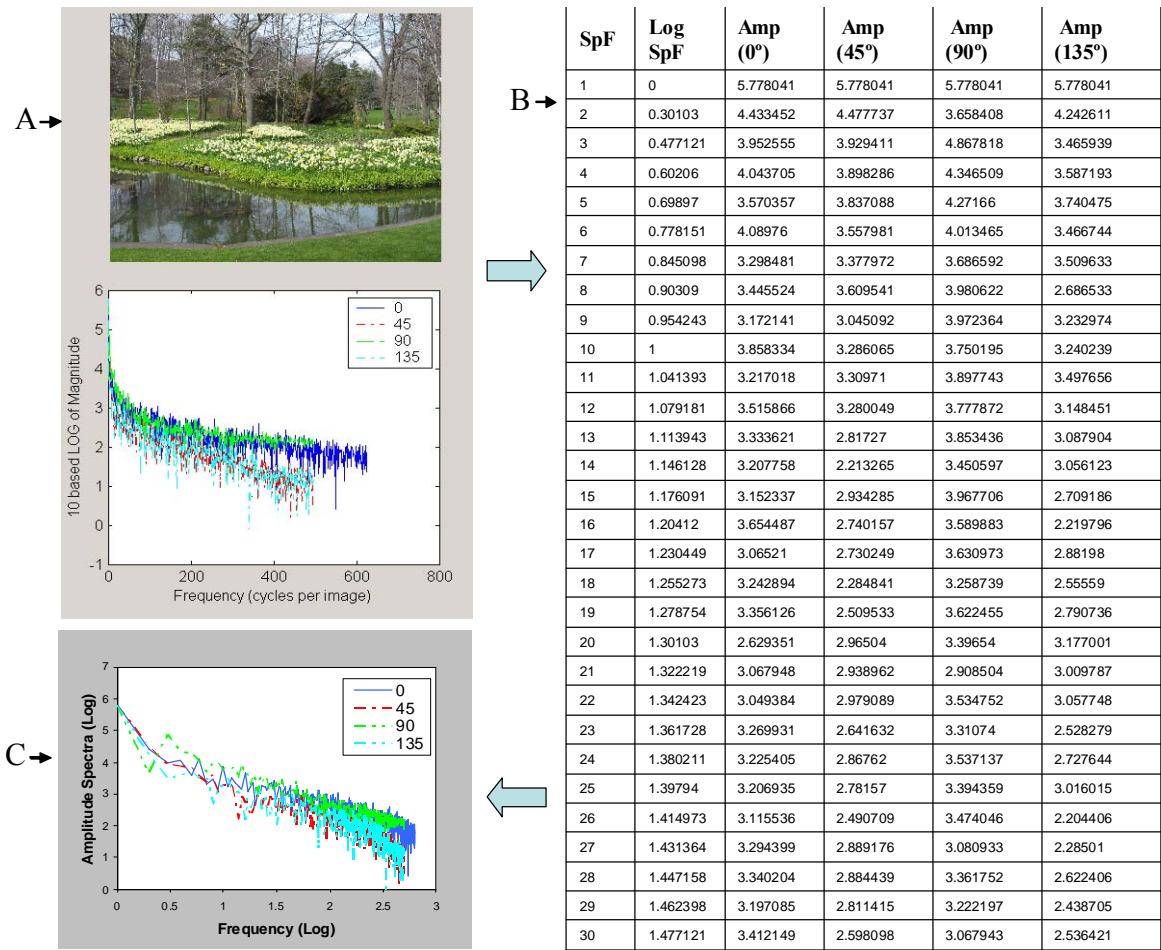


Figure 5-1. An example of image analysis. A. Original image and plot with amplitude spectrum (log) versus spatial frequency (cycles per image) in a linear scale at the four orientations of 0°, 45°, 90°, and 135°, where 0° corresponds to the horizontal meridian and the others are measured counter-clockwise from there. B Part of the values of amplitude spectrum at each spatial frequency at the four orientations retrieved from A. C. Log of the amplitude spectrum plotted versus log spatial frequency.

Figure 5-2 shows that amplitude spectra of the two oblique directions are considerably superimposed. This was true for all the images that were analyzed. Therefore

the values of amplitude and spectra of these two orientations were averaged to give one spectrum for oblique orientations.

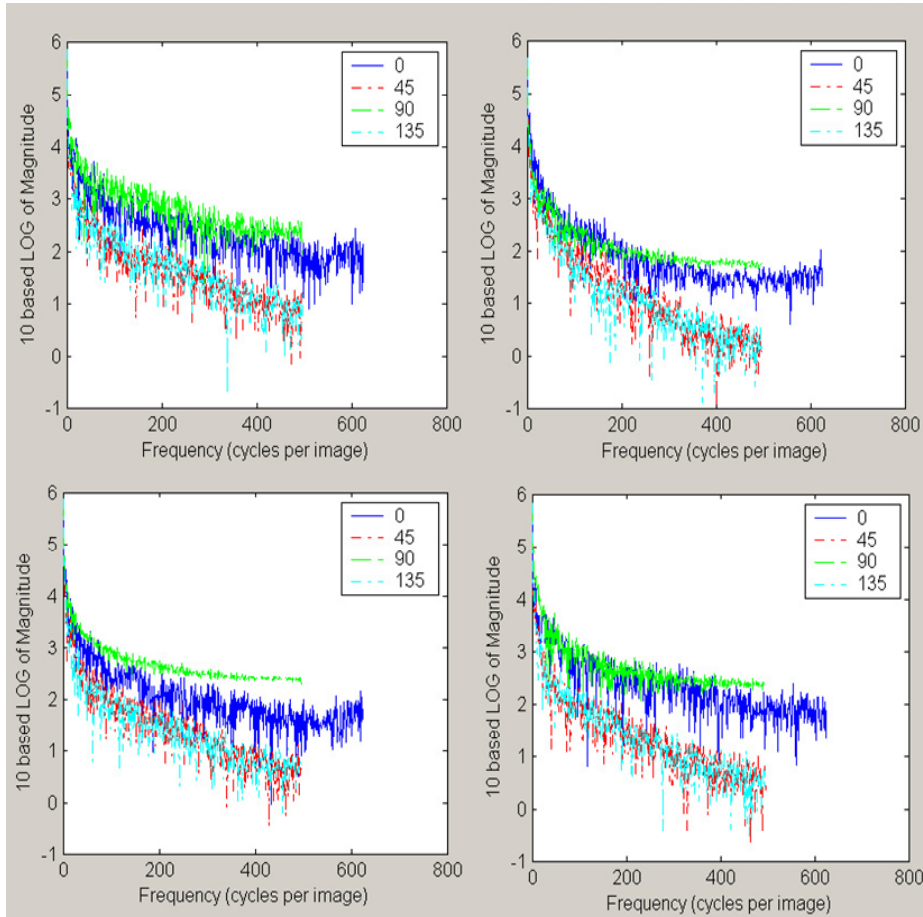


Figure 5-2. Examples of amplitude spectra plots for four images showing the four orientations of 0°, 45°, 90°, and 135°. The two oblique orientations are superimposed and are lower in amplitude than the vertical and horizontal.

5.3 Results

The average amplitude versus slope of the 132 images (average of three orientations) is plotted in Figure 5-3A. Since the horizontal dimension of the images was greater than the

vertical, this limited the highest spatial frequencies measured in the vertical direction. The graph of amplitude versus slope for all meridians was truncated at the maximum value for the vertical meridian, so as to be able to compare the average amplitudes. It can be seen that there is a continuous distribution of data and no obvious clusters are formed. When each category of image is shown differently, as in Figure 5-3B, it can be seen that face images seem to make a separate cluster, distinct from other groups of images, being located superior and left of the plot. The other images all seem to cluster together, although there may be a slight tendency for the natural scene images to be located superior and right in the plot and for indoor images to be located inferiorly. Other groups of images are all overlapping and grouped together. The amplitude and slope in three separate orientations and the averages for all three orientations of six groups of images are shown in Table 5-1.

Analysis of amplitude with mixed ANOVA (6 image categories x 3 orientations) shows that there are differences among the six groups of images ($p < 0.001$) and among the different orientations ($p < 0.001$). There was an interaction between orientation and image group ($p = 0.003$). Similar analysis for the slope also showed an effect of group ($p = 0.001$) and orientation ($p < 0.001$) but no interaction ($p > 0.05$). Significant differences between image groups from post-hoc analyses (Bonferroni) are shown in Table 5-2A. Face images show the most frequent differences from other types of images, having a significant difference in at least one orientation compared to all other image types except one-person images. For slope (Table 5-2A) there are fewer differences, with natural images tending to be different from the other groups. Post-hoc analysis for differences in orientation for amplitude and slope showed significant differences ($p < 0.001$) among all the orientations.

One-way ANOVA was also performed on the average of the three orientations for amplitude (6 groups) and slope. There were significant effects of group in both cases (for amplitude $p < 0.001$ and for slope $p = 0.001$). The Bonferroni post-hoc analyses are shown in Table 5-2B. The amplitudes of face images are different from all other images types and the slopes of the natural images are more consistently different from other types of images than any other category. Indoor images show some differences of either slope or amplitude from other types (Table 5-2 A and B). Thus, looking at these results as a whole, it seems that faces, natural scenes and indoor images tend to be different from some other categories in either slope or amplitude.

Considering the results shown in Table 5-1 and the average of the three orientations, the amplitude varies from 1.8 to 2.15 with face images having the smallest amplitude and miscellaneous images the largest. As for the standard deviation of the averaged orientations, indoor images show the smallest variability and one-person images the largest. Considering the amplitudes in the separate orientations, all six groups of images show a similar trend: vertical amplitude > horizontal > oblique, with the exception of the indoor images which show little difference between the horizontal and vertical. The face images show the smallest amplitude in all three separate and the average orientations.

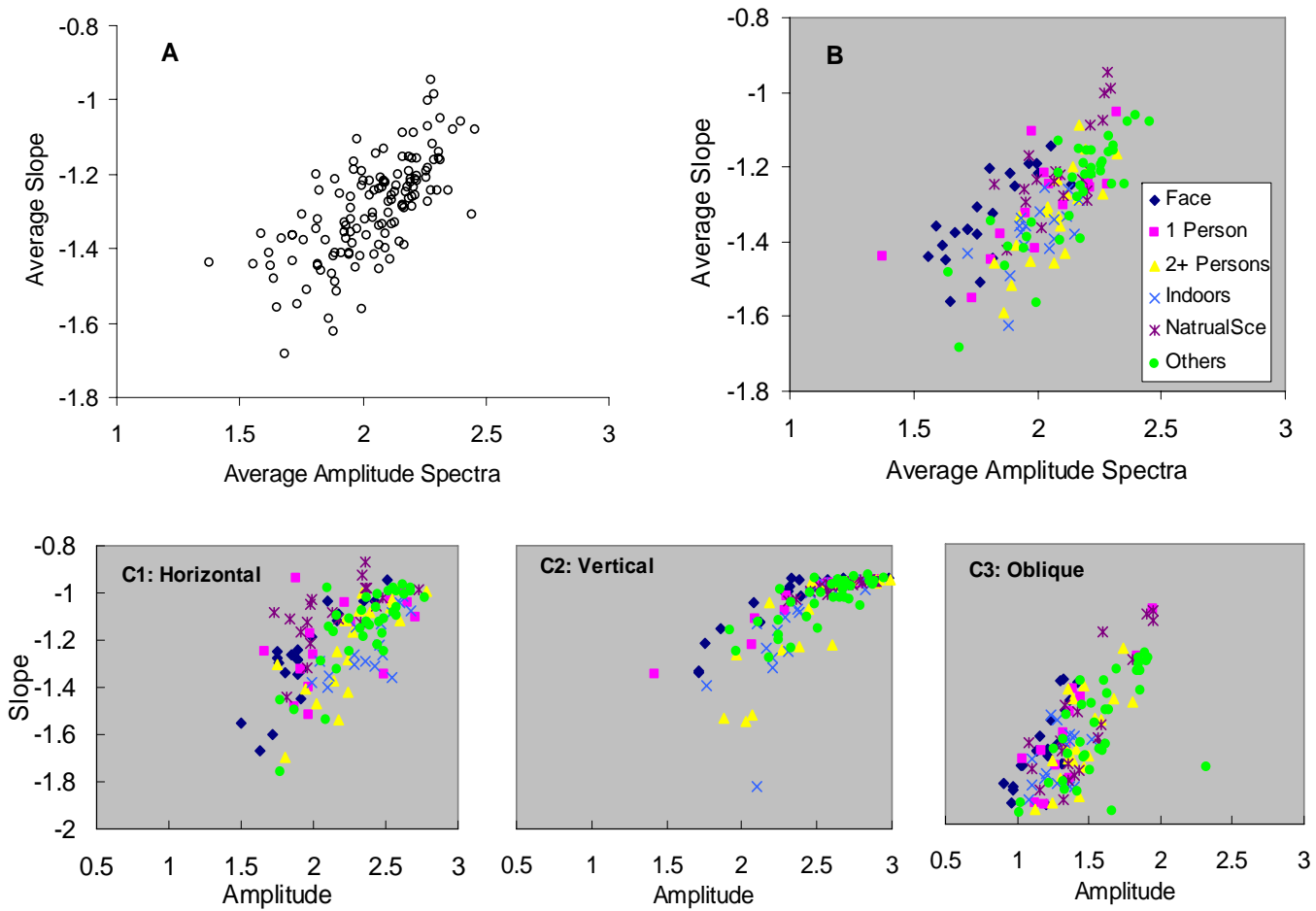


Figure 5-3. Plots of slope versus amplitude for all images. A. All data showing a continuous range without obvious clusters. B. Data split into the six categories of images. C1-Horizontal, C2-Vertical, C3-Oblique orientations, according to image category.

Table 5-1. Average amplitude and slope \pm one standard deviation for the six groups of images in the three orientations and the average of three orientations.

<i>Amplitude</i>	<i>Horizontal</i>	<i>Vertical</i>	<i>Oblique</i>	<i>Average</i>
Face	1.95 \pm 0.26	2.30 \pm 0.34	1.16 \pm 0.17	1.80 \pm 0.16
1 Person	2.18 \pm 0.34	2.49 \pm 0.40	1.32 \pm 0.28	2.00 \pm 0.24
2+ Persons	2.27 \pm 0.26	2.53 \pm 0.35	1.42 \pm 0.19	2.07 \pm 0.13
Indoor	2.37 \pm 0.21	2.35 \pm 0.28	1.27 \pm 0.13	2.00 \pm 0.12
Natural	2.16 \pm 0.27	2.67 \pm 0.17	1.48 \pm 0.26	2.10 \pm 0.19
Miscellaneous	2.36 \pm 0.24	2.54 \pm 0.26	1.55 \pm 0.27	2.15 \pm 0.19
<i>Slope</i>	<i>Horizontal</i>	<i>Vertical</i>	<i>Oblique</i>	<i>Average</i>
Face	-1.26 \pm 0.19	-1.04 \pm 0.13	-1.68 \pm 0.19	-1.33 \pm 0.12
1 Person	-1.20 \pm 0.18	-1.02 \pm 0.12	-1.66 \pm 0.28	-1.30 \pm 0.13
2+ Persons	-1.22 \pm 0.20	-1.10 \pm 0.21	-1.66 \pm 0.21	-1.33 \pm 0.13
Indoor	-1.23 \pm 0.12	-1.16 \pm 0.22	-1.74 \pm 0.15	-1.37 \pm 0.09
Natural	-1.07 \pm 0.15	-0.97 \pm 0.03	-1.56 \pm 0.26	-1.20 \pm 0.12
Miscellaneous	-1.15 \pm 0.17	-1.03 \pm 0.10	-1.61 \pm 0.24	-1.27 \pm 0.14

Table 5-2. Post-hoc Bonferroni analysis of ANOVA for amplitude and slope for separate orientations and averaged across orientations.

<i>A: Separate amplitude and slope in each of three orientations</i>		
Amplitude-Horizontal	Amplitude-Vertical	Amplitude-Oblique
Face vs. 2+Persons, $p = 0.002$	Face vs. Natural, $p = 0.002$	Face vs. 2+Persons, $p = 0.006$
Face vs. Indoor, $p < 0.001$	Face vs. Miscellaneous, $p = 0.047$	Face vs. Naturals, $p < 0.001$
Face vs. Miscellaneous, $p < 0.001$	Indoor vs. Natural, $p = 0.025$	Face vs. Miscellaneous, $p < 0.001$
		Indoor vs. Miscellaneous, $p = 0.001$
		1 Person vs. Miscellaneous, $p = 0.022$
Slope-Horizontal	Slope-Vertical	Slope-Oblique
Natural vs. Face, $p = 0.006$	Natural vs. Indoor, $p = 0.002$	
<i>B: Average amplitude and slope</i>		
Amplitude	Slope	
Face vs. 1 Person, $p = 0.013$	Natural vs. Face, $p = 0.018$	
Face vs. 2+Persons, $p < 0.001$		
Face vs. Indoor, $p = 0.008$	Natural vs. Indoor, $p = 0.001$	
Face vs. Natural, $p < 0.001$		
Face vs. Miscellaneous, $p < 0.001$	Natural vs. 2+Persons, $p = 0.027$	
Indoors vs. Miscellaneous, $p = 0.041$		

For the average slope of three orientations, the β value varies from 1.20 to 1.37 with the natural scene group being the shallowest and indoor the steepest. For slope in the separate orientations, all six groups of images show the same trend as the amplitude: vertical > horizontal > oblique. The natural scene group shows the shallowest slopes in all three orientations which suggest that there is relatively more high spatial frequency content in these images.

5.4 Discussion

Our visual cortex is highly differentiated to perceive specific images (such as single faces, chairs, buildings, etc). Correspondingly, it would be expected that there would be differentiation in the physical characteristics of images. The current study provides evidence that there are differences in some types of images. This finding is in agreement with Torralba and Oliva (2003) in that amplitude spectra can distinguish image characteristics of natural images. They did not include faces or scenes with human made content. The current study also extends an analysis of image characteristics from single objects (such as face, chair) to a wide range of image types, including everyday scenes. From Table 5-1 and 5-2 it can be seen that there are significant differences between some image groups in amplitude and slope. A study using computer simulation and psychophysical methods with city and beach scenes showed that the amplitude spectrum alone is sufficient to categorize the images (Guyader, et al., 2004). Our findings also demonstrate that amplitude spectrum is a good parameter to distinguish images according to spatial frequency content.

There are differences in amplitude and slope with respect to orientation. The present results show that, for most image groups, the amplitude is greater in the cardinal orientations than the oblique. This is consistent with former findings (Baddeley & Hancock, 1991; Coppola et al., 1998; Keil & Cristobal, 2000; Switkes et al., 1978; van der Schaaf & van Hateren, 1996). According to the anisotropy in visual perception for complex scenes (Essock et al., 2003), the horizontal has the least gain and the oblique the most in the order of oblique > vertical > horizontal. This is the reverse of the current finding of greater average amplitude for horizontal contours (vertical meridian) and least in the oblique orientation, which was found for almost all image types in this study. Thus, it would seem that the anisotropy of the visual system tends towards equalizing the anisotropy of real world images, resulting in a more equal perception of differently orientated contours.

For slopes, the current study found the same trend in all six groups of images: vertical > horizontal > oblique i.e. shallower in the vertical. This implies that there is relatively more high frequency content in the vertical meridian i.e., for horizontal contours. Again, the anisotropy of the visual system would tend to equalise these differences. Former studies on slopes with amplitude versus spatial frequency focused on natural images and found the average values of β were from 0.70 to 1.50. In the current study, we focused on a broader range of images that people encounter in daily life. The average β values (1.20 to 1.37) are within this published range for natural images, which suggests that all kinds of daily encountered scenery images could presumably be analysed with the same cortical neural machinery as natural scene images.

According to all the analyses of amplitudes and slopes among the six groups of images categorized in this study, three groups stand out as possibly different: single faces, indoors, and natural scenes.

Single face images

Single faces turn out to be the most consistently distinctive image type (according to spatial frequency content) among all six groups, with significantly lower average amplitudes than other groups of images. However, they are similar to other images in having the smallest slope in the vertical meridian thus having relatively more high spatial frequency information in the vertical meridian (horizontal contours). The physical uniqueness of single face images is consistent with the uniqueness of single face perception in the visual cortex (Farah et al., 1998; Ishai et al., 2000; Wang et al., 1998, Hasson, et al., 2001).

However, the images used in this study represent only one kind of face stimulus (straight on view and showing details of the face structure). Faces can be viewed from any angle and may be represented diagrammatically e.g. the Rubin vase-face illusion. This visual illusion can be perceived either as a vase or two faces which means that the same stimulus activates two different cortical perception centers. Two studies (Andrews et al., 2002; Hasson et al., 2001) showed that, when subjects perceived a face, there was higher activation in face-selective regions but, when the stimulus was perceived as a vase, there was more activity in the object-selective regions. This, again, gives more evidence for face-specific regions in the cortex. It has been found that the fusiform gyrus and the superior temporal sulcus (Allison et al., 1999; Grill-Spector et al., 2004; Haxby et al., 1994; Kanwisher et al., 1997; Loffler et al., 2005; Puce et al., 1995; Sergent et al.,

1992;) selectively respond to face images and that the superior temporal sulcus is more concerned with the details of facial structure (Haxby et al., 2000; Allison et al., 2000; Andrews et al., 2002). Therefore, it would be expected that single face images, such as used in this study, would stimulate the temporal sulcus face-selective region.

Indoor images

Indoor images show similar amplitudes in horizontal and vertical orientations. This is different from the other groups of images which showed bigger amplitudes in the vertical orientation (horizontal contours) than the horizontal. Therefore, indoors images have relatively larger amplitude in the horizontal orientation (vertical contours) compared to other images. This could be caused by the human-made vertical lines indoors such as the table legs and edges of walls.

Natural scenes

Natural scenes have moderate amplitudes but their main difference from other images is in their shallower slopes for all orientations (Table 5-1 and 2B). This suggests that there is relatively more high spatial frequency structure in all three orientations compared to other image types. The irregular content of natural scenes such as mountain edges, leaves, or clouds could explain this finding. Natural scenes also stand out with significantly shallower average slopes compared to single faces.

Future work

While the present analysis of the spatial frequency spectrum and slope reveals some capability to distinguish among image categories, it may be possible to extract more effective discriminating features from a more detailed analysis of the spatial frequency

spectrum. Specifically, a study of the amplitudes in the four orientations at different centre spatial frequency and bandwidths would comprise a multidimensional feature space within which statistical pattern recognition techniques could be used. Specifically we would determine the maximally discriminating sub-spaces for given image categories. The two-dimensional space used in this chapter is in fact a particular feature pair that could be extracted directly from the filter bank outputs.

5.5 Conclusions

This study demonstrated that the amplitude spectra and slope in three orientations can be used to describe the physical characteristics of images and to distinguish among different groups of images. We have shown that most everyday scenes have more spatial frequency power in the vertical and horizontal than oblique orientations. Single face images are the most unique images of those tested, having a lower amplitude spectrum. This may correspond to the fact that there is evidence that they are dealt with uniquely in the visual cortex. Natural scenes are special in having much shallower slopes indicating more high spatial frequency structures, and are most different in this respect compared to face images. Indoor images show less anisotropy compared to other images.

Chapter 6

The Perceived Visibility Enhancement in Maculopathy by Image Enhancement Techniques

6.1 Introduction

People with maculopathy lose central vision. Visual functions, such as visual acuity, visual field, contrast sensitivity (CS) and supra-threshold contrast as well (see chapter 4), are decreased due to the loss of cone and rod cells. Viewing images and reading are two tasks that present difficulties for people with maculopathy. Many different treatments have been investigated, such as laser and radiation therapies, retinal transplants, gene therapies, ozone and hyperbaric therapies, antioxidant and zinc therapies (Eger, 1998; Seddon et al., 1994). There has been no great breakthrough in the development of treatment to date (Elliot, et al., 2001). Most treatments slow the progression of the disease process to a greater or lesser degree, but none can completely restore vision that has been lost. Therefore, many investigations have focused on visual rehabilitation and a large number of optical and non-optical devices or instruments have been developed to compensate for the visual function loss. Much of this research has aimed at improving text for reading. However, the increasing use of television and personal computers has made digital image enhancement a new and potentially useful area for vision researchers. In the last two decades, digital image processing was introduced to enhance the visibility of digital images for the visually impaired.

The luminance information of a digital image can be decomposed to different spatial frequencies with a variety of contrast levels. People with maculopathy lose sensitivity to spatial frequencies not only at contrast threshold but also at supra-threshold levels (see chapter 4). In the early stages of maculopathy, high spatial frequency sensitivity loss occurs first. Later the whole range of spatial frequencies is influenced but the high spatial frequency loss is more severe. Therefore, increasing amplitude of the lost spatial frequencies has been the basic strategy for image enhancement for visually impaired viewers. However, when this approach was based on threshold losses it was not found to be very effective by Leat et al. (2005) and no filters were effective in ARMD. Therefore, the current study will investigate a wider range of filters, including filters based on supra-threshold contrast matching, with the aim of finding filters that may be effective in maculopathy.

The former chapter (chapter 5) on image analysis and classification has shown that single full faces have different spatial frequency information compared to other categories of images such as indoor scenes and natural scenes. We would deduce that the filters that result in visibility improvement for single faces and other images might be different.

As described in Chapter 1, quite a few image enhancement techniques may be effective at increasing the perceived visibility for the visually impaired. The present study will aim to investigate the beneficial filters for three groups of maculopathy—atrophy ARMD, exudative ARMD, and JMD. Also, due to the uniqueness of single faces, the test images are separate into two groups—single faces and general scenes. This study aims to further the investigation based on Leat et al. (2005)'s work. Some filters not found useful

in that study (e.g. the adaptive thresholding filter) will not be included for further study. The effective filters found in that study will be retested with a wider range of parameters. The custom-devised filters will be based on supra-threshold contrast loss as well as CS loss. But the gain will be applied in a different way (not only the full gain but also part of the full gain will be applied).

6.2 Methods and Materials

6.2.1 Subjects

Thirty five subjects aged 20- 92 years with maculopathy were recruited from the Optometry Clinic at the School of Optometry, University of Waterloo and the Canadian National Institute for the Blind (CNIB). Three groups of subjects with maculopathy (13 atrophic ARMD, 14 exudative ARMD, and 8 JMD) participated (shown in Table 6-1). All subjects gave written informed consent for participating in the study, which was approved by the Office of Research Ethics at the University of Waterloo. Subjects' refractive errors were checked by subjective refraction. If there was no improvement in visual acuity, then they wore their spectacles plus a working distance correction. If there was a significant change, the refractive correction, plus working distance lens, was worn in a trial frame. Monocular visual acuity of the preferred eye was measured with the University of Waterloo log MAR chart (Strong & Woo, 1985). A +1.75 D spherical lens was added for the 57cm viewing distance.

Table 6-1. The subjects' diagnosis, ages, and visual acuities. ARMD = age-related macular degeneration; JMD = juvenile macular dystrophy.

Subject	Diagnosis	Age	VA (logMAR)
1	Atrophic ARMD	75	1.10
2	Atrophic ARMD	79	1.00
3	Atrophic ARMD	84	0.70
4	Atrophic ARMD	82	1.43
5	Atrophic ARMD	83	0.70
6	Atrophic ARMD	77	1.10
7	Atrophic ARMD	78	1.20
8	Atrophic ARMD	81	0.70
9	Atrophic ARMD	82	0.51
10	Atrophic ARMD	89	0.51
11	Atrophic ARMD	79	0.51
12	Atrophic ARMD	83	1.11
13	Atrophic ARMD	92	0.92
14	<i>Exudative ARMD</i>	79	<i>1.03</i>
15	<i>Exudative ARMD</i>	91	<i>1.03</i>
16	<i>Exudative ARMD</i>	75	<i>1.30</i>
17	<i>Exudative ARMD</i>	83	<i>1.15</i>
18	<i>Exudative ARMD</i>	85	<i>1.33</i>
19	<i>Exudative ARMD</i>	59	<i>0.70</i>
20	<i>Exudative ARMD</i>	86	<i>1.12</i>
21	<i>Exudative ARMD</i>	86	<i>1.12</i>
22	<i>Exudative ARMD</i>	86	<i>1.12</i>
23	<i>Exudative ARMD</i>	89	<i>0.60</i>
24	<i>Exudative ARMD</i>	81	<i>1.12</i>
25	<i>Exudative ARMD</i>	77	<i>1.03</i>
26	<i>Exudative ARMD</i>	77	<i>0.90</i>
27	<i>Exudative ARMD</i>	85	<i>1.33</i>
28	JMD	20	1.51
29	JMD	47	1.20
30	JMD	64	0.92
31	JMD	47	0.90
32	JMD	47	1.12
33	JMD	48	0.80
34	JMD	40	1.15
35	JMD	64	0.90

6.2.2 Images

Two smaller 24 bit color images of half the width of the monitor (488 x 616 pixels or 14.05 x 17.73 cm) were selected. One was a single full face, and the other was a general scene. Twenty eight larger images of the full size of the monitor (990 x 1250 pixel or 28.5 x 35.98 cm) were also selected from our image pool (14 single full face images and 14 general scene images). Two half-sized images and one full-sized image are shown in Figure 6-1. The two half-sized images were used to determine the preferred parameters of each filter for each subject. The full-sized images were used to rate the whole range of filters. All of the images were low pass filtered at a maximum spatial frequency of 15 cpd. This was to optimize the images for the future study of people with visual impairment, so as to avoid unnecessarily enhancing high frequencies beyond the subject's acuity limit which would further compromise the dynamic range of an enhanced image (Peli, 1992; Leat et al, 2005). Fifteen cpd (equivalent to 6/12 Snellen acuity) is the maximum spatial frequency that would be perceived by this population based on the definition of low vision being visual acuity worse than 6/12 in visual acuity (Leat et al., 1999). The average luminance of the screen was 60 cd/m² measured with a Minolta Chromatic Meter CS-100. The display had a linear relationship between pixel value and luminance. This was measured by creating a grey square image of one pixel value, the pixel values were all varied between 0 and 255 and the luminance was measured with the same luminance meter.



Figure 6-1. Two half-sized images and one full-sized image showing their relative sizes

6.2.3 Apparatus and Filters

A high resolution 21-inch Sony Trinitron monitor was used to display the images which were processed with Matlab-based software, the Image Processing Tool. It was programmed by Gordon Deng, a software programmer from the System Design Engineering Department of the University of Waterloo. This software can provide a variety of image processing/enhancement functions to process/enhance an image. The interface of this software is shown in Figure 6-2. The Image Processing Tool software is similar to the ImageLab software used by Kennedy, Leat, & Jernigan (1998) and Leat et al. (2005) but run through Matlab. Two modifications were made. First, the kernel-based filters could be applied with various “strengths”. Second, the spatial frequency filters could be applied with a polynomial envelope and with a two-octave bandwidth as well as a one-octave bandwidth.

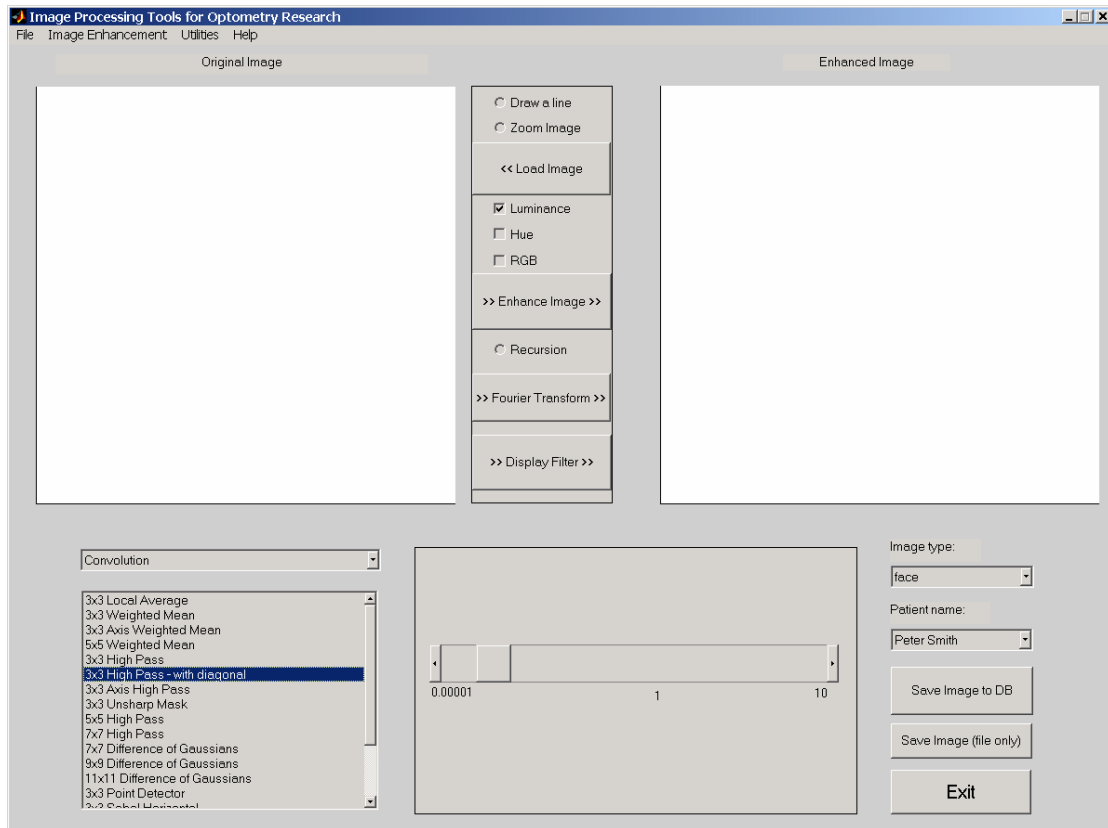


Figure 6-2. The interface of the Image Processing tool. The interface can be divided into six areas: original image display area (top left), execution area (top middle), enhanced image display area (top right), enhancement option area (bottom left), enhancement parameter area (bottom middle), and image saving area (bottom right).

Three main groups of filters were tested: generic filters, custom-devised filters, and unenhancing filters. The generic filters include the spatial domain filters, Peli's adaptive enhancement filter, contrast enhancement filter and DoG FFT filter. The custom-devised filters mainly are band-pass filters based on individual spatial frequency perception loss. The band-pass filter based on equi-emphasis of spatial frequencies was an exception because it is not based on individual spatial frequency loss. However, it used the same parameters as the other custom-devised filters so it was grouped as a

custom-devised filter. Table 6-2 shows the two groups of filters applied in the current study. The two unenhancing filters were used to degrade the image to prevent the subjects from having an expectation set that all filtered images should be more visible than the unfiltered ones. For each filter, there was a variety of parameters which could be changed and these are shown in Table 6-2. Examples of these filters are shown in Appendix C.

6.2.3.1 Generic filters

The description and codes of the generic filters are shown in Appendix D, and the details of the different parameters that were used are shown in Table 6-2.

Table 6-2. Filter parameters

Filter	Parameter
<i>Generic Filters</i>	
High-pass/unsharp masking	Mask size (3x3, 5x5, 7x7), mode (high-pass, unsharp), & scale (1, 2, 4, 8)
Sobel edge enhancement (horizontal & vertical)	Mode (RGB, HSB), scale (1, 2, 4, 8)
Contrast enhancement	Mode (RGB/HSB), power (20, 40, 80, 160)
DoG convolution	Mask size (7x7, 9x9, 11x11), scale (1, 2, 4, 8)
DoG FFT	Central frequency (0.5, 1, 2, 4, 8 cpd), maximum gain (2, 4, 8, 16), cutoff frequency (15 cpd)
Peli's adaptive enhancement	Kernel (9, 15, 21, 25), gain (2, 4, 8, 16), Slope (0.9), start value (13)
Equi-emphasis of spatial frequencies *	Mode (Gabor or polynomial), gain (1.5, 2, 4, 8), octave span (one, two)
<i>Custom-devised Filters: Band-pass based on</i>	
Contrast matching at 3.6%	Mode (Gabor or polynomial), gain (0.5, 1, 1.5, 2, 4), octave span (one, two)
Contrast matching at 27.9%	Mode (Gabor or polynomial), gain (0.5, 1, 1.5, 2, 4), octave span (one, two)
CS loss	Mode (Gabor or polynomial), gain (1, 1/2, 1/4, 1/8, 1/16, 1/32), octave span (one, two)
Peak-emphasis of spatial frequencies	Mode (Gabor or polynomial), gain (1.5, 2, 4, 8), octave span (one, two)
<i>Unenhancing Filters</i>	
Low Pass	Cut-off frequency = 1 cpd
DoG FFT	Gain = 0.3

*Since the filter based on equi-emphasis of spatial frequencies is also implemented with an FFT and it has similar parameters to the custom-devised filters, it is discussed together with the custom-devised filters rather than generic filters.

6.2.3.2 Custom-devised Filters

Band-pass filters were applied with FFT filtering. The Gabor filters were one or two octaves wide at half-height. The polynomial filters summed the gains of each spatial frequency span at one or two octaves wide. The band-pass filters based on the contrast matching at 3.6% and 27.9% were based on the contrast matching at these two contrast levels (an example for a particular subject is shown in Table 6-3-1). The ratios of the contrast matching of the subject with maculopathy to the control at each spatial frequency were calculated (M/C). The basic gain (M/C ratio) was multiplied by various gains (in an appropriate log scale) to obtain different strengths of the filter. The gains used in this case were 1, 2, 4, and 8. If the ratio was less than 1, then a gain of 1 was used. Usually with the gain of 8, the processed image would appear quite exaggerated. Therefore, the gain of 8 was chosen as the biggest gain. The rule was that the smallest gain could go down until all the inputs of all spatial frequencies were below 1. For the example shown in the Table 6-3-1, with the gain of 1, all the inputs of all spatial frequencies were close to 1. If the gain was taken lower, all the individual gains would be below 1, in which case the processing would not give any enhancement. Therefore, a gain of 1 was used as the smallest gain for this filter for this subject.

Table 6-3-1. An example of the band-pass filter based on the contrast matching at 27.9%. CM represents contrast matching. For this subject, the contrast matching at 27.9% was not available at 4.29 cpd and 8.53 cpd. The ratio (M/C) represents the ratio of the contrast matching of the test subject to the control. The black represents the spatial frequencies at which the subject could not make contrast matching at 27.9%. The grey shows the frequencies at which a gain was input for the 2-octave filters.

Spatial frequency	CM @ 27.9% -Control (%)	CM @ 27.9% - Test (%)	1x Ratio (M/C)	2x Ratio (M/C)	4x Ratio (M/C)	8x Ratio (M/C)
0.26 cpd	35.71	31.47	0.88	1.76	3.52	7.04
0.58 cpd	27.81	28.62	1.03	2.06	4.12	8.24
1.11 cpd	23.92	26.13	1.09	2.18	4.37	8.74
2.17 cpd	22.53	25.49	1.13	2.26	4.52	9.04
4.29 cpd	30.76					
8.53 cpd	32.69					

With the gain of 4 from the example in Table 6-3-1, the band-pass filter obtained is displayed in Figure 6-3. The left plot shows the filter using a Gabor filter with 1-octave. The right shows the polynomial with 1-octave. Gabor function was modulated by a Gaussian envelope for each specified spatial frequency span. The polynomial function was modulated by an envelope with a boundary line connecting the peaks of the gains for all spatial frequencies. For the 1-octave mode, gain was applied at all the specified spatial frequencies (every octave). For the 2-octave mode, gain was applied at every other specified spatial frequencies (i.e. every other octave). For the example shown in Table 6-3-1, the available specified spatial frequencies are 0.26, 0.58, 1.11, and 2.17 cpd. For the

1-octave mode, all these gains were inputted for these frequencies. For the 2-octave mode the gains at 0.26 and 1.11 cpd (highlighted in grey) were inputted.

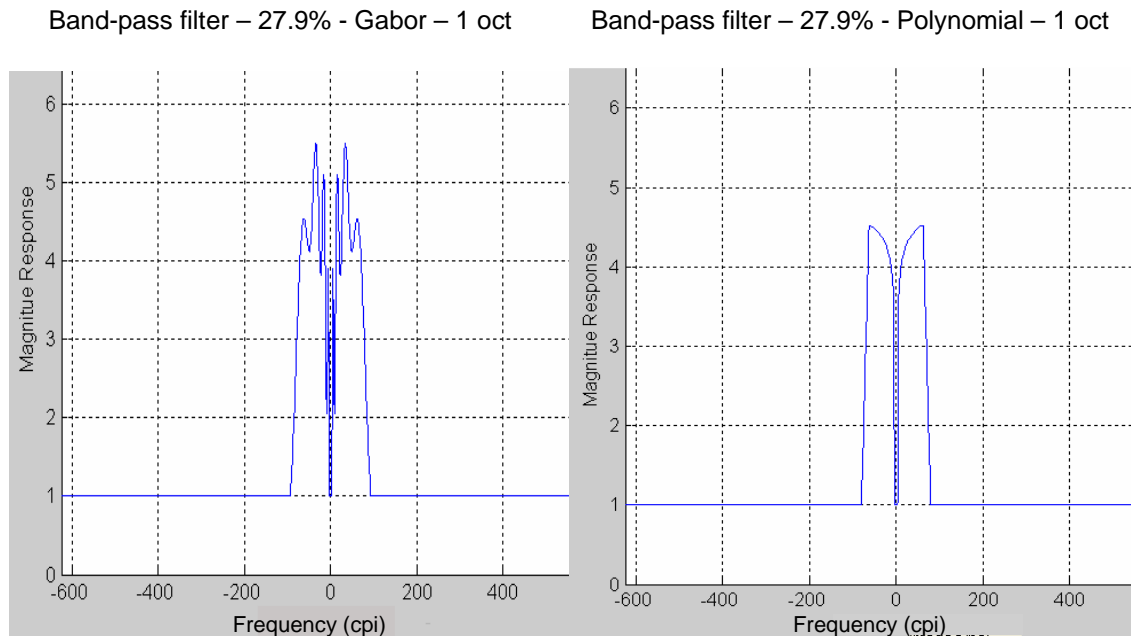


Figure 6-3. Example of frequency domain plots of the band-pass filter based on CM of 27.9% with a gain of 4 from Table 6-3-1 showing two versions (Gabor filter with 1-octave, & polynomial with 1-octave). The x axis shows the spatial frequency in cycles per image (cpi) and the y axis shows the magnitude response of the filter. 1 cpd = 28 cpi.

An example of the band-pass filter based on CS loss is shown in Table 6-3-2 and the filter profiles are shown in Figure 6-4. The ratio of the contrast threshold of the maculopathy subject to the control was calculated. This was the full gain of the filter. Usually with a full gain, the processed image would be quite exaggerated. The study of Leat et al. (2005) showed that the full gain was not preferred and could often not be implemented. Therefore, reduced gains in log steps were used such as 1/2, 1/4, 1/8, 1/16 etc. The rule was that gain could do down to the point before all the inputs for all the spatial frequencies were below 1. In the example shown in Table 6-3-2, the smallest

reduced gain would be 1/32. At each spatial frequency where the ratio was < 1 a gain of 1 was used. Thus for the 1/32 filter, gains of 1, 1, 1, 1, 1.40 would be used for spatial frequencies of 0.26, 0.58, 1.11, 2.17, and 4.29 cpd respectively.

Table 6-3-2. An example of the band-pass filter based on the contrast sensitivity loss. CTh represents contrast threshold. The ratio (M/C) represents the ratio of the contrast threshold of the test subject to the control. The black represents the un-available contrast threshold at 8.53 cpd for this subject.

Spatial frequency	CTh – Control (%)	CTh – Test (%)	1x Ratio (M/C)	1/2 x Ratio	1/4 x Ratio	1/8 x Ratio	1/16 x Ratio	1/32 x Ratio
0.26 cpd	1.06	3.09	2.92	1.46	0.73	0.36	0.18	0.09
0.58 cpd	0.62	2.32	3.76	1.88	0.94	0.47	0.23	0.12
1.11 cpd	0.41	3.39	8.30	4.15	2.08	1.04	0.52	0.26
2.17 cpd	0.50	4.13	8.30	4.15	2.07	1.04	0.52	0.26
4.29 cpd	0.61	27.51	44.83	22.42	11.21	5.60	2.80	1.40
8.53 cpd	1.56							

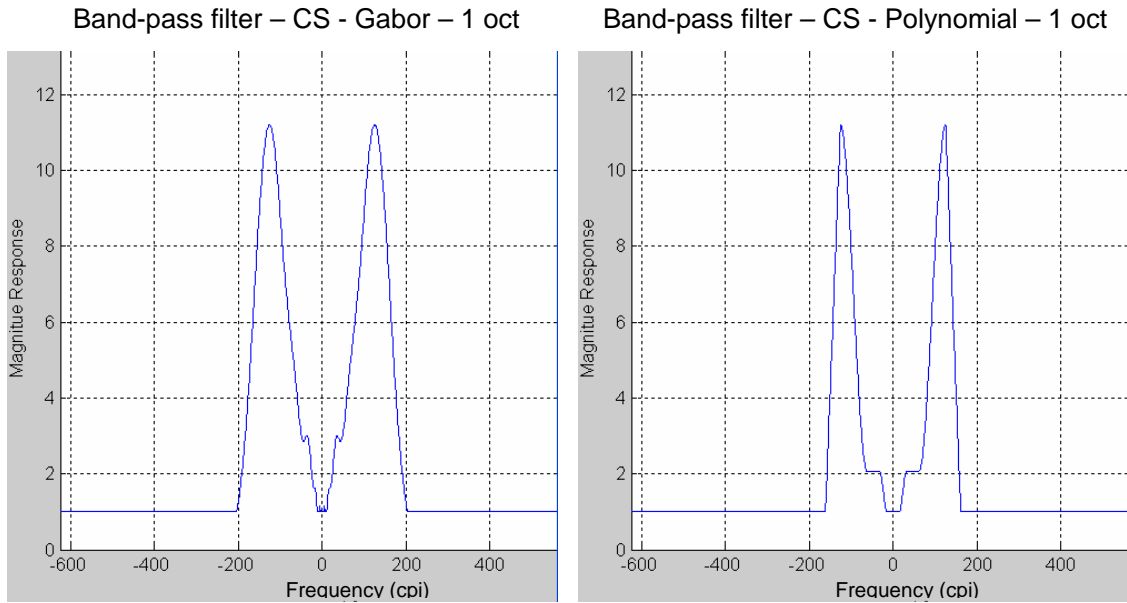


Figure 6-4. Examples of frequency domain plots of the band-pass filter based on CS loss with a gain of 1/4 ratio from Table 6-3-2 showing two versions (Gabor filter with 1-octave, and polynomial with 1-octave). The x axis shows the spatial frequency (cpi) and the y axis shows the magnitude response of the filter. 1 cpd = 28 cpi.

An example of the band-pass filter based on the peak-emphasis of spatial frequencies is shown in Table 6-3-3 and the filter profiles are shown in Figure 6-5. With this filter, the most sensitive spatial frequency (peak of the CS curve) was the most exaggerated and the least sensitive spatial frequency was the least exaggerated. For the example shown in Table 6-3-3, the most sensitive spatial frequency was 0.58 cpd. The ratios of contrast threshold of 0.58 to other spatial frequencies were calculated. The multiplied factors of 1.5, 2, 4 and 8 were the gains used for this filter. Any calculated input of below 1 would be replaced with 1.

Table 6-3-3. An example of the band-pass filter based on peak-emphasis of the spatial frequencies. CTh = contrast threshold, s.f. = spatial frequency. The ratio of CTh (0.58 cpd/other s.f.) represents the ratio of the contrast threshold of the most sensitive spatial frequency to another spatial frequency. The black represents the un-available contrast threshold at 8.53 cpd for this subject.

Spatial frequency	CTh – Test (%)	Ratio of CTh (0.58 cpd/ other s.f.)	1.5 x Ratio	2 x Ratio	4 x Ratio	8 x Ratio
0.26 cpd	3.09	$2.32/3.09 = 0.75$	1.13	1.51	3.01	6.02
0.58 cpd	2.32	$2.32/2.32 = 1$	1.5	2	4	8
1.11 cpd	3.39	$2.32/3.39 = 0.68$	1.03	1.37	2.74	5.48
2.17 cpd	4.13	$2.32/4.13 = 0.56$	0.84	1.12	2.25	4.49
4.29 cpd	27.51	$2.32/27.51 = 0.08$	0.13	0.17	0.34	0.67
8.53 cpd						

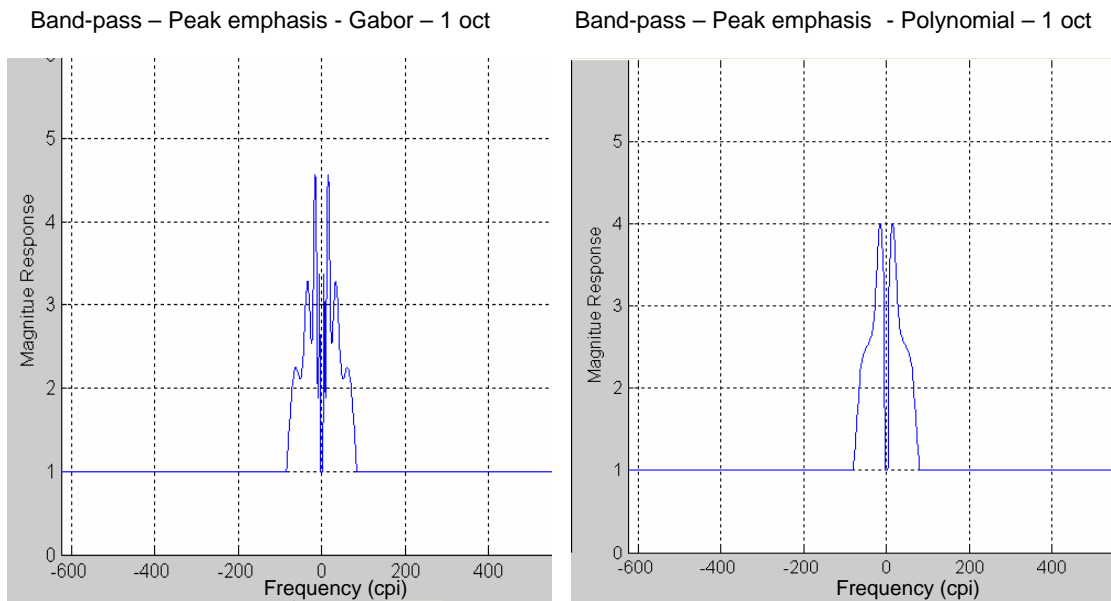


Figure 6-5. Examples of frequency domain plots of the band-pass filter based on peak-emphasis of spatial frequencies with a gain of 4 from Table 6-3-3 showing two versions (Gabor with 1-octave and polynomial with 1-octave). The x axis shows the spatial frequency (cpi) and the y axis shows the magnitude response of the filter. 1cpd = 28 cpi.

An example of the band-pass filter based on the equi-emphasis of spatial frequencies is shown in Table 6-3-4 and the filter displays are shown in Figure 6-6. This filter does not need contrast sensitivity or contrast matching information. All the spatial frequencies tested were equally exaggerated with gains of 1.5, 2, 4, and 8.

Table 6-3-4. An example of the band-pass filter based on equi-emphasis of the spatial frequencies. All the spatial frequencies were exaggerated by the same gains (1.5 x, 2 x, 4 x, and 8 x).

Spatial frequency	1.5 x	2 x	4 x	8 x
0.26 cpd	1.5	2	4	8
0.58 cpd	1.5	2	4	8
1.11 cpd	1.5	2	4	8
2.17 cpd	1.5	2	4	8
4.29 cpd	1.5	2	4	8
8.53 cpd	1.5	2	4	8

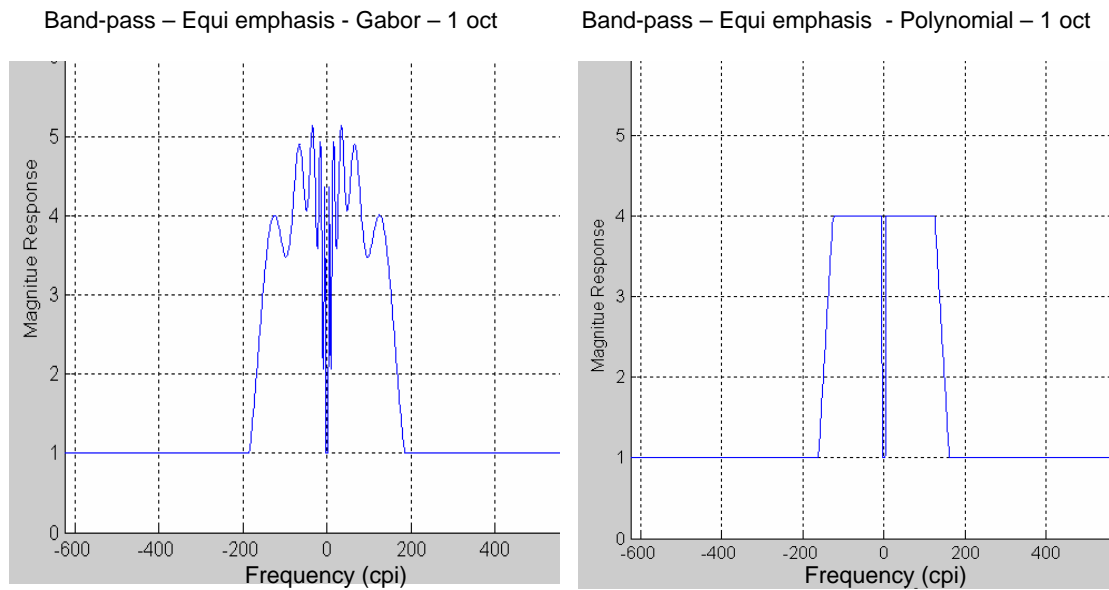


Figure 6-6. Examples of frequency domain plots of the band-pass filter based on equi-emphasis of spatial frequencies with a gain of 4 and two versions (Gabor and 1-octave, polynomial and 1 octave). The x axis shows the spatial frequency (cpi) and the y axis shows the magnitude response of the filter.

6.2.4 Procedure

Each subject made three or four visits during the study.

6.2.4.1 First Visit

Preliminary tests were done for each subject with the preferred eye including visual acuity (VA), intraocular pressure, and fundus examination with ophthalmoscope. Contrast threshold and supra-threshold contrast matching were measured (see Chapter 4) to obtain the gains to be used for the custom-devised band pass filters.

6.2.4.2 Second Visit

Within-Filter Ranking – First phase

The purpose of this phase was to determine the optimal power, scale or gain of each filter. Each of the two half-sized images was processed with each filter using different powers. Four of the processed half-sized images (in a randomized placement) were displayed together as shown in Figure 6-7. The subject, sitting at 57cm, was permitted to look freely among the four images. If there were four or fewer versions of a filter, the subject was required to indicate the one that provided the best visibility. If there were more than four versions of a filter, the subject was first required to indicate the worst one, i.e. which provided the poorest visibility. The worst version was then replaced with a fifth version with another scale, and the subject would be required to choose the worst one until there were four versions of images left. Then, the subject was required to determine the best version i.e. which provided the best visibility. Taking the Sobel edge enhancement filter as an example, the ranking was between scale of 1, 2, 4 and 8 for RGB and HSB modes, i.e. the subject compared among four versions of the filter. Using

this process, the best (most preferred) filter version was selected, i.e. the optimum power for each filter.

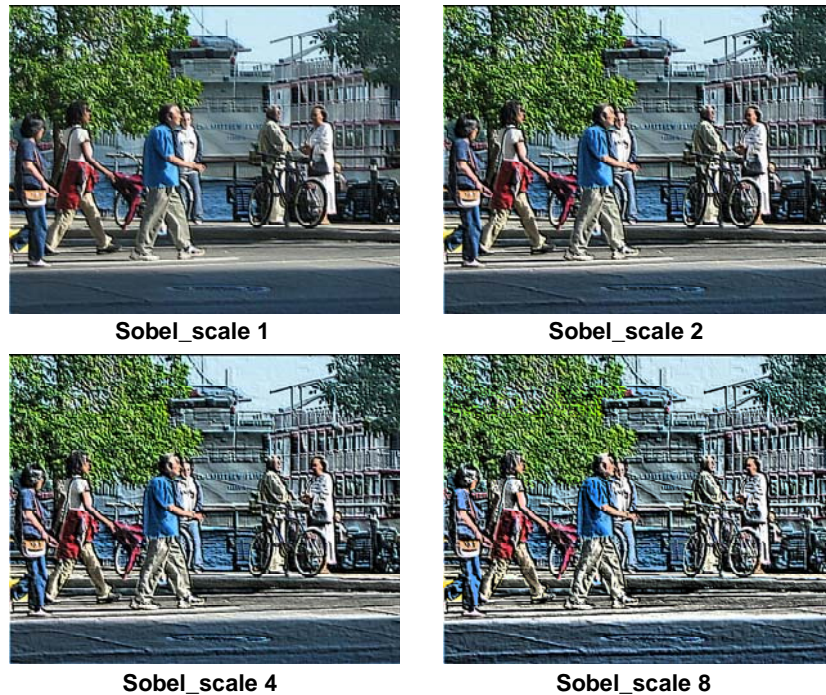


Figure 6-7. Four versions of the half-sized general scene image processed with different scales of the 3x3 Sobel horizontal and vertical edge enhancement filter. The four versions were located randomly on the screen.

Within-Filter Ranking – Second phase

Since the optimal scale/power/gain was selected from the first phase ranking, the purpose of the second phase was to determine the optimal kernel size or mode for each filter or group of similar filters using the optimal scale/power/gain of each filter version. The kernels and modes of each filter are shown in Table 6-2. Similar to the first phase of within-filter ranking, the filtered images with different kernels or modes of each filter were shown in a random placement on the screen. The subjects were required to rank the different versions and determined the kernel or mode which provided the best perceived

visibility. Taking the Sobel edge enhancement filter as an example again, the first phase ranking was between scale of 1, 2, 4 and 8 for each of the RGB and HSB modes, and the second phase ranking was between RGB mode and HSB mode using their corresponding optimal scales. After these two phases of within-filter rankings, each filter had been chosen with the best scale and the best mode so that comparison between filters in the final phase would be with the optimum version of each filter for each subject.

6.2.4.3 Third Visit — between-filter ratings

At the third visit, subjects evaluated the whole range of filters each in its optimal version. Fourteen faces and 14 general scene images were assigned to 14 filters for processing using a Latin Square (see Table 6-4) so that each image would be processed by one filter once. The 14 filters (11 test filters, 2 unenhancing filters and 1 control) were labeled from F1 to F14 shown in the top row of Table 6-4, and the 14 images of either single face or general scene were labeled from I1 to I14 shown in the left column. For the first subject of each maculopathy group, I1 was assigned to F1, I2 to F2, and so on to I14 was assigned to F14. For the second subject of each group, I1 was assigned to F2 and I14 to F1. This pattern was repeated for each subject until each image was assigned to a filter without any repetition.

To measure the display order effect, two blocks of ratings were undertaken. In the first block, the original picture was shown first, followed by the processed one. The subjects were told that the processed image could be better, the same, or worse than the original image in visibility. Examples were demonstrated for training before the real test. The subjects were asked to give a number in a scale of 0 to 200 to represent perceived improvement or decrement in visibility. The value of 100 represented the same in

perceived visibility as the original image. If processed image was more visible, a value from 101 and 200 was assigned; if less, then a value from 0 to 99 was assigned. In the second block, the processed image was shown ahead of the original, yet the subject was not informed of this display order. The subjects were first asked to determine which one was more visible, the first or the second. Then they were to assume that the worse one was 100 and rated the better one with a value either more or less than 100. If they did not see any difference between the two, they were allowed to say no difference and rate with 100. The two unenhancing filters were used to prevent the subjects from having an expectation set that all filtered images should be more visible than the un-filtered ones. To measure the repeatability, the control unfiltered images were displayed in each block.

To show the rating results more clearly, 100 was subtracted from each rating. Thus, if the perceived visibility with an enhanced image was better than the original, the displayed ratings would be higher than 0; if worse, then below 0.

Table 6-4. Latin Square. F₁ to F₁₄ represent the filters. I₁ to I₁₄ represent the images. S₁ to S₁₄ represent the subjects.

	F ₁	F ₂	F ₃	F ₄	F ₅	F ₆	F ₇	F ₈	F ₉	F ₁₀	F ₁₁	F ₁₂	F ₁₃	F ₁₄
I ₁	S ₁	S ₂	S ₃	S ₄	S ₅	S ₆	S ₇	S ₈	S ₉	S ₁₀	S ₁₁	S ₁₂	S ₁₃	S ₁₄
I ₂	S ₁₄	S ₁	S ₂	S ₃	S ₄	S ₅	S ₆	S ₇	S ₈	S ₉	S ₁₀	S ₁₁	S ₁₂	S ₁₃
I ₃	S ₁₃	S ₁₄	S ₁	S ₂	S ₃	S ₄	S ₅	S ₆	S ₇	S ₈	S ₉	S ₁₀	S ₁₁	S ₁₂
I ₄	S ₁₂	S ₁₃	S ₁₄	S ₁	S ₂	S ₃	S ₄	S ₅	S ₆	S ₇	S ₈	S ₉	S ₁₀	S ₁₁
I ₅	S ₁₁	S ₁₂	S ₁₃	S ₁₄	S ₁	S ₂	S ₃	S ₄	S ₅	S ₆	S ₇	S ₈	S ₉	S ₁₀
I ₆	S ₁₀	S ₁₁	S ₁₂	S ₁₃	S ₁₄	S ₁	S ₂	S ₃	S ₄	S ₅	S ₆	S ₇	S ₈	S ₉
I ₇	S ₉	S ₁₀	S ₁₁	S ₁₂	S ₁₃	S ₁₄	S ₁	S ₂	S ₃	S ₄	S ₅	S ₆	S ₇	S ₈
I ₈	S ₈	S ₉	S ₁₀	S ₁₁	S ₁₂	S ₁₃	S ₁₄	S ₁	S ₂	S ₃	S ₄	S ₅	S ₆	S ₇
I ₉	S ₇	S ₈	S ₉	S ₁₀	S ₁₁	S ₁₂	S ₁₃	S ₁₄	S ₁	S ₂	S ₃	S ₄	S ₅	S ₆
I ₁₀	S ₆	S ₇	S ₈	S ₉	S ₁₀	S ₁₁	S ₁₂	S ₁₃	S ₁₄	S ₁	S ₂	S ₃	S ₄	S ₅
I ₁₁	S ₅	S ₆	S ₇	S ₈	S ₉	S ₁₀	S ₁₁	S ₁₂	S ₁₃	S ₁₄	S ₁	S ₂	S ₃	S ₄
I ₁₂	S ₄	S ₅	S ₆	S ₇	S ₈	S ₉	S ₁₀	S ₁₁	S ₁₂	S ₁₃	S ₁₄	S ₁	S ₂	S ₃
I ₁₃	S ₃	S ₄	S ₅	S ₆	S ₇	S ₈	S ₉	S ₁₀	S ₁₁	S ₁₂	S ₁₃	S ₁₄	S ₁	S ₂
I ₁₄	S ₂	S ₃	S ₄	S ₅	S ₆	S ₇	S ₈	S ₉	S ₁₀	S ₁₁	S ₁₂	S ₁₃	S ₁₄	S ₁

6.2.5 Statistical Analysis

For the two phases of within-filter rankings, there were too many groups and parameters for meaningful statistical analysis. Therefore a statistical analysis was undertaken only for phase 3, the between-filter ratings. The coefficient of repeatability (1.96 x SD of block one rating minus block two rating) was calculated to show the repeatability. Since the filters were all rated twice in different orders, a paired t-test was applied to test order effect for all filters. If no order effect was found, the ratings of the two blocks were averaged and a one sample t-test was applied to show if the filter was rated significantly different from zero.

6.3 Results

6.3.1 Within-Filter Rankings – First phase

The number of subjects who preferred each power/scale/gain value is shown in Tables 6-5-A to 6-5-K.

High-pass/unsharp masking filter (Table 6-5-A)

For the general scene, the JMD group preferred a power of 4 or 8 less often than the two ARMD groups. For the face images, the exudative ARMD group preferred a power of 8 more often than the other two groups. Compared to the general scene, the face image seems to be preferred with higher powers.

Table 6-5-A. First phase rankings of the high-pass/unsharp masking filter. HP = high-pass filter. P1 to P8 represent power of 1 to power of 8. The powers were set in log scales. The numbers of subjects who preferred the scale of each version of the filter are shown.

Image	Version & Kernel	Atrophic ARMD				Exudative ARMD				JMD			
		P1	P2	P4	P8	P1	P2	P4	P8	P1	P2	P4	P8
General Scene	Unsharp 3*3	4	4	5	0	4	2	6	2	5	2	0	1
	HP 3*3	2	3	6	2	4	1	3	6	3	3	1	1
	HP5*5	2	7	3	1	9	0	4	1	6	1	1	0
	HP7*7	4	6	2	1	6	0	6	2	5	3	0	0
Face	Unsharp 3*3	4	6	1	2	4	1	5	4	0	3	1	4
	HP 3*3	1	5	3	4	4	0	5	5	1	3	0	4
	HP5*5	1	8	2	2	4	1	5	4	1	3	2	2
	HP7*7	3	7	3	0	3	1	7	3	2	4	1	1

3x3 horizontal and vertical Sobel edge enhancement filter (Table 6-5-B)

For the general scene, the atrophic ARMD group preferred scales of 1 and 2. The exudative ARMD group tended to prefer higher scales more often. Most subjects with JMD preferred a scale of 1. For the face, both the atrophic ARMD and JMD preferred lower scales of 1 and 2, while the exudative ARMD tended to prefer higher scale of 4.

Table 6-5-B. First phase rankings of the 3x3 Sobel horizontal and vertical edge enhancement filter. S1 to S8 represent scale 1 to scale 8. The subject numbers who preferred the scale of each version of the filter are shown.

Image	Mode	Atrophic ARMD				Exudative ARMD				JMD			
		S1	S2	S4	S8	S1	S2	S4	S8	S1	S2	S4	S8
General Scene	HSB	5	7	1	0	8	3	1	2	6	1	0	1
	RGB	7	5	1	0	5	5	4	0	7	1	0	0
Face	HSB	7	4	2	0	3	4	5	2	2	4	1	1
	RGB	9	4	0	0	5	3	5	1	3	3	0	2

Contrast Enhancement filter (Table 6-5-C)

For the general scene, the preferences of both the atrophic ARMD and JMD groups were spread among the powers, but the subjects with exudative ARMD preferred a higher λ value of 80 or 160. For the face, a λ value of 40 was most often preferred by the atrophic ARMD and JMD groups while a λ value of 160 was preferred by the subjects with exudative ARMD.

Table 6-5-C. First phase rankings of the contrast enhancement filter. λ 20 to λ 160 represent the percentage of the enhanced image which was added back to the original image. The subject numbers who preferred the λ value of each version of the filter are shown.

Image	Mode	Atrophic ARMD				Exudative ARMD				JMD			
		λ 20	λ 40	λ 80	λ 160	λ 20	λ 40	λ 80	λ 160	Λ λ 20	40	λ 80	Λ 160
General Scene	HSB	4	3	5	1	1	1	7	5	2	3	2	1
	RGB	1	3	3	6	1	2	6	5	1	2	3	2
Face	HSB	5	6	2	0	4	1	5	4	1	4	0	3
	RGB	3	8	2	0	3	1	3	7	2	3	1	2

DoG Convolution filter (Table 6-5-D)

For the general scene, the JMD group preferred a scale of 1 or 2. The two ARMD groups showed more spread in their preference for scales. For the face, the atrophic ARMD group preferred a scale of 1 or 2 while the exudative ARMD group showed more spread in preference and the JMD group preferred a scale of 2 most frequently.

Table 6-5-D. First phase rankings of the DoG Convolution filter. S1 to S8 represent the power of the filter. The subject numbers who preferred each scale of each version of the filter are shown.

Image	Kernel	Atrophic ARMD				Exudative ARMD				JMD			
		S1	S2	S4	S8	S1	S2	S4	S8	S1	S2	S4	S8
General Scene	7x7	6	3	3	1	5	3	3	3	4	3	1	0
	9x9	5	4	2	2	5	4	4	1	4	3	0	1
	11x11	5	4	1	3	5	4	1	4	3	4	0	1
Face	7x7	6	3	3	1	4	2	4	4	1	6	0	1
	9x9	5	6	0	2	3	3	6	2	1	6	0	1
	11x11	4	7	0	2	3	4	5	2	1	7	0	0

DoG FFT filter (Table 6-5-E)

As central spatial frequency increases, the preferred gain tends to be higher. For the general scene, both ARMD groups showed more spread in preferred gains; the JMD group preferred the gain of 2 or 4 most frequently. For the face, the atrophic ARMD group preferred gains of 2 or 4 for central spatial frequencies of 0.5 to 2cpd. The exudative ARMD group showed more spread in their preferences. The JMD preferred gain 2 for central spatial frequencies of 0.5 to 1cpd or gain 4 for 2 to 8 cpd.

Table 6-5-E. First phase rankings of the DoG FFT filter. S.F. = spatial frequency. G2 to G16 represent gain of 2 to gain of 16.

Image	Central S.F.	Atrophic ARMD				Exudative ARMD				JMD			
		G2	G4	G8	G16	G2	G4	G8	G16	G2	G4	G8	G16
General Scene	0.5cpd	4	4	2	3	3	4	5	2	4	3	1	0
	1cpd	5	4	3	1	2	6	6	0	5	1	1	1
	2cpd	3	4	4	2	3	5	5	1	3	3	2	0
	4cpd	4	3	5	1	3	3	5	3	2	4	1	1
	8cpd	0	4	4	5	3	2	5	4	1	3	2	2
Face	0.5cpd	9	4	0	0	5	4	4	1	5	2	0	1
	1cpd	8	5	0	0	5	3	4	2	3	3	0	2
	2cpd	9	2	1	1	6	1	4	3	0	6	1	1
	4cpd	5	3	4	1	3	2	5	4	0	5	2	1
	8cpd	1	4	5	3	2	0	6	6	0	3	3	2

Peli's Adaptive Enhancement Filter (Table 6-5-F)

For the general scenes, the atrophic ARMD and JMD groups preferred lower gains of 2 or 4. The exudative ARMD group showed more spread in preference. For the face, the three maculopathy groups showed a similar trend as they did for the general

scene. Relative to the general scene, the two ARMD groups preferred lower gains for the face, while the subjects with JMD preferred bigger gains for the face image.

Table 6-5-F. First phase rankings of the Peli’s adaptive enhancement filter. G2 to G16 represent the gain of 2 to 16.

Image	Kernel	Atrophic ARMD				Exudative ARMD				JMD			
		G2	G4	G8	G16	G2	G4	G8	G16	G2	G4	G8	G16
General Scene	9	5	5	2	1	5	2	4	3	5	3	0	0
	15	5	4	2	2	6	2	3	3	6	1	1	0
	21	5	7	0	1	6	3	3	2	6	2	0	0
	25	6	6	0	1	5	3	3	3	6	1	1	0
Face	9	6	6	1	0	5	4	4	1	1	4	3	0
	15	8	5	0	0	5	4	5	0	2	6	0	0
	21	9	4	0	0	6	4	4	0	4	3	1	0
	25	10	3	0	0	8	2	4	0	5	3	0	0

Band-pass filter based on contrast matching of 3.6% (Table 6-5-G)

For the general scene, both the atrophic ARMD and JMD groups tended to prefer gains of not more than 1.5, while the exudative ARMD group showed more preference for higher gains. This is also the trend for the face image. All subjects tended to prefer relatively smaller gains more frequently for the face than the general scene.

Band-pass filter based on the contrast matching at 27.9% (Table 6-5-H)

For both types of image, the atrophic ARMD and JMD groups preferred gains of 1 to 2, while the exudative ARMD group tended to prefer bigger gains more often. The subjects preferred relatively smaller gains more frequently for the face than the general scene.

Band-pass filter based on CS loss (Table 6-5-I)

For the general scene, the subjects with atrophic ARMD preferred the middle gains of 1/16 to 1/2. The subjects with exudative ARMD showed a wide spread in preference. The subjects with JMD preferred smaller gains of 1/32 to 1/4. For the face image, the atrophic ARMD group preferred gains of 1/8 to 1/2. The exudative ARMD preferred gains of 1/8 to 1 and the JMD group tended to prefer to gain of 1/8 to 1/4. Relative to the preferred gains for the general scene, those for the face tend to be higher.

Band-pass filter based on peak emphasis of spatial frequency (Table 6-5-J)

For the general scene, both the atrophic ARMD and JMD groups preferred a smaller gain of 1.5 or 2 most frequently, while the exudative ARMD group showed a wider spread in preference. For the face, the atrophic ARMD and JMD groups showed the same trend as for the general scene while the exudative ARMD showed less preference for the biggest gain of 8.

Band-pass filter based on equi-emphasis of spatial frequencies (Table 6-5-K)

For the general scene, the atrophic ARMD preferred lower gains of 1.5 to 4, the JMD preferred gains of 1.5 and 2 while the exudative ARMD group showed spread in preference. For the face, both the atrophic ARMD and JMD groups preferred the smallest gains of 1.5 and 2 while the exudative ARMD showed a spread in preference.

Generally speaking, two trends are demonstrated at this stage of rankings. Firstly, the atrophic ARMD and the JMD groups tended to prefer smaller gains more often than the exudative ARMD group. Secondly, it seemed that relative to the general scene, the face image was preferred more frequently with smaller gains.

Table 6-5-G. First phase rankings of the band-pass filter based on contrast matching of 3.6%.

Image	Envelope-octave span	Atrophic ARMD					Exudative ARMD					JMD				
		G0.5	G1	G1.5	G2	G4	G0.5	G1	G1.5	G2	G4	G0.5	G1	G1.5	G2	G4
General Scene	Gabor 1oct	1	5	4	1	1	2	0	1	1	5	2	3	0	1	1
	Gabor 2oct	1	7	2	1	1	1	0	2	1	5	2	3	1	1	0
	PolyN 1oct	1	6	2	1	2	2	0	1	0	6	2	3	0	0	2
	PolyN 2oct	1	6	2	2	1	1	0	2	0	6	3	4	0	0	0
Face	Gabor 1oct	1	7	2	2	0	2	2	1	2	2	3	3	1	0	0
	Gabor 2oct	1	7	3	1	0	1	1	2	3	2	4	2	0	0	1
	PolyN 1oct	2	6	3	1	0	3	1	1	2	2	4	2	1	0	0
	PolyN 2oct	1	6	4	1	0	1	1	2	3	2	4	2	0	1	0

Table6- 5-H. First phase rankings of band-pass filter based on the contrast matching at 27.9%.

Image	Envelope-octave span	Atrophic ARMD					Exudative ARMD					JMD				
		G0.5	G1	G1.5	G2	G4	G0.5	G1	G1.5	G2	G4	G0.5	G1	G1.5	G2	G4
General Scene	Gabor 1oct	0	4	5	3	1	0	1	4	2	7	0	3	2	3	0
	Gabor 2oct	0	3	6	3	1	0	2	3	4	5	0	5	0	2	1
	PolyN 1oct	0	5	6	1	1	0	2	3	4	5	0	2	3	3	0
	PolyN 2oct	0	6	5	2	0	0	2	2	3	7	0	4	1	3	0
Face	Gabor 1oct	0	6	4	1	2	0	3	2	3	6	1	2	4	0	1
	Gabor 2oct	0	7	5	1	0	0	3	3	2	6	0	5	2	1	0
	PolyN 1oct	0	8	5	0	0	0	3	4	2	5	1	3	4	0	0
	PolyN 2oct	1	5	7	0	0	0	4	2	2	6	0	3	2	3	0

Table 6-5-I. First phase rankings of the band-pass filter based on CS loss

Image	Envelope-octave	Atrophic ARMD						Exudative ARMD						JMD					
		1/32	1/16	1/8	1/4	1/2	1	1/32	1/16	1/8	1/4	1/2	1	1/32	1/16	1/8	1/4	1/2	1
General Scene	Gabor 1oct	0	3	2	4	3	1	3	2	3	2	2	2	2	0	3	3	0	0
	Gabor 2oct	0	1	4	4	3	1	2	0	4	4	2	2	1	1	0	4	2	0
	PolyN 1oct	0	3	5	2	3	0	1	2	5	1	2	3	3	1	1	2	1	0
	PolyN 2oct	0	2	2	5	3	1	1	3	3	1	3	3	2	2	2	2	0	0
Face	Gabor 1oct	0	1	3	3	5	1	1	0	4	3	3	3	1	2	1	2	2	0
	Gabor 2oct	0	1	3	4	5	0	0	0	5	2	5	2	1	1	3	1	2	0
	PolyN 1oct	0	0	2	5	5	1	0	2	5	1	4	2	1	1	4	2	0	0
	PolyN 2oct	0	0	3	6	4	0	1	1	4	2	4	2	1	1	1	5	0	0

Table 6-5-J. First phase rankings of the band-pass filter based on peak emphasis of spatial frequency

Image	Envelope-octave	Atrophic ARMD				Exudative ARMD				JMD			
		G1.5	G2	G4	G8	G1.5	G2	G4	G8	G1.5	G2	G4	G8
General Scene	Gabor 1oct	8	5	0	0	3	2	6	3	1	5	1	1
	Gabor 2oct	8	4	1	0	6	2	3	3	4	2	1	1
	PolyN 1oct	5	8	0	0	5	2	5	2	4	3	0	1
	PolyN 2oct	7	5	1	0	5	3	3	3	4	3	0	1
Face	Gabor 1oct	7	5	1	0	4	4	4	2	4	3	0	1
	Gabor 2oct	8	5	0	0	4	4	5	1	4	3	0	1
	PolyN 1oct	7	6	0	0	5	3	6	0	4	4	0	0
	PolyN 2oct	9	4	0	0	5	2	7	0	6	2	0	0

Table 6-5-K. First phase rankings of the band-pass filter based on equi-emphasis of spatial frequencies

Image	Envelope-octave	Atrophic ARMD				Exudative ARMD				JMD			
		G1.5	G2	G4	G8	G1.5	G2	G4	G8	G1.5	G2	G4	G8
Scene	Gabor 1oct	6	2	5	0	4	0	4	6	3	3	2	0
	Gabor 2oct	5	6	2	0	3	1	5	5	5	2	0	1
	PolyN 1oct	4	5	4	0	4	0	4	6	5	2	1	0
	PolyN 2oct	4	6	2	1	4	0	3	7	3	3	1	1
Face	Gabor 1oct	11	2	0	0	6	1	4	3	5	3	0	0
	Gabor 2oct	10	3	0	0	4	3	6	1	5	2	1	0
	PolyN 1oct	10	3	0	0	5	3	5	1	5	2	1	0
	PolyN 2oct	8	5	0	0	5	3	4	2	5	3	0	0

6.3.2 Within-Filter Rankings – Second Phase

The purpose of the second phase of within-filter rankings was to determine the preferred kernel or mode of each filter. The results are shown in Table 6-6.

High-pass/unsharp masking filter

For the general scene, the three maculopathy groups seemed to prefer the kernel of 5x5 and 7x7 more frequently. For the face, it seemed that the smaller kernels were more often preferred by the subjects with atrophic ARMD and JMD.

DoG convolution filter

For both image types, the subjects with atrophic ARMD and JMD preferred the two smaller kernels (7x7 and 9x9) more frequently while the subjects with exudative ARMD preferred the largest kernel (11x11) more frequently.

Peli's adaptive enhancement filter

For the general scene, the subjects with atrophic ARMD preferred the smallest kernel of 9 and the biggest of 25 most often, while the subjects with exudative ARMD and JMD preferred the kernel of 21. For the face, all three groups preferred the small kernels of 9 and 15 more often.

Sobel edge enhancement (horizontal and vertical) filter

There was no obvious difference between the two modes HSB and RGB, by observation.

Contrast enhancement filter

RGB was the more frequently preferred mode in all situations except for the face image for the atrophic ARMD observers.

DoG FFT filter

The DoG filter versions with the peak at the two highest central spatial frequencies (4 and 8cpd) were not generally preferred by all three groups. The two ARMD groups preferred a central frequency of 1 or 2cpd more frequently for the general scene but preferred 0.5cpd more often for the face. For JMD, the opposite pattern is seen – they preferred enhancement at a lower frequency of 0.5 or 1cpd for the general scene, but preferred enhancement at 1 or 2cpd for the face image.

Table 6-6. Second phase of within-filter rankings between kernels/modes for each generic filter

Filter	Kernel /mode	Atrophic ARMD		Exudative ARMD		JMD	
		Scene	Face	Scene	Face	Scene	Face
High-Pass & Un-sharp masking	Un-sharp 3x3	2	7	3	4	0	0
	HP 3x3	1	2	1	1	2	4
	HP5x5	7	1	6	7	2	2
	HP7x7	3	3	4	2	4	2
DoG Convolution	7x7	5	4	3	3	4	3
	9x9	7	6	4	4	3	4
	11x11	1	3	7	7	1	1
Peli's Adaptive Enhancement	Kernel 9	5	6	4	6	1	2
	Kernel 15	1	6	2	4	2	4
	Kernel 21	2	1	6	2	4	0
	Kernel 25	5	0	2	2	1	2
Sobel Edge Enhancement	HSB	7	6	8	9	4	4
	RGB	6	7	6	5	4	4
Contrast Enhancement	HSB	4	9	4	5	2	2
	RGB	9	4	10	9	6	6
DoG FFT	0.5cpd	1	7	3	9	3	0
	1cpd	4	4	5	0	2	2
	2cpd	4	2	4	3	1	3
	4cpd	2	0	2	0	1	1
	8cpd	2	0	0	2	1	2
Band-pass_3.6%	Gabor 1oct	3	3	5	4	0	4
	Gabor 2oct	3	3	1	2	2	2
	PolyN 1oct	3	5	3	3	2	0
	PolyN 2oct	3	1	1	1	3	1
Band-pass_27.9%	Gabor 1oct	4	5	8	5	3	3
	Gabor 2oct	4	3	1	4	1	4
	PolyN 1oct	4	4	3	2	2	1
	PolyN 2oct	1	1	2	3	2	0
Band-pass based on CS loss	Gabor 1oct	4	5	3	4	1	0
	Gabor 2oct	2	2	5	5	2	5
	PolyN 1oct	0	4	3	2	2	1
	PolyN 2oct	7	2	3	3	3	2
Band-pass based on peak-emphasis of s.f.	Gabor 1oct	5	5	4	4	3	3
	Gabor 2oct	2	3	0	1	1	0
	PolyN 1oct	2	3	5	4	3	4
	PolyN 2oct	4	2	5	5	1	1
Band-pass_Equi-emphasis of s.f.	Gabor 1oct	4	4	3	4	3	2
	Gabor 2oct	1	1	3	2	0	3
	PolyN 1oct	4	4	3	2	0	2
	PolyN 2oct	4	4	5	6	5	1

Each of the custom-devised filters has four versions (Gabor applied with 1-octave band-width, Gabor with 2-octave, polynomial with 1-octave, and polynomial with 2-octave). To investigate the preference for Gabor versus polynomial and 1 versus 2 octave span, the data were combined so as to compare the preference for these parameters: Gabor versus polynomial and 1-octave versus 2-octave band-widths, which are shown in Table 6-7-A and B.

Gabor versus polynomial functions

Generally speaking, the two ARMD groups preferred the Gabor function more frequently than the polynomial function. The JMD group preferred the Gabor function more often for the general scene but the polynomial more often for the face. The three band-pass filters based on the CM of 3.6%, 27.9% and the CS loss tended to be preferred with the Gabor function more often, while the peak-emphasis and the equi-emphasis were more frequently preferred when applied with the polynomial. Thus there is no great advantage in using the polynomial over the Gabor.

1-octave versus 2-octave band-width

For the band-pass filter based on CM of 3.6%, 27.9% and the peak-emphasis, the 1-octave band-width was preferred more often than the 2-octave band-width. For the band-pass filter based on CS loss and the equi-emphasis, it seemed that the 2-octave was preferred more often. The atrophic ARMD group preferred the 1-octave band-width more often. Thus there was no overall advantage of 2-octave band-width over 1-octave band-width for filtering.

Table 6-7-A. Second phase of within-filter rankings for the custom-devised filter applied with Gabor or polynomial function.

Band-pass filter based on	Mode	Atrophic ARMD		Exudative ARMD		JMD	
		Scene	Face	Scene	Face	Scene	Face
CM of 3.6%	Gabor	6	6	6	6	6	2
	PolyN	6	6	4	4	1	5
CM of 27.9%	Gabor	8	8	9	9	7	4
	PolyN	5	5	5	5	1	4
CS loss	Gabor	7	6	9	8	5	3
	PolyN	6	7	5	6	3	5
Peak-emphasis of spatial frequencies	Gabor	8	7	5	4	3	4
	PolyN	5	6	9	10	5	4
Equi-emphasis of spatial frequencies	Gabor	5	5	6	6	5	3
	PolyN	8	8	8	8	3	5

Table 6-7-B. Second phase of within-filter rankings for the custom-devised filter according to 1-octave and 2-octave band-width.

Band-pass filter based on	Mode	Atrophic ARMD		Exudative ARMD		JMD	
		Scene	Face	Scene	Face	Scene	Face
CM of 3.6%	1-oct	8	6	7	8	4	2
	2-oct	4	6	3	2	3	5
CM of 27.9%	1-oct	9	8	7	11	4	5
	2-oct	4	5	7	3	4	3
CS loss	1-oct	9	4	6	6	1	3
	2-oct	4	9	8	8	7	5
Peak-emphasis of spatial frequencies	1-oct	8	7	8	9	7	6
	2-oct	5	6	6	5	1	2
Equi-emphasis of spatial frequencies	1-oct	8	8	6	6	4	3
	2-oct	5	5	8	8	4	5

6.3.3 Between Filter Ratings

6.3.3.1 Repeatability

For the unfiltered control images, a paired t-test showed no difference between the two orders of ratings ($p > 0.05$). This suggests there was no display order effect when

subject rated the images. Therefore the two ratings were averaged for each subject. A one sample *t*-test was applied between the averaged ratings and 100. Again no difference was shown ($p > 0.05$), which suggests that subjects could make accurate ratings. The averaged results across subjects are shown in Figure 6-8 A.

6.3.3.2 Ratings for two un-enhancing filters

The average ratings across subjects for the two un-enhancing filters are shown in Figure 6-8 B & C. A one sample *t*-test was applied. Except with faces in atrophic ARMD, all showed significances indicating a poorer visibility of the filtered images compared to the original images ($p < 0.05$).

6.3.3.3 Ratings of the generic filters

The average ratings for the generic filters are shown in Figure 6-9. A one-sample *t*-test was applied to determine which were significantly different from zero. For the general scenes, the subjects with atrophic ARMD showed perceived improvement with the high-pass/un-sharp mask filter ($p < 0.001$) and the Peli's adaptive enhancement filter ($p = 0.007$). The subjects with exudative ARMD showed improvement with Peli's adaptive filter ($p = 0.036$) and the subjects with JMD with the high-pass/un-sharp masking filter ($p = 0.009$), Sobel edge enhancement filter ($p = 0.001$), contrast enhancement filter ($p = 0.014$), and Peli's adaptive enhancement ($p = 0.009$). Peli's adaptive enhancement filter was shown to be effective for all three categories of maculopathy for the general scenes.

As for the single faces, the subjects with atrophic ARMD showed significantly perceived improvement with the contrast enhancement filter ($p = 0.017$), DoG convolution filter ($p = 0.005$) and Peli's adaptive enhancement filter ($p = 0.029$). The

subjects with exudative ARMD showed no filter that gave significantly improvement and the subjects with JMD showed significantly improved visibility with the contrast enhancement filter ($p = 0.003$).

Generally speaking, the DoG FFT filter did not give perceived improvement. Peli's adaptive enhancement filter most often gave perceived improvement followed by the high-pass/un-sharp masking and contrast enhancement and the Sobel edge enhancement filter for general scenes. The contrast enhancement followed by Peli's adaptive and DoG convolution most often gave perceived improvement for faces. The Subjects with JMD gained perceived improvement with more filters compared to the atrophic ARMD and subjects with exudative ARMD.

6.3.3.4 Ratings of the custom-devised filters

With custom-devised filters, for the general scenes (shown in Figure 6-10), both the atrophic and subjects with exudative ARMD only showed perceived improvement with the band-pass filter at a contrast of 27.9% ($p = 0.013$ and $p = 0.008$) while the subjects with JMD only showed perceived improvement with the equi-emphasis filter ($p = 0.025$) and 3.6% band-pass filter ($p = 0.004$).

For the single faces, the subjects with atrophic ARMD showed perceived improvement with 3.6% band-pass filter ($p = 0.001$), the subjects with exudative ARMD with no filter, and the subjects with JMD with the equi-emphasis filter ($p = 0.014$). The peak-emphasis filter and band-pass filter based on CS loss did not give perceived improvement for any group.

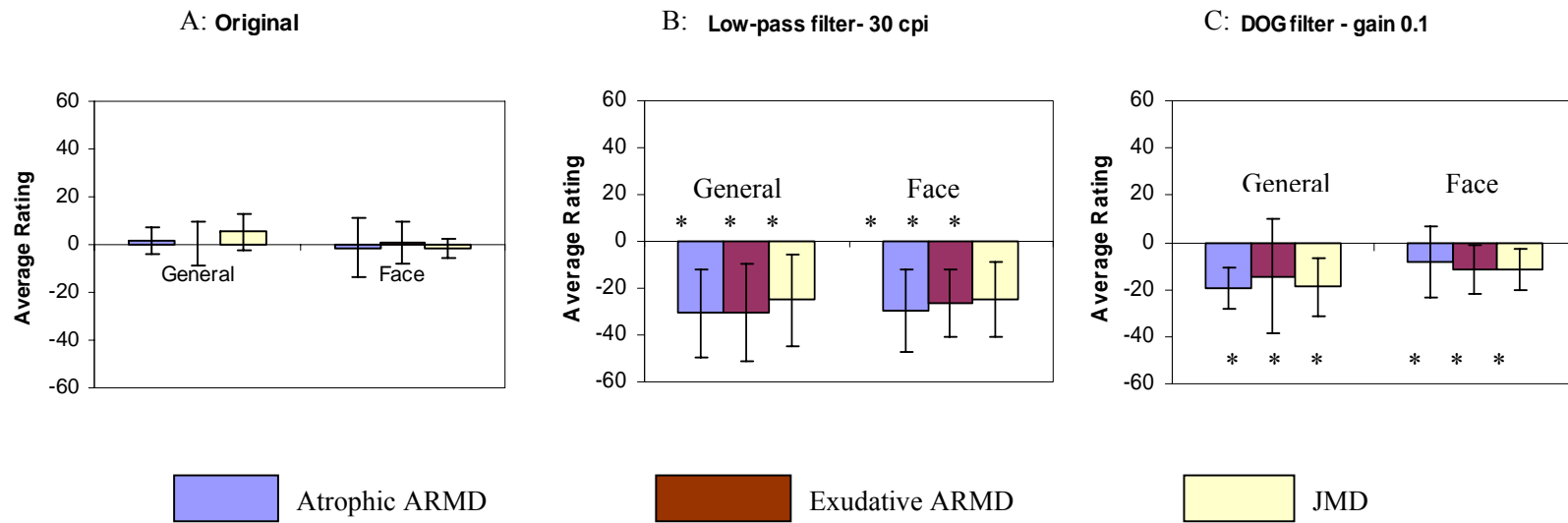


Figure 6-8. Average perceived visibility ratings of the control and two un-enhancing filters. The error bars represent +/- one standard deviation. The stars show those that were significantly at the $p < 0.05$.

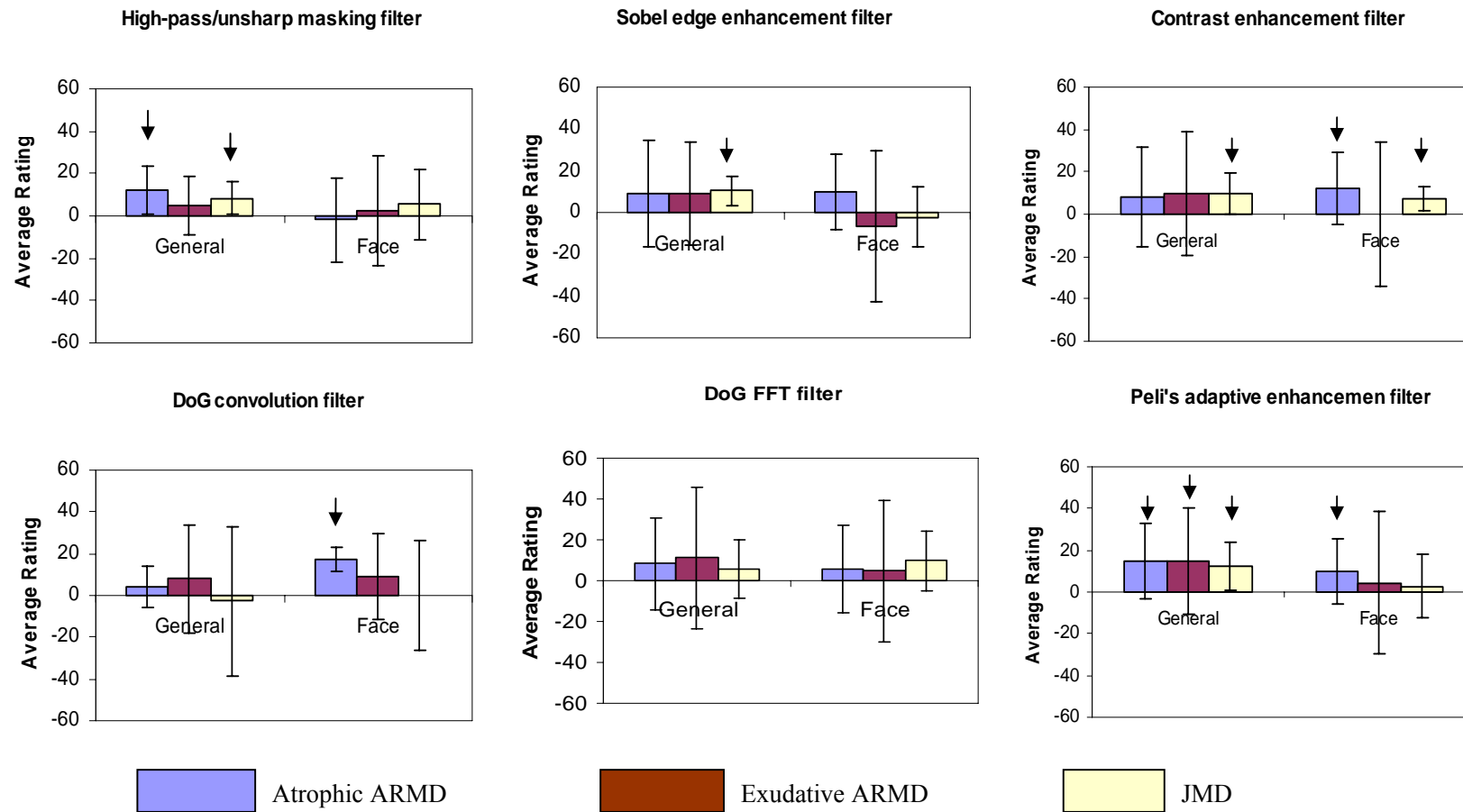


Figure 6-9. Average ratings for generic filters for two groups of images (general scenes and faces). The error bars represent +/- one standard deviation. The arrows show those that were significant at the $p < 0.05$ level.

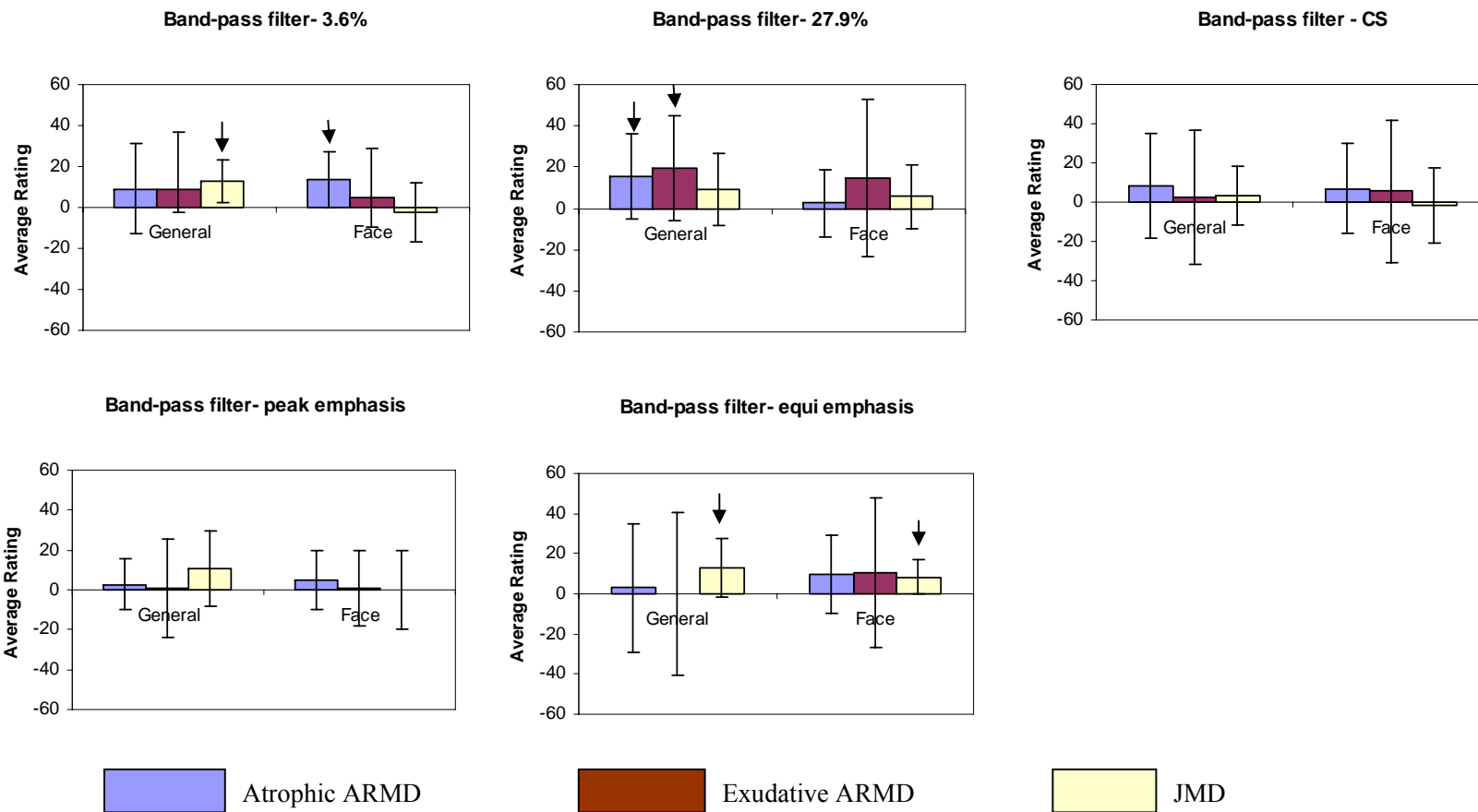


Figure 6-10. Evaluations of the custom-devised filters. The error bars represent +/- one standard deviation. The arrows show those that were significantly preferred at the $p < 0.05$ level.

6.3.3.5 Bonferroni adjustment

To control the Type 2 errors (false positives), all the significant p values of the filters from t-test were adjusted by the adjusted Bonferroni (Jacard and Wan, 1996) method (shown in Table 6-8). The current study was done according to two types of groupings – three maculopathies and two image categories. Therefore, the adjusted Bonferroni was applied to each of the six combinations: atrophic ARMD – general scenes, exudative ARMD – general scenes, JMD – general scenes, atrophic ARMD – faces, exudative ARMD – faces, JMD – faces. The results showed that all the initially significant p values of the filters remained significance (shown with *).

Table 6-8. Bonferroni adjustment for all the significant p values. The final column shows the modified p values for each significance from *t*-test (shown in the fourth column).

Those that reach significance after being adjusted by Bonferroni are shown with *.

Maculopathy- Image type	Filter	Mean rating	P value	Divisor	Modified p level for significance
Atrophic ARMD-general scene	High-pass/unsharp masking	112.3	<0.001*	3	0.017
	Peli's adaptive enhancement	114.9	0.007*	2	0.025
	Band-pass (27.9%)	115.5	0.013*	1	0.05
Exudative ARMD-general scenes	Band-pass (27.9%)	119.4	0.008*	2	0.025
	Peli's adaptive filter	115.0	0.036*	1	0.05
JMD-general scene	Sobel edge enhancement	110.3	0.001*	6	0.008
	Band-pass (3.6%)	112.9	0.004*	5	0.01
	Highpass/unsharp masking	108.4	0.009*	4	0.0125
	Peli's adaptive enhancement	112.5	0.009*	3	0.017
	Contrast enhancement	109.9	0.014*	2	0.025
	Band-pass (equi- emphasis)	113.1	0.025*	1	0.05
	Band-pass (3.6%)	113.9	0.001*	4	0.0125
Atrophic ARMD-Face	DoG convolution	117.6	0.005*	3	0.017
	Contrast enhancement	112.0	0.017*	2	0.025
	Peli's adaptive enhancement	109.9	0.029*	1	0.05
	Contrast enhancement	107.3	0.003*	2	0.025
JMD-face	Band-pass (equi- emphasis)	108.4	0.014*	1	0.05

6.4 Discussion

This study found that eight filters were effective at improving the perceived visibility of images. They were the contrast enhancement, Peli's adaptive enhancement, DoG convolution, high-pass/unsharp masking, Sobel edge enhancement, band-pass based on CM at 3.6% and 27.9%, and the band-pass filter based on equi-emphasis of spatial frequencies. Three filters were not effective in enhancing the perceived visibility of any type of image and any group of subjects with maculopathy. These were the DoG FFT filter, the band-pass based on CS loss, and the peak-emphasis filter. The effective filters were specific to one or several combinations of type of maculopathy and category of image. This is summarized in Table 6-9. It can be seen that there are more effective filters for the subjects with atrophic ARMD and JMD than for the subjects with exudative ARMD and there are more effective filters for general scenes than for single faces. The most commonly preferred filter was the Peli's adaptive enhancement (shown in bold italic font) followed by the contrast enhancement (underlined).

Table 6-9. The filters that gave significant improvement in perceived visibility

Maculopathy	General Scenes	Single Faces
Atrophic ARMD	<ul style="list-style-type: none"> • <i>Peli's adaptive enhancement</i> • High pass/unsharp masking • Band pass - 27.9% 	<ul style="list-style-type: none"> • <i>Peli's adaptive enhancement</i> • <u>Contrast enhancement</u> • DoG convolution • Band pass - 3.6%
Exudative ARMD	<ul style="list-style-type: none"> • <i>Peli's adaptive enhancement</i> • Band pass - 27.9% 	
JMD	<ul style="list-style-type: none"> • <i>Peli's adaptive enhancement</i> • <u>Contrast enhancement</u> • High pass/unsharp masking • Sobel edge enhancement • Band pass - Equi-emphasis • Band pass - 3.6% 	<ul style="list-style-type: none"> • <u>Contrast enhancement</u> • Band pass - Equi-emphasis

6.4.1 Comparison with former studies

Peli's studies

A few of Peli's studies applied the adaptive enhancement filter for people with visual impairment (Fullerton, & Peli, 2006; Peli et al., 1991; Peli, 1994a, 1994b). All the studies claimed effective enhancement in image visibility. For example, Peli et al. (1991) demonstrated that the adaptive enhancement filter improved face recognition (celebrity and unfamiliar faces) for subjects with central scotomas. In that study, 9 out of 21 patients with macular disease showed significant improvement ($p < 0.05$). Peli (1994b) applied individually tuned enhancement to face images for people with a central scotoma. The filter depended on the patient's contrast sensitivity function and on the spatial

frequency content of the image. This study found that the individually tuned enhancement filter had a similar effect to the uniformly applied adaptive enhancement filter. There were 3 out of 11 subjects who showed significant improvement and the level of improvement was similar in magnitude to the effect found in the previous study (Peli et al., 1991). The level of significance was calculated for each subject but not across all subjects as a group. In the present study, the Peli's adaptive enhancement filter gave significant improvement in perceived visibility for single faces only for the subjects with atrophic ARMD. In the present study, the significance was calculated across the whole group with maculopathy instead of for each subject. Unfortunately, in Peli's two studies the exact type of retinal disease for each subject with central scotoma was not recorded. Therefore, it is hard to know the extent of agreement between Peli's studies and the present study.

Peli (1994b) showed that 48 subjects with a central scotoma selected a face image filtered with a gain factor of 2.4 ± 1.5 . In the current study, the majority of subjects in all maculopathy groups preferred filtered images with a gain of 2 or 4 (see Table 6-5-F) which basically supports Peli's finding.

The study of Leat et al. (2005)

The current study was continuation of the study of Leat et al. (2005). Generally speaking the current study found more filters to be effective for improving perceived visibility than the previous one. Eight filters were found to be effective in the current study compared to only two by Leat et al (2005). Several factors can explain this

difference. Firstly, the subjects in the current study were diagnosed with only maculopathy, and the subjects were further separated into three groups (atrophic ARMD, exudative ARMD, and JMD) while Leat et al. (2005) included subjects with low vision due to a variety of disorders. It may be easier to find effective filter(s) for a more homogeneous population than for a whole group of low vision subjects with mixed visual pathologies. Secondly, the tested images were grouped into single faces and general scenes instead of the four categories of images used in the study of Leat et al. (2005). This grouping was based on the analysis of the image spatial frequency characteristics rather than the subjective grouping according to the scenes in the images used in Leat et al.'s study. Single faces were found to be distinctive from other general scene images (see Chapter 5) having significant lower amplitude spectra in all three orientations (horizontal, vertical, and oblique). Similar to the grouping of maculopathy, the single face image group or the general scene group may be more homogeneous, possibly making it easier to find effective filters. Thirdly, the current study based the custom-devised filters on supra-threshold contrast loss instead of CS loss. As was discussed in Chapter 3, supra-threshold contrast perception may be more important than contrast threshold for daily visual function. Fourthly, the current study instructed subjects to rate image "visibility" rather than "preference" which was adopted by Leat et al. (2005). That is, the subjects were required to choose the image version from which they could gain more information rather than the one which was more "pleasing". During the current study, the author did notice that some subjects said "I do see better with the processed image but I like the smoother (original) one". This suggests that the low vision patients with maculopathy can perceive

the exaggerated information in an enhanced image. Although this exaggeration is not always pleasant, it does help with visibility. Peli (1994) noticed this point and stated that “since the degradation of performance by low vision is larger than the effect of distortion, the enhancement that reduced performance for normal observers may still be beneficial for the visually impaired observer”. This different rating criterion may have resulted in the higher scores. Fifthly, the enlarged parameter span in the current study also may have contributed to the different findings. For example, Peli’s adaptive enhancement filter resulted in borderline improvement in the study by Leat et al. (2005). The tested parameters were three kernel sizes (9, 15, and 21) with a gain of 5. In the current study four kernels (9, 15, 21 and 25) and four gains (2, 4, 8, and 16) were tested. The results showed that the kernel size of 25 and the gain of 2 or 4 were frequently chosen by the subjects. This suggests that, in the previous study, some filters probably did not show effects because of the narrower span of parameters. Another two filters also resulted in borderline improvement in the earlier study. These were edge enhancement and histogram equalization.

Two effective filters from the study of Leat et al. (2005) were again found to be effective in the current study. These were the high-pass/unsharp masking and Peli’s adaptive enhancement filter. Leat et al. showed that, for maculopathy, unsharp masking had no effect for single faces but was effective for multiple faces and outdoors images (see their Figure 4). In the current study, unsharp masking and high-pass were grouped as one type of filter. We found that high-pass/unsharp mask had no effect for single faces but was effective for both the subjects with atrophic ARMD and JMD for general scenes.

Thus the findings with regards to the high-pass/unsharp masking filter in the two studies show some agreement with each other.

Generally, Leat et al did not find any significant effects for subjects with maculopathy with the Peli's adaptive enhancement filter. The current study did find an effect for single faces for atrophic ARMD and effects for general scenes for all three maculopathy groups which is in disagreement with Leat et al. The possible explanation is the sample size. In the study of Leat et al (2005), there were 18 subjects with maculopathy and 2 out of these 18 had both ARMD and diabetic retinopathy. Plus, the three types of maculopathy were treated as one group. If the filter were effective for only one type of maculopathy but ineffective for the others (as found in the current study), the significance for maculopathy as a whole group would be reduced.

6.4.2 What can be drawn from the current study?

If one filter has to be chosen to enhance the perceived visibility of one type of image, Peli's adaptive enhancement filter could be used to enhance the perceived visibility of general scenes (shown in *italic and bold font* in Table 6-9); and the contrast enhancement filter would be chosen for single faces (shown with underline in Table 6-9) except for people with exudative ARMD.

If one filter had to be chosen to enhance the visibility for each type of maculopathy, Peli's adaptive enhancement would be used for people with atrophic ARMD, and contrast enhancement or equi-emphasis for people with JMD. Unfortunately,

no effective filter was found for people with exudative ARMD. The parameters of these filters are discussed below.

6.4.2.1 Effective filters according to image category

General scenes

Peli's adaptive enhancement stood out in this study as being effective for general scenes for all three types of maculopathy.

In the first phase of within-filter rankings, subjects with atrophic ARMD and JMD preferred lower gains of 2 and 4. Relatively more subjects with exudative ARMD chose gains of 8 and 16 (Table 6-5-F). The filtering effects with different gains are shown in Figure 6-11 with the top two images. Bigger gains lead to stronger enhancement effects and usually cause more exaggeration. Therefore, the subjects with exudative ARMD seem to prefer stronger filtered images compared to the subjects with atrophic ARMD and JMD. In the current study, no difference was shown in visual acuity and CS between the three types of maculopathy. Maybe some other aspects of the disease process or the functional deficits between the three maculopathy types caused this difference. For example, spatial phase may be more disrupted in those with exudative ARMD. Spatial frequency phase may be one factor that affects between these ocular disease groups.

Kernel 15 – Gain 2



Kernel 15 – Gain 8



Kernel 9 – Gain 4



Kernel 25 – Gain 4



Figure 6-11. Demonstration of Peli's adaptive enhancement. The top two images show filtering with gains of 2 and 8 with the same kernel size of 15. The bottom two images show filtering with two different kernel sizes of 9 and 25 with a gain of 4.

In the second phase of within-filter rankings for viewing general scenes, the subjects with atrophic ARMD tended to prefer the biggest kernel of 25 and the smallest kernel of 9 while the subjects with exudative ARMD and JMD tended to prefer a kernel of 21 more often. Smaller kernels result in a wider range of spatial frequencies being enhanced (demonstrated in Figure 6-11 with the bottom two images). The larger kernels

21 and 25 are more often preferred by all three groups of maculopathies than the smaller kernels. This suggests that for the general scenes, the enhancement of wider range of spatial frequencies works better than the enhancement of a narrower band of spatial frequencies.

Therefore, for the general scenes, the subjects with exudative ARMD preferred higher gains with larger kernels, and the subjects with atrophic ARMD and JMD preferred smaller gains with bigger kernels. This suggests that a stronger filtering effect is more beneficial to the subjects with exudative ARMD than the subjects with atrophic ARMD and JMD. It also suggests that if one filter version was to be chosen for all subjects with maculopathy, the kernel size should be 21 or 25 and the gain should be 4 or 8.

Single faces

The contrast enhancement filter was shown to be effective for single faces for subjects with atrophic ARMD and JMD. Again we will consider the optimum version of this filter.

In the first phase of within-filter rankings, the subjects with atrophic ARMD preferred smaller power/scales of 20 or 40 while subjects with JMD showed more spread in their preference for scales (some preferred 80 or 160). For modes HSB and RGB, the bigger the power/scale, the more enhanced the filtered image tends to be (shown in Figure 6-12).

In the second phase of within-filter rankings, more subjects with atrophic ARMD preferred the HSB mode, while more subjects with JMD preferred the RGB mode. With the same power/scale, the RGB mode filtered image appears more intense in color than the HSB mode (shown in Figure 6-12) because each color is also enhanced. In general, subjects with atrophic ARMD preferred smaller gains with the HSB mode, and Subjects with JMD showed more spread in their preferred power/scales with the RGB mode. This suggests the subjects with JMD preferred more colourful and a stronger filtered image compared to the subjects with atrophic ARMD.

Generally for all preferred filters, the face images seem to need less gain/strength of filtering than the general scenes. What causes this difference? Chapter 5 has shown that single face images have lower amplitude spectra of spatial frequencies in all three orientations (horizontal, vertical, and oblique) than general scene images. However, there is no significant difference in slopes (amplitude spectrum versus spatial frequency) between the two categories of images. This suggests that single face images have less high spatial frequency content than the general scenes. It is already known that high spatial frequency perception is more damaged for people with maculopathy. In that case, viewing general scenes (with relatively more high spatial frequency information) should be more negatively affected than viewing single faces (with relatively less high spatial frequency information) for people with maculopathy. As compensation, the optimum digital filtering gains/strengths for single faces should be smaller than those for general scenes.



Figure 6-12. Face images enhanced with the contrast enhancement filter in two scales (20 and 80) and two modes (HSB and RGB).

6.4.2.2 Effective filters according to maculopathy group

Atrophic ARMD

Peli's adaptive enhancement filter was effective in atrophic ARMD for both single faces and general scenes. The first phase of within-filter rankings showed that more subjects preferred smaller gains when viewing single faces than general scenes. The

second phase of within-filter rankings showed that subjects with atrophic ARMD preferred the smallest and the biggest kernels of 9 and 25 for general scenes but preferred the two small kernels of 9 and 15 for single faces. In general, single faces need smaller gains with smaller kernels while general scenes need bigger gains with either the smallest or the biggest kernel. This suggests that general scenes for subjects with atrophic ARMD need stronger enhancement.

Exudative ARMD

There was no effective filter for single faces although the Peli's adaptive enhancement and the band-pass filter based on the CM at 27.9% were shown to be effective for general scenes. Therefore, no filter could be chosen for all types of images for this type of maculopathy based on the current study.

JMD

The contrast enhancement and band-pass based on equi-emphasis of spatial frequency were effective for both image types.

Regarding the contrast enhancement filter, it has been discussed above that it was effective for single faces with a preference for scales of 20 or 40 and the RGB mode. For subjects with JMD viewing general scenes, the first phase of between-filter rankings showed that more subjects tended to prefer higher scales of 40 and 80 (see Table 6-5-C). The second phase of between-filter rankings showed that the RGB mode was more often preferred (see Table 6-6). These results indicate that general scenes needed stronger enhancement than single faces for subjects with JMD. Both single faces and general scenes were preferred with color enhanced images in the RGB mode.

Regarding the equi-emphasis band-pass filter, the first phase of within-filter rankings showed that more subjects with JMD preferred lower gains (1.5 and 2) for the single faces than the general scenes (Table 6- 5-K), which could be attributed to the differences of physical characteristics between the two categories of images. The second phase of within-filter rankings showed that more subjects tended to prefer the Gabor mode for the general scenes but more tended to prefer the polynomial mode for the single faces (Table 6-7-A). The subjects did not show a preference for 1 or 2 octave band widths for the general scenes, but more often preferred the 2-octave filtering for the single faces. With the same gain, the Gabor mode filtered images appear more exaggerated to the normally sighted eye compared to the polynomial filtered image and the 2-octave mode filtered face images look smoother than the 1-octave mode filtered images (shown in Figure 6-13 & 14). Therefore, for single faces the polynomial and 2-octave modes were preferred i.e. relatively smoother looking images were preferred. General scenes benefited from the Gabor filter, which means that more exaggerated images can be acceptable. However, this difference between the preference to Gabor and polynomial was almost unnoticeable to subjects with maculopathy for the smaller gains for the general scene image.

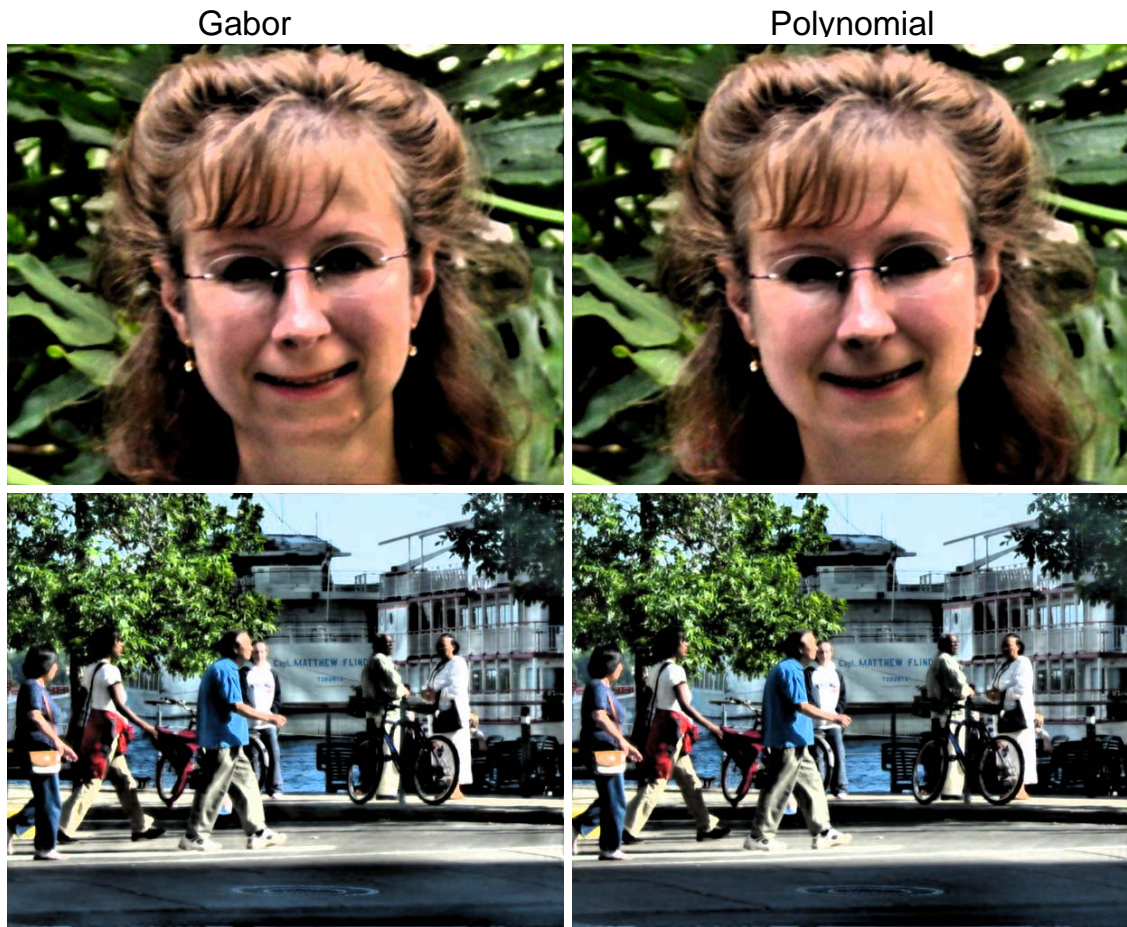


Figure 6-13. Demonstration of the band-pass filter based on equi-emphasis of spatial frequencies showing the filtering effects with Gabor and polynomial for the face and the general scene.

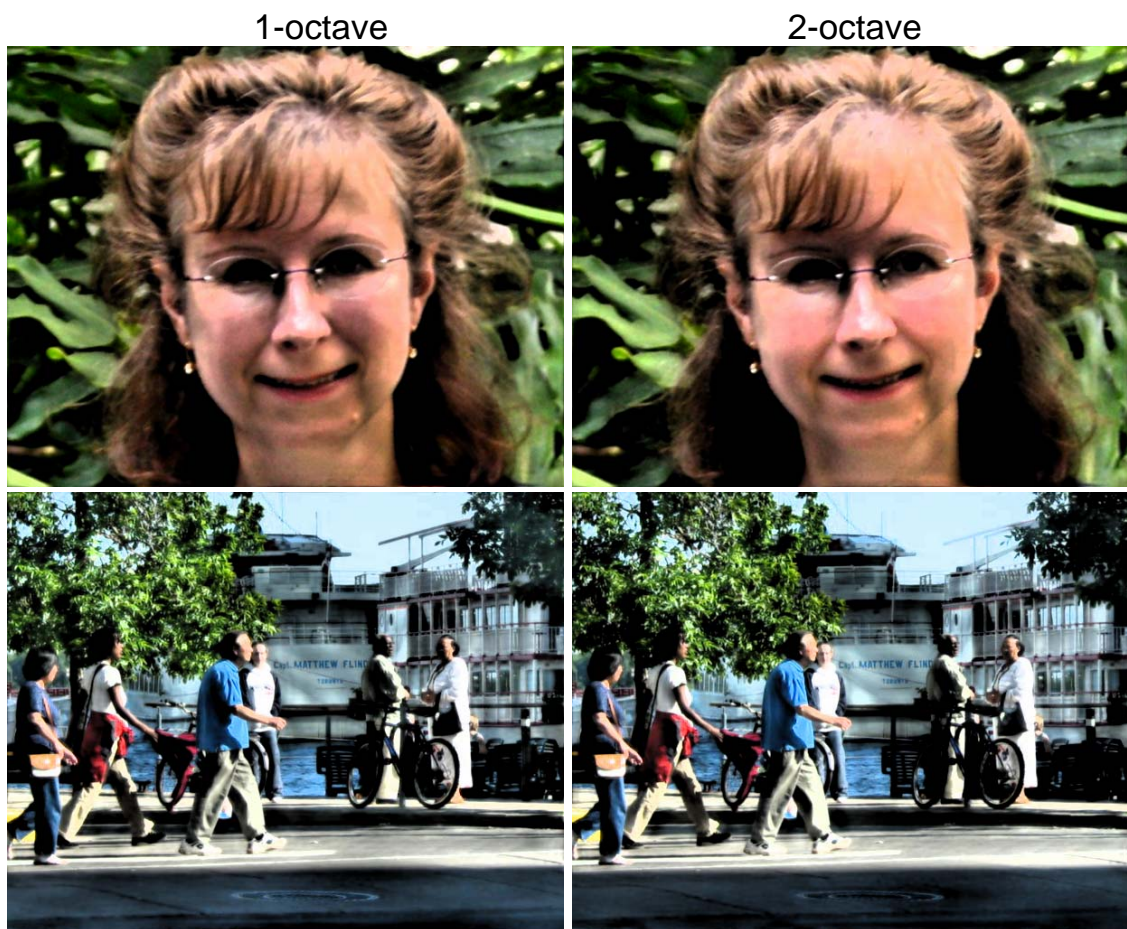


Figure 6-14. Demonstration of the band-pass filter based on equi-emphasis of spatial frequencies for 1-octave and 2-octave filtering with the face and general scene.

6.4.2.3 Custom-devised filters

In the former study of Leat et al. (2005), the custom-devised filter was derived from contrast sensitivity loss and no significant improvements were found. In the current study, the custom-devised filters were derived from both contrast perception loss at supra-threshold levels and contrast threshold. Also, a band-pass filter based on equi-emphasis of spatial frequencies was tested.

The results showed that several modes derived from supra-threshold contrast loss were effective (shown in Table 6-9). This supports previous findings that the visual system does not process contrast linearly (Georgeson & Sullivan, 1975). There are different gains in different channels, so that contrast constancy is achieved. For people with maculopathy, contrast constancy was demonstrated although supra-threshold contrast perception was influenced by the presence of maculopathy (Mei & Leat, 2007; chapter 4). The filtered images derived from contrast threshold loss look more exaggerated than those from supra-threshold contrast loss (shown in Figure 6-15). Leat et al. (2005) found the band-pass filter derived from CS loss was not effective and the full gain could not be applied because of unwanted effects due to exceeding the dynamic range. The current study also showed that the band-pass filter based on CS loss was not effective and the full gain was not preferred (the most preferred gains were 1/8 to 1/2 of the full gain). However, with the filters based on supra-threshold contrast loss at 3.6% and 27.9% were both effective. Most subjects with atrophic ARMD and JMD chose gains of around 1 (1x the ratio of CM of abnormal/CM of normal) while quite a few subjects with exudative ARMD chose gains of 2 or 4 (2x or 4x of the ratio). For the equi-emphasis mode, the subjects with atrophic ARMD and JMD chose the two smaller gains of 1.5 and 2 (1.5x and 2x of the ratio), while more subjects with exudative ARMD chose bigger gains of 4 and 8.

Band-pass (CM @ 27.9%) - Gain 2



Band-pass (CS) – Gain 0.5



Figure 6-15. Demonstration of the filtering effects of the band-pass filter based on CM at 27.9% with a gain of 2 and band-pass filter based on CS loss with gain of 0.5.

Three points are drawn from these findings. Firstly, custom-devised filters derived from supra-threshold contrast loss are effective for people with maculopathy, but those derived from CS loss are not, even when the gains were reduced. Secondly, a full gain or a bigger gain is required for the supra-threshold based filter to function well. Thirdly, subjects with exudative ARMD preferred bigger gains than subjects with atrophic ARMD or JMD. This seems to be the rule for all custom-devised filters. This finding is in agreement with the generic filters. Consistently, people with exudative ARMD prefer larger gains or stronger filtering effects than those with atrophic ARMD and JMD. The first phase of within-filter rankings also showed that smaller gains were preferred for the faces than for the general scenes. This finding is consistently shown for the generic filters and the custom-devised filters.

The second phase of between-filter rankings showed subjects' preferences for Gabor and polynomial modes and 1-octave and 2-octave modes. For the band-pass filter at a contrast of 3.6% and 27.9%, in most situations, subjects preferred the Gabor mode, while for peak-emphasis and equi-emphasis filters, in most situations, subjects preferred the polynomial mode (Table 6-7-A). Table 6-7-B demonstrates that the subjects preferred 1 octave more frequently than 2 octave filtered images. With normal vision, the 2 octave filtered images look less exaggerated than the 1 octave filter when applied to the same image.

6.4.2.4 The comparison between generic and custom-devised filters

Although the custom-devised filters functioned better when based on supra-threshold contrast loss than CS loss, this group of individualized filters did not show superiority to the generic filters (shown in Table 6-8 in this chapter). The Peli's adaptive enhancement filter and contrast enhancement filter were the two most effective filters (demonstrated in Table 6-9), not custom-devised filters. Peli (1994) compared an individually tuned enhancement filter which was derived from CS loss with the generic Peli's adaptive enhancement filter. Peli stated that the level of improvement for each subject was similar for the two filters, but only 3 out of 11 subjects with retinal diseases showed significant improvement in visibility with the individually tuned filter.

Considering all these findings, it could be concluded that enhancing the contrasts at certain spatial frequencies where there is loss of sensitivity due to visual impairment back to a "normal" level is not the only optimal way to improve the visibility of images.

6.5 Conclusions

The results of this study show that some generic and custom-devised filters improved perceived visibility of images (general scenes and full single faces) for subjects with maculopathy (atrophic ARMD, exudative ARMD, and JMD). For each combination of image category and maculopathy type, there are corresponding effective filters except for the case of subjects with exudative ARMD viewing single faces. According to the ratings of perceived image visibility, Peli's adaptive enhancement and the contrast enhancement filter stood out as the two most frequently effective filters. Next were the high-pass/unsharp masking, band-pass filter based on contrast matching of 3.6% and 27.9%, and the equi-emphasis filter. The DoG convolution and the Sobel edge enhancement were occasionally effective. Three filters did not lead to improvement. They are the DoG FFT filter, the band-pass based on CS loss, and the peak-emphasis filter. The custom-devised filter derived from supra-threshold contrast loss functioned better than that derived from CS loss. However, the custom-devised filters did not show superiority to the generic filters. Subjects with exudative ARMD preferred relatively bigger gains and smaller kernels than the subjects with atrophic ARMD and JMD. Subjects viewing general scenes preferred bigger gains and smaller kernels than when viewing single faces. Further study is required to find effective filter(s) for subjects with exudative ARMD for viewing single faces.

Chapter 7

Quantitative Assessment of Perceived Visibility Enhancement with Image Processing

7.1 Introduction

In chapter 6, it was shown that digital image processing can improve the perceived visibility of digital images for people with maculopathy. Other studies have shown similar findings for people with visual impairment due to a variety of conditions (Leat et al., 2005; Peli, 1994b). But one remaining question is whether this perceived enhancement can be demonstrated quantitatively or objectively i.e., does it result in measurable improvement in performance.

To answer this question, several methods have been attempted by previous investigators. The earliest one was based on the use of receiver operating curves (ROCs). A number of Peli's studies of image processing for the visually impaired were based on this method (Peli et al., 1991; Peli, 1994; Peli, 2005) For example, in the 1994 study, to investigate the individually tuned Peli's adaptive enhancement for face recognition, they measured the recognition of familiar faces, i.e., celebrities compared to unfamiliar faces. The original and filtered images were shown to people with low vision. Subjects indicated on a scale of 1 to 6 their level of confidence in recognizing a face as a celebrity. These ratings were used to calculate ROCs, plotting the probability of recognizing a true

celebrity versus a false celebrity. Then, the ratio of the area under the ROC obtained from the filtered images to the area under ROC obtained from the unfiltered images was calculated. These ratios could demonstrate if the face recognition with filtered images of familiar faces was improved or not, compared to the un-filtered images in some degree. This method obviously has restrictions. It may function well with certain people who are interested in celebrities and know these faces. But for people who are not well-informed about politics and entertainment, it will not work at all. Sometimes, even for a subject who knows a celebrity, it may be hard for the subject to recognize the face if the face is making an unusual expression. The false positive rate might be high. Considering these two concerns, it is hard to say whether this method is reliable and valid.

In several other studies (Peli, 1999; Peli & Fine, 1996), performance with the enhanced image was evaluated by questions following sequential viewing of either the enhanced and unenhanced versions of the test images. These questions were about visual details contained in the images. In these studies, the low vision subjects answered the questions quite accurately even with the un-enhanced images which renders many questions useless, i.e., there was a “ceiling effect”. This made it hard to show any change between filtered and unfiltered images. The 1994 study of Peli et al. tested the individually-selected enhancements with 16 subjects. The results showed that subjects were able to correctly identify 57% of the details when the image was un-enhanced, and 74% with enhancement ($p = 0.0012$). Interestingly, Peli did not continue with this method in subsequent publications and adopted a new method. This deserves some attention. One can deduce that there must be some shortcomings or restrictions that led Peli in other

directions. The questions developed for the test images were not recorded in the paper and it seems that these questions were not tested on normal control subjects. That is, the reliability of these questions is unknown. It is possible that the questions were too general to reflect a difference between filtered and unfiltered images.

In a recent study (Peli, 2005), Peli developed a similar method to assess the effect of individually-selected Peli's adaptive enhancement. The enhancement was applied to motion video segments. Recognition was tested by measuring the number of visual details that could be correctly identified in response to the questions after observing either the original or the enhanced video segments. The visual details were reflected in questions which were multiple-choice such as, "The woman has... (1) gray hair; (2) black hair". The questions were based on "Audio Description (AD)" used by some US TV stations to describe video for people with visual impairment. The overall means of the number of questions answered correctly for the enhanced segments and unenhanced segments were compared using paired sample statistics. Twenty-five subjects completed this assessment. The results showed that the subjects could answer over 71% of the questions correctly with enhancement and 66% without enhancement. Therefore, this method of quantitative assessment failed to show that the enhanced images significantly increase visibility. This conclusion is contrary to Peli's previous findings (Peli et al., 1994). Peli suggested that "the failure could be attributed to the big variability of AD program itself and it could detect improvement if the effect of enhancement was relatively large". Peli stated in the 2005 paper that "the best methodologies to assess the

effects of enhancement on perceived image quality, and even more so, on recognition performance have yet to be developed”.

The current study was designed to quantitatively assess the visibility enhancement with processed images for people with maculopathy in a valid, reliable, and sensitive way. Since single faces are such a unique type of image that they are perceived differently from general scenes, and since facial discrimination is a difficult task for people with maculopathy, separate methods for assessing improvements in face images and general scenes were developed. The study had two stages. Stage one was a preliminary study to develop a methodology to be used in quantitative measurement of image visibility enhancement. Stage two was the application of this method for people with maculopathy.

7.2 Methods and Materials

To measure improvement in image perception quantitatively, the task should give a good indication of the detail and meaning in the images. For single full face images, facial expression recognition is a good parameter to reflect image visibility. For general scene images, detailed questions developed from the image were considered to be a good parameter to measure visibility.

7.2.1 Images

Full sized images (990 x 1250 pixel or 28.5 x 35.98 cm) were displayed on the same high resolution 21-inch Sony Trinitron monitor which was used in Chapter 6. Images were again displayed with Matlab software named Imageshow which was

programmed by a software programmer from the System Design Engineering Department, University of Waterloo.

Single Full Face Images A CD of full face images with different expressions named JACFEE (Japanese and Caucasian Facial Expressions of Emotion) was used (<http://www.paulekman.com/researchproducts.html>). JACFEE consists of 56 photographs of different people, half of whom are male and half female, and half of whom are Caucasian and half Japanese. The photographs are in color and each photograph illustrates one of seven different emotions (anger, contempt, disgust, fear, happiness, surprise, and sadness). There were eight images for each emotion giving a total of 56 images. Among the eight images, there were two male and two female Caucasians, and two male and two female Asians.

General Scene images Ten general scene images out of the image pool described in Chapter 5 were selected. These images did not include those used in the subjective preference ratings described in Chapter 6. These images were chosen to be complex images including many objects so that questions could be devised about the content.

7.2.2 Preliminary study

Subjects Six subjects with normal vision (aged 25 to 35) and two subjects with maculopathy (aged 59 and 78) participated in this preliminary study.

Single faces The task for the subjects was to tell the facial expression of a briefly presented single face image. Using all the images from the JACFEE CD, subjects needed to choose one expression from 7 possibilities (anger, contempt, disgust, fear, happiness,

surprise, and sadness). Because most of the subjects participated in the quantitative measurement were seniors, the number of facial expressions (7) was considered to be too many for them to keep in mind during the test. Initial testing showed that the image display duration was a critical factor; the longer the display duration, the higher the accuracy of expression recognition. If the display time were not short enough, the task would be too easy and any enhancement in recognition with the filtered images compared to the un-filtered images would not be shown (a ceiling effect). A critical duration time should be determined to eliminate the ceiling effect to show the enhancement effect with the filtered images. Also, it was noted that some facial expressions were easier to recognize than others, while other expressions were very similar to each other. Yet other images did not seem to fit the intended type of expression. The contempt expression was excluded from the beginning because even normally-sighted observers made quite a number of errors about the expression, which means this face expression is confusing to subjects. Therefore, a preliminary study was done to find out the critical display duration time so that the enhancement could be shown, and to eliminate expressions which were too easy or too confusing, and to lower the number of expressions so that the senior subjects could keep the choices of expression in mind while undertaking the test.

The six facial expressions were displayed to the six subjects with normal vision with various durations preceded (duration of 2 seconds) and followed (unlimited duration) by a plain grey image. In total, 48 images were shown with all 6 expressions. The image display sequence is shown in Figure 7-1. An image duration of 2 seconds was used at the beginning. The results showed that no subjects made any mistakes in

recognizing the expressions with this duration. Then, the duration was shortened to 1 second and the subjects with normal vision began to make a very few mistakes. Lastly, the duration was shortened again to 0.73 second which is the minimum duration that the image display program could provide. The normally sighted subjects made more mistakes with this display duration. The results are shown in Table 7-1. The normally sighted subjects did not make any mistakes with the expressions of happiness, and only one with the expression of surprise. Therefore, these two expressions were excluded. Thus, only four face expressions were left (anger, disgust, fear, and sadness), which is relatively easy for senior people to remember at one time. Next the two subjects with maculopathy were tested with the four face expressions using 32 images displayed with a duration of 0.73 second. The results are also shown in Table 7-1. It can be seen that the subjects with maculopathy made more mistakes than the normal subjects under the same experimental conditions. This suggests that the duration of 0.73 second can show a difference between normal subjects and subjects with maculopathy. According to the subjective responses of the two subjects with maculopathy, a choice of four facial expressions was easy for the seniors to undertake. From this preliminary study, the face expression image duration of 0.73 and the four face expressions (anger, disgust, fear, and sadness, shown in Figure 7-2) were chosen for the further quantitative measurement of image visibility.

Grey Image	Face Expression Image	Grey Image
2 seconds	?	Unlimited duration

Figure 7-1. Face expression image display durations, used to determine the optimum duration for the face images. It was preceded with a grey image in 2 seconds and followed by the same grey image for an unlimited duration time.



Figure 7-2. Examples of the four facial expressions finally chosen from JACFEE.

Table 7-1. Number of mistakes of facial expression recognition with face expression image display duration of 0.73 second

Subject	Anger	Disgust	Fear	Sadness	Happiness	Surprise
	N = 8	N = 8	N = 8	N = 8	N = 8	N = 8
Normal S1	0	1	0	2	0	0
Normal S2	1	1	1	1	0	0
Normal S3	0	1	0	0	0	0
Normal S4	1	0	1	1	0	0
Normal S5	0	0	1	0	0	1
Normal S6	1	1	0	1	0	0
Maculopathy S1	3	4	2	3		
Maculopathy S2	4	3	4	3		

General scenes

The purpose of the preliminary study was to develop the same number of questions for each of the ten images and to determine standard answers to these questions. The first step was to develop as many questions as possible from each of the ten images for testing. The rule for the question development was to adopt “how many” questions instead of “yes” or “no” questions, “what”, “where” or “why” questions. Thus, the answer of these “how many” questions would provide a wide range of potential answers which could be qualified. It was possible to develop at least 8 questions based on this condition for each image. Therefore 8 questions from each image were adopted. One example is shown in Figure 7-3. The eight questions for that image were: 1) How many street lamps can you see? 2) How many cars can you see? 3) How many wheels can you see? 4) How many trees can you see? 5) How many garbage cans can you see? 6) How

many driving signs can you see? 7) How many Canadian flags can you see? 8) How many gorillas can you see? The second step was to decide how many images should be involved in this quantitative visibility measurement. The highest rated two filters would be tested plus a control (no filter) to test any learning effect and repeatability. Considering this and the testing time, it was decided that seven images would be optimal. The seven images would be randomized in order. The first three would be assigned for filter 1, another three for filter 2, and the seventh one for the control. The last step was to develop the standard answers for these questions and to validate the questions using the same 6 control subjects who participated in the validation of facial expressions. The general scene images were displayed for unlimited duration. Subjects were allowed to infer from their general knowledge, based on what they could see in the image. After answering each “how many” question, the subject was asked to point to the positions in the image of each object. Thus, standard answers to these questions were gained from the subjects with normal vision. If subjects with normal vision could not answer the question accurately or consistently missed an object, then that question had to be eliminated, or the “correct” standard answer modified. Next, these images were displayed to the two subjects with maculopathy and they were required to answer the same questions. This showed that the subjects with maculopathy made quite a number of mistakes compared to the standard answers from the subjects with normal vision. This indicated that these developed questions do not produce a “ceiling effect”. That is, the questions provide room for improvement with the filtered images.



Figure 7-3. One example of a general scene image for performance measurement.

7.2.3 Subjects

Nine subjects with maculopathy from the group of subjects who participated in the study described in Chapter 6 participated in this session. These were subjects who had recently been involved in the qualitative assessment part of the study and who were willing to attend for a further session. Three of them had atrophic ARMD, four had exudative ARMD, and two had JMD. The two subjects with maculopathy who participated in the preliminary study were not included.

7.2.4 Digital filters

At the fourth visit, the two highest rated filters for each subject (filter 1 and filter 2) were chosen for re-evaluation using the quantitative measures. The names of “filter 1” and “filter 2” were used to distinguish the two filters. Because the intention was to test the enhancement difference between the two filters, they were named according to the rating rate from the qualitative measurement (Chapter 6). 1st filter represents the highest rated filter, and 2nd filter represents the second highest rated filter. For some subjects, the top two filters had been rated equally. In these cases “filter 1” or “2” was assigned arbitrarily.

7.2.5 Procedure

Facial Expression Images

For each subject, the 32 images showing the four emotions were randomized in order. The first 1-15 images were processed by filter 1. The next 16-30 images were processed by filter 2. Images 31 and 32 were not processed and used as controls. These 32 images were mixed and then put into a randomized order for image display. Each image was shown twice in random order, in an original and processed version with one rule that the same face (filtered and unfiltered) would not be shown consequently. The two unfiltered control images were shown twice to measure any practice effect.

The subjects were told that there were four expressions to recognize and a list of the possible 4 expressions in large print was given to them. They were shown one separate image example of each emotion at the beginning to explain the purpose of this session. When testing began, similar to the preliminary study, a plain grey image was

shown before and after the test image. The first grey image was displayed for 2 seconds, the face image for 0.73 second and the second grey image for an unlimited time until the subject gave a response (see Figure 7-1).

Each face expression image presentation was marked as incorrect or correct and the numbers of errors were recorded. For the control images, the coefficient of repeatability was calculated across all subjects (Bland and Altman, 1986) and a paired t -test was applied to consider any practice effect. To study the effect of enhancement with the test images, a paired t -test was also applied across subjects.

To test if there was any enhancement difference between two tested effective filters, the results from the two filters were separated according to 1st filter and 2nd filter, and a paired t -test was applied, excluding those subjects who had rated filter 1 and filter 2 equally.

General Scene Images

For each subject, the seven general scene images used for objective measurement of visibility were randomized in order. Images 1-3 were processed with filter 1. Images 4-6 were processed with filter 2. Image No. 7 was a control and was not processed by any filter. These 7 images were mixed with the 7 original images randomly to determine a display order for each subject with one rule that the same image (filtered and unfiltered versions) could not be displayed consecutively. Each image in its two versions (original and processed) was then shown twice. The control image was shown twice, both in the unfiltered version. The subjects were asked to answer the 8 oral consecutive questions

about each image and the image remained on the screen for as long as the subject needed. Therefore each set of questions were answered two times by each subject, but the order (filtered or unfiltered first) was randomized. After each answer, the subject was asked to point to each object on the screen.

The number given in answer to each question was transferred to an error score. For example, there are five cars in the image of Figure 7-4 so that for the question “how many cars are in the image?” the full correct answer would be scored as 5. If a subject only saw four cars and pointed to them correctly, a score of 4 would be given. The error score was the difference between the correct score and the subject’s answer. In some cases, the subjects gave false positive answers when pointing. For example, there should be 5 cars in the image. The subject may have said 4 cars were seen, but pointed incorrectly to the position of one car, i.e., misidentified another object for a car. In this situation there are two methods to calculate the score. Method 1: Positive mark for each correctly identified car = 3; Method 2: (positive mark for each correctly identified object) – (negative mark for each erroneously pointed to object) = $3 - 1 = 2$. Both of these two methods of scoring were used for comparison.

For the control images, the coefficient of repeatability was calculated across all subjects. For the test images, a paired *t*-test was applied for each subject comparing the error score with the filtered and unfiltered images.

To test if there was any enhancement difference between two tested effective filters, the results from two filters were separated according to 1st filter and 2nd filter, and

a paired *t*-test was applied. For this analysis those subjects who had rated their two best filters equally were excluded.

7.3 Results

7.3.1 Repeatability

Facial Expression Images

The coefficient of repeatability was 1.73 and the mean difference was 0.44. This can be compared with the whole range of the scale. There could be a total of 30 (or 23 taking into account the 25% guessing rate) possible errors. Compared to 30 or 23, 1.73 is relatively small which implies that this facial expression task has good repeatability. It also means that an improvement of 2 or more with the filtered image is a significant improvement at the 95% level. The mean difference of 0.44 suggests that there was hardly any practice effect.

General scenery images

The randomly decided No. 7 control image was displayed twice and the eight questions for this image were answered twice. The coefficient of repeatability for the error score was 0.227 for both methods of scoring and the mean difference was 0.11. The maximum error score for any image ranged from 20 to 32 and the total number of possible errors is between 140 and 224. This is large in comparison to this level of repeatability. This repeatability also means that a significant difference at the 95% level between the filtered and unfiltered image is 1 or more. The mean difference of 0.11 suggests that there was hardly any practice effect.

7.3.2 The effects of filters with test images

Facial Expression Images

The results are shown in Table 7-2. The two-tailed paired *t*-test showed that the best two filters significantly decreased the errors of facial expression recognition across the 9 subjects with maculopathy ($p = 0.004$). Considering this in terms of the coefficient of repeatability (1.73), only subjects 8 and 9 did not show a decrease of 2 or more errors. All other subjects showed significantly fewer recognition errors with the filtered images.

General scenery images

According to the two-tailed paired-*t*-test for each subject (Table 7-2), 6 subjects using scoring method 1, and 7 subjects using scoring method 2 showed significantly fewer errors with filtered images. Considering the coefficient of repeatability of 0.227, all of the 9 subjects showed significantly fewer errors. This suggests that image processing did enhance visibility using a performance measure for all subjects.

Table 7-2. Results of the performance measure of visibility enhancement. D represents the mean error difference per image between unfiltered and filtered images. * shows significance at the level of $p = 0.05$.

Subject	Face Expression Images		General Scenes	
	Errors with original image	Errors with enhanced image	Scoring method 1	Scoring method 2
S1 (Atrophic)	9	6	D = 0.35 p = 0.005 *	D = 0.29 p = 0.029 *
S2 (Exudative)	14	6	D = 0.27 p = 0.026 *	D = 0.31 p = 0.012 *
S3 (Atrophic)	4	2	D = 0.21 p = 0.017 *	D = 0.44 p = 0.003 *
S4 (JMD)	15	11	D = 0.15 p = 0.09	D = 0.15 p = 0.164
S5 (Atrophic)	11	7	D = 0.19 P = 0.027 *	D = 0.29 P = 0.029 *
S6 (JMD)	15	8	D = 0.29 p = 0.005 *	D = 0.31 p = 0.017 *
S7 (Exudative)	15	13	D = 0.60 p = 0.021 *	D = 0.60 p = 0.021 *
S8 (Exudative)	8	8	D = 0.13 p = 0.057	D = 0.17 p = 0.04 *
S9 (Exudative)	12	11	D = 0.10 P = 0.255	D = 0.21 P = 0.077
Mean	11.4	8		
<i>t</i> -test, $p = 0.004$				

7.3.3 The comparison between two best-rated filters

The qualitative average ratings (from Chapter 6) of the 1st and 2nd filters for the 9 subjects are shown in Table 7-3. Since subjects 7 and 9 for faces and 3 and 8 for general scenes had rated the 1st and 2nd filter equally, they were excluded from this statistical analysis. A paired *t*-test showed that the qualitative ratings of the two groups of filters were significantly different ($p = 0.034$ for single faces and $p = 0.015$ for general scenes).

The quantitative measurement results of 1st filter and 2nd filter were separated and analyzed using a *t*-test which is shown in Table 7-4. For the facial-expression-recognition task, a *t*-test was applied to the two groups of errors from the 1st and 2nd filters (subject 7 and 9 were excluded from the analysis). The *p* value = 0.33. This shows that there was no significant difference in visibility enhancement with face expression images between the two groups of effective filters. The higher rated 1st filters did not show better enhancement than the 2nd filters.

For the general scenes, data comparing 1st and 2nd filter were also shown in Table 7-4. Subjects 3 and 7 were excluded from the analysis because they rated the 1st and 2nd filters equally in the qualitative measurement. Only subjects 1 and 9 demonstrated significant differences between their 1st and 2nd filters. However, the *D* values of the 1st filters for subjects 1 and 9 were both smaller than those of the 2nd filters, i.e., the difference was in the unexpected direction. This shows that the highest rated 1st filter did not give better performance than the 2nd highest rated filter.

Table 7-3. Qualitative ratings and type of filter of the 1st and 2nd filters for the 9 subjects for the single faces and the general scenes. S1 to S9 represent the subjects 1 to 9. S7 and S9 for faces and S3 and S9 for scenes rated the two filters equally (shown in grey). p value shows the difference between the qualitative ratings of 1st and 2nd filter excluded the equally rated filters.

Subjects	Face		General Scene	
	1 st Filter	2 nd Filter	1 st Filter	2 nd Filter
S1 (JK)	145 (BP_Equi Emphasis)	117.5 (BP_3.6%)	125 (High-pass)	120 (DOG Convolution)
S2 (BT)	115 (BP_Peak Emphasis)	107.5 (BP_Equi Emphasis0	110 (BP_Equi Emphasis)	107.5 (BP_CS)
S3 (LL)	132.5 (DOG Convolution)	130 (BP_3.6%)	127.5 (Peli Enhancement)	127.5 (BP_CS)
S4 (NA)	127.5 (BP_CS)	122.5 (BP_27.9%)	145 (BP_Equi Emphasis)	140 (BP_Peak Emphasis)
S5 (LG)	150 (DOG Convolution)	135 (Peli Enhancement)	145 (BP_Equi Emphasis)	140 (DOG Convolution)
S6 (DG)	135 DOG Convolution	127.5 (DOG FFT)	130 (BP_Peak Emphasis)	128.5 (BP_3.6%)
S7 (SF)	175 (BP_27.9%)	175 (BP_Equi Emphasis)	175 (BP_Equi Emphasis)	175 (DOG FFT)
S8 (GC)	107.5 (BP_3.6%)	106.5 (BP_27.9%)	105 (High-pass)	104.5 (Peli Enhancement)
S9 (BS)	125 (High-pass)	125 (BP_27.9%)	142.5 (BP_27.9%)	132.5 (Contrast Enhancement)
Paired <i>t</i> -test	p = 0.034		p = 0.015	

Table 7-4. The comparison of quantitative assessment of performance between the 1st filter and 2nd filter. D represents the mean differences of error per image (original-filtered) for each subject. The bigger the D value the more effective the filter. * shows significance at the level of $p = 0.05$. The blank data are where the 1st filter and 2nd filter were equally rated from the qualitative measurement.

Subject	Facial Expression Images		General Scene Images		
	Errors with 1 st Filter	Errors with 2 nd Filter	1 st Filter	2 nd Filter	p
S1 (Atrophic)	2	4	D = 0.00	D = 0.71	p = 0.003 *
S2 (Exudative)	2	4	D = 0.33	D = 0.21	p = 0.60
S3 (Atrophic)	2	0			
S4 (JMD)	4	7	D = 0.13	D = 0.17	p = 0.81
S5 (Atrophic)	4	2	D = 0.25	D = 0.13	p = 0.45
S6 (JMD)	4	4	D = 0.42	D = 0.17	p = 0.21
S7 (Exudative)					
S8 (Exudative)	2	6	D = 0.08	D = 0.17	p = 0.52
S9 (Exudative)			D = -0.13	D = 0.33	p = 0.01 *
Mean	2.86	3.86			
p (between 1 st and 2 nd filter) = 0.33					

7.4 Discussion

The method developed in this study used to measure performance-based assessment of visibility improvement with image processing for the visually impaired overcame the limitations of previous methods. The use of familiar versus unfamiliar face recognition (Peli, 1994b) was obviously limited by the familiarity of the celebrities to each subject. If a subject did not know any of the celebrities or only a limited number of celebrities, the method would not be successful. The current study used facial expressions

to reflect the visibility of the single face images. This method is applicable to all people and does not rely on specific knowledge. Besides, the faces were from both Caucasians and Asians, both men and women. Thus people from different racial backgrounds were included making the application more generalizable. Also, the four face emotions chosen for the quantitative measurement were selected through preliminary study with subjects with normal vision. The ease of the task and the difficulty for recognizing particular facial expressions for the older maculopathy population were considered.

Details regarding the specific questions for general images (Peli et al., 1994a) were not well recorded in literature. The kind of questions or how many questions were derived for one image has not been published. Other studies with questions (Fine, Peli, & Brady, 1998; Peli, 1999; Peli & Fine, 1996) turned out to be ineffective. The most recent study, based on audio described questionnaires (Peli, 2005), did not show a significant difference between filtered and unfiltered video sequences, and therefore the questions may have had poor sensitivity. The current study developed questions according to certain rules. The questions and answers were first tested by subjects with normal vision. This ensures some validity to the questions. Additionally, all the answers were numbers varying from 0 to 12 which gave a wide span for measurement of change. This eliminated the “ceiling effect” shown in Peli’s studies.

With these methods, image visibility enhancement with digital filtering was demonstrated quantitatively for people with maculopathy. Although the current study was only undertaken on a subset of subjects, the results confirm the improvements perceived by the subjects. When comparing many filters it is quicker to use subjective ratings, but

here we have confirmed that when subjects prefer an image it does lead to improved performance i.e. people do actually see more accurate information in an image.

As for the relation between qualitative measures and the quantitative measures, the current study seems to suggest that they are not necessarily directly related. This is demonstrated by the comparison of the two effective filters of 1st and 2nd effective filters. Five out of seven subjects did not show any difference between the two filters, and two subjects even showed that the lower rated 2nd filter gave better performance than the higher rated 1st filter. Therefore, people's visual subjective rating of how much improvement they perceive may be not very reliable. The objective measurement of visual enhancement demonstrates how much more detail the subjects can detect in the filtered images.

The methods developed and used in this study not only overcome the limitations of previous methodologies and turned out to be effective, but also have the potential of being a widely applicable standard method because they meet the criteria of validity, reliability, and sensitivity.

Validity

Validity is the degree to which a measure actually reflects that which it purports to measure (Anastasi & Urbina, 1997, p114). In the current study, the purpose was to directly measure visibility enhancement with filtered images compared to unfiltered images. The recognition of facial expression is important in daily life and therefore this measure has face, i.e., apparent validity and we would seem to be measuring an important

aspect of viewing a face. The facial expression images were professionally made. All the expressions shown in the images were previously tested by large numbers of subjects and shown to have accurate expressions (Biehl et al., 1997). Therefore, this group of facial expression images could be used in the current and subsequent research of image enhancement techniques applied to face images.

For the general scene images, the measurement of image detail perception differences between filtered and unfiltered images provided evidence about the amount of improvement in performance gained with image enhancement. Eight questions for each image were developed about details in the image. It seems intuitively obvious that correctly identifying details within an image is important. Therefore, there is face validity regarding this measure. Also, the fact that we did measure an improvement with the preferred filters indicated validity.

Reliability

In research, the term reliability means “repeatability” or “consistency” (<http://trochim.human.cornell.edu/kb/reliabl.htm>). A measure is considered reliable if it gives us the same result over and over again when administered at different times, locations, or with different populations. In the current study, the measurement of objective visibility was administered to the same subjects at two points in time. Therefore, the test-retest reliability can be considered. The coefficient of repeatability is one method to calculate test-retest reliability. This is 1.96x the standard deviation of the differences and thus 95% of differences are less than this value. In the current study, the

coefficient of repeatability (Bland & Altman, 1986), for face expression images was 1.73, which is a small number compared to the total possible mistakes which is 30. This suggests that this method of facial expression recognition is reliable. For the general scene images, the coefficient of repeatability was 0.227. The total possible number of mistakes was 187 and, therefore, the coefficient of repeatability is a small proportion of the total measurement range. This suggests that the questions developed to show objective image visibility enhancement are reliable. There were no large practice effects, i.e., the subjects did not gain benefit from seeing the image a second time, even within a short space of time (the experimental session).

Sensitivity

Sensitivity is the ability of a measurement to detect a disease, condition or change. In this study, the condition to be detected is an objective measure of improvement in visibility as a result of digital image enhancement.

For the facial expression recognition task, the paired-*t* test for 9 subjects showed that there was a significant effect of image processing on image visibility ($p= 0.004$), e.g. fewer errors were made with filtered images than with the unfiltered images. For the general scenes, a paired-*t* test for each subject indicated that 6 or 7 subjects (depending on scoring method) out of a total of 9 showed significantly enhanced visibility with filtered images than with unfiltered images. These two groups of results suggest that the measurements used to demonstrate the objective visibility enhancement are sensitive enough to detect the improvements in visibility suggested by the subjective ratings. For

the general scene, each question had quite a range of possible answers. For example, if the standard answer obtained from the normal observers was 5, there could be at least 5 possible answers from the subject (0, 1, 2, 3, 4, 5, or more than 5 with false positives). Accordingly, the errors between the normal answer and the answer from the subject have a relatively large potential range. These questions encouraged the subjects to observe almost every detail of an image. These kind of questions could be generated for almost any general scene. This helped to ensure the sensitivity of the methodology.

7.5 Conclusions

The method developed in the preliminary study turned out to be effective in objective (quantitative) measurement of the image visibility enhancement with digital filtering for people with maculopathy. The results of the objective measurement were not directly in proportion to those of the qualitative measurements. The facial expression task was valid for measuring single face perception. The questions developed for general scenes also appeared to be a valid method. The methodology developed and validated in the current study is proposed as a standard method to be utilized in other future studies of image enhancement.

Chapter 8

General Discussion

Compared to the former studies of application of digital filtering for people with visual impairment to enhance image visibility (Peli, 1991; Peli, 1994b; Leat et al., 2005), the current study has some unique aspects. First, this project focused on people with maculopathy only, and the maculopathy was further grouped according to the diagnosis of atrophic ARMD, exudative ARMD, and JMD. Therefore effective filter(s) were found for each specific type of maculopathy. Secondly, this study grouped the test images into single full faces and general scenes according to the image spatial frequency characteristics. Effective filter(s) were also found specifically for each image category. Thirdly, this study tested custom-designed filters based on supra-threshold contrast loss rather than just CS loss. The CS loss derived custom-devised filters were tested in some former studies (Leat et al, 2005; Peli, 1994b) and found to be ineffective. The results showed that the supra-threshold contrast loss derived custom-devised filters were effective. Fourthly, this study compared generic filters with custom-devised filters derived from supra-threshold contrast loss. The results showed that the custom-devised filters were not superior to the generic filters. Fifthly, not only was a qualitative measurement of visibility enhancement used but also a quantitative measurement. The method designed for the quantitative enhancement was able to demonstrate improvement in visibility.

8.1 Supra-threshold contrast matching in control groups

In order to develop the custom-devised filters derived from supra-threshold contrast loss for people with maculopathy, two age groups of control data of supra-threshold contrast matching were collected. The main purpose was to develop a control data set against which the subjects with maculopathy could be compared to calculate the gain for the various custom-devised filters. The effects of age and contrast threshold on supra-threshold were investigated at this stage.

The supra-threshold contrast matching results for the two groups were quite similar to Georgeson and Sullivan's findings (1975). At low contrast, the matching curves resembled the threshold curve, while at medium and higher levels, the curves became flatter, described as contrast constancy. This study extends their data to show that contrast constancy exists in a larger group of naïve subjects of different ages. The data showed that, at 55.9% contrast, the matching functions against spatial frequency were best fit with a quadratic function, rather than a straight line ($p < 0.001$) and the matching was still spatial frequency dependant, with a peak at 1 to 2cpd. This indicates that contrast constancy was still not complete up to 55.9%.

Aging increased contrast thresholds for spatial frequencies between 0.26 and 8.53 cpd in the current study. The interesting question here is whether, as thresholds change with age, there is a change in the supra-threshold gain of the system to compensate. By calculating the regression lines of the matched test grating contrast against the standard grating contrast, it was found that the slopes of the regression lines were similar for the two age groups (two-sample t -test, $p > 0.05$ in all cases). Whether age-related supra-

threshold differences in slope would be found would depend on the relative thresholds of the standard and the test grating. The threshold curves in Figure 3-1 showed that the relative thresholds for 0.58 cpd and other spatial frequencies for the two age groups are similar. Since the older subjects showed a decrease of contrast sensitivity at all spatial frequencies, there is little change in the relative thresholds. Also, as it happened, there was no example where the data points for the relative thresholds in Figure 3-2 or 3-3 were above the line for unity for one group and below it for the other. Thus, the present data cannot answer the question of whether there are changes in the gain to compensate for thresholds changes with age.

To test whether contrast matching can be accounted for by subtracting the thresholds (Kulikowski, 1976), and to examine the differences of contrast matching with respect to age, the data were normalized by subtracting the linear threshold for 0.58 cpd from the standard contrast and the threshold at each matched frequency from the matched contrast (McIlhagga, 2004) and then taking the logarithm. Similar to the non-normalized data, the regression lines were still affected by their corresponding thresholds.

In general, at most levels of contrast the two groups matched supra-threshold contrast similar statistically although the contrast thresholds were significantly different.

8.2 Supra-threshold contrast matching in maculopathy

To investigate the supra-threshold contrast loss in maculopathy and as a basis for the custom-devised filters, the supra-threshold contrast matching was tested for the three groups of subjects with maculopathy (atrophic ARMD, exudative ARMD, and JMD).

The results were compared to the older control group for statistical analysis. There were two reasons that the younger control group data were not used in this comparison. First, there was no main effect of age in supra-threshold contrast matching for the two control age groups. Second, most of the maculopathy subjects belonged to older age group. To test the effect of threshold on supra-threshold contrast, the contrast threshold was measured as well.

The results showed that the average contrast thresholds of maculopathy patients were significantly higher than the 95% age-matched normal range at all spatial frequencies tested. In all three groups of subjects with maculopathy, the peaks of the CSF shifted to lower spatial frequencies. The supra-threshold contrast matching results plotted across contrast levels appear quite similar to the previous findings with subjects with normal vision. At low contrasts, the matching curves resemble the threshold curve, while at medium and higher levels, the curves become flatter, demonstrating contrast constancy. Contrast matching at 3.6% and 27.9% was analyzed with ANOVA. There were differences between the normal control and the maculopathy group at both levels of contrast. Thus, the results are also in agreement with a previous study (Leat & Millodot, 1990), showing that there are deficits of supra-threshold contrast perception in people with maculopathy. Similar to this previous study, these deficits are not as great as the deficits in contrast threshold - there is some compensation for contrast sensitivity loss. Also, similar to normal vision, there is a connection between contrast threshold and supra-threshold contrast perception. This is in agreement with previous studies which have suggested neural compensation by means of a change in gain.

Gain Compensation

Variations of contrast gain in the visual system which is located at the retina and visual cortex are usually used to explain contrast constancy (Georgeson & Sullivan, 1975). For normal vision, contrast gain was found to change so that contrast perception was fairly accurate even under different visual conditions such as dark adaptation. In ocular disorders, it has also been suggested that there is a gain adjustment (Dickinson & Abadi, 1992; Leat & Millodot, 1990). In the present study, the gains for people with maculopathy were significantly different than the normals especially at higher spatial frequencies, and these differences were in the direction expected to compensate for differences in thresholds (Figure 4-4). For higher spatial frequencies, where contrast sensitivity is more reduced compared to the lower spatial frequencies in maculopathy (Figure 4-2), the slopes were reduced compared to the controls, i.e., more contrast is required to make a match nearer threshold and less contrast is required at higher contrasts. The subjects with maculopathy are, therefore, showing modification of the gain, presumably as a result of the contrast sensitivity loss due to the disease process. Gain control has been suggested in various stages in the visual pathway; retina (Albrecht & Hamilton, 1982), Lateral geniculate nucleus (Webb et al., 2003; Webb et al., 2002; Przybyszewski et al., 2000), visual cortex (Geisler & Albrecht, 1992; Carandini & Ferster, 1997; Truchard et al., 2000) or by feedback from extrastriate cortex (Gardner et al., 2005) and may, of course, occur at all these locations. There is evidence that damage in ARMD is not only limited to photoreceptors, but occurs in the various retinal layers from photoreceptors, horizontal cells, bipolar cells to ganglion cells (Enoch, 1978; Dunaief

et al., 2002; Kim et al., 2002). For advanced maculopathy, as in the current study, the retinal gain control may be expected to be damaged. It would therefore appear that the contrast gain compensation does happen in the cortex or that the cortex is able to compensate for damage to the gain control in the retina.

One interesting question is, how long the visual system needs to adjust the contrast gain as a result of CS loss. One case with bilateral congenital cataract removal resulting in improved CS showed that the contrast of high spatial frequencies was overestimated by the patient's visual system as long as one year after the surgery (Fine et al., 2002). In the current study, all the subjects were recruited from the Low Vision Clinic or CNIB and had had maculopathy at least 2 years before they took part in the study. Some participants with age-related maculopathy (a progressive condition) may have experienced changes in their condition fairly recently prior to the study. However, juvenile macular degeneration progresses earlier in life and is more stable later. These subjects would be less likely to have changes in the period prior to the study. Yet, these groups (ARMD and JMD) performed similarly in the present study. This would seem to indicate that initial changes in gain occur quite rapidly. However, there were significant differences between the maculopathy and the normal group. This would seem to indicate that, although some adaptation occurs, it does not completely compensate for CS losses, even after many years.

Overconstancy

Another explanation for the apparent contrast constancy may be in overconstancy. Observers with advanced maculopathy use a PRL for fixation, at which location normal observers show overconstancy (Georgeson & Sullivan, 1975). Georgeson's data (1991), shown in his Figure 3a, is replotted in Figure 8-1. A trend of overestimating of test gratings' contrast at higher spatial frequencies (> 3 cpd) can be seen, especially at low contrasts and high spatial frequencies. Observers with maculopathy who were doing contrast matching with PRL fixation and peripheral vision (shown in Figure 4-3) did not show this trend but rather underestimated test grating contrast at higher spatial frequencies (> 0.5 cpd). Considering the partial contrast constancy shown by the subjects with maculopathy, there are two possible ways to explain this. First, the PRL functions as a new "fovea" losing the normal overconstancy of eccentric vision but with adjustment of the gain to compensate for the loss of CS due to the disease process. Second, the PRL still functions as eccentric retina with contrast overconstancy which in itself partially tends to compensate for loss of CS due to the disease process. The present data are not able to distinguish between these two situations.

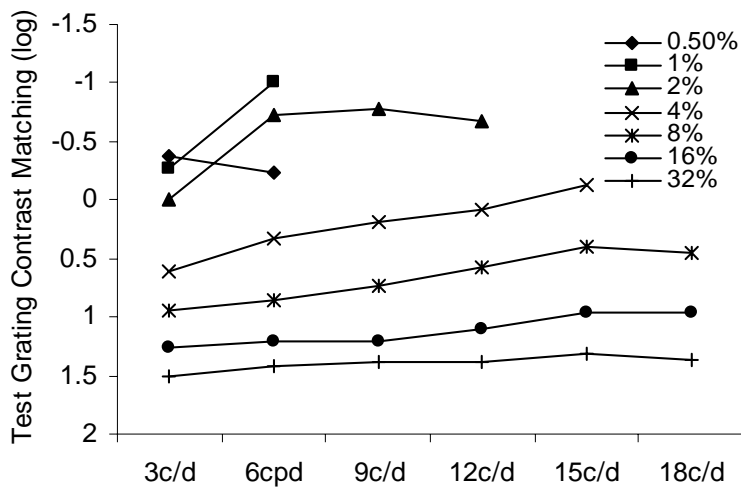


Figure 8-1. Replotting of Figure 3a from Georgeson (1991). Contrast overconstancy was shown with eccentric fixations for both standard and test gratings.

Is there any evidence that there is plasticity of the cortex, so that the PRL may function like the fovea? There is early evidence that there is considerable plasticity in the visual cortex, even in adults. Some researchers have shown evidence of retinotopic cortical re-organization. Animal studies with monkey and cat (Gilbert & Wiesel, 1992; Darian-Smith & Gilbert, 1994; Calford et al., 2000) have shown that reorganization in adult mammalian visual cortex occurred following visual field loss. Studies in humans (Morland et al., 2001; Baseler et al., 2002) reported abnormal retinotopic organization in cases of congenital vision loss and in long-standing macular degeneration of over 20 years (Baker et al., 2005). They found that parts of the visual cortex that normally respond only to central visual stimuli were strongly activated by peripheral stimuli. However a recent study reported no retinotopic re-mapping of a 60-year-old subject with

a 3-year history of atrophic ARMD (Sunness et al., 2004). Thus, so far no studies have provided evidence for reorganization of visual cortex in older adults with visual loss which is less long standing. However, in the present study, no difference was found in supra-threshold contrast matching between the three maculopathy groups, although some were more long standing (those with JMD) and some of more recent onset (ARMD). These results seem to support the view that there may be some cortical reorganisation (so that the PRL functions more like the fovea) or that there are changes in the gain which is likely located in the cortex.

An alternative explanation could be based on Brady and Field's work (1995). Maculopathy would result in an increase in noise resulting in an increase in thresholds, but supra-threshold performance, which depends on average signals rather than signal to noise ratio, would be affected to a lesser extent or not at all. With this model there would be no need to suggest a change in gain. In fact, the partial contrast constancy might indicate some deficit in gain.

This study has shown that there is a supra-threshold contrast perception defect in people with maculopathy compared to those with normal vision, although this deficit is not as great as that for CS. Thus, one would conclude that the actual performance of people with AMD may not be as poor as CS predicts. Whether this is found to be true is a subject for future research.

8.3 Image analysis and grouping

The effective digital filters were found to be not only specific to type of maculopathy but also specific to the category of image. Leat et al. (2005) also demonstrated this in their study. However, in their study the image grouping was according to the subject content in the images. There was no objective evidence to support their grouping. Spatial frequency, amplitude, orientation and phase are the basic parameters which describe the spatial frequency content of an image. In this study, phase was not considered (which will be one interest in the future study). Amplitude spectrum of spatial frequencies and the slope of the amplitude against spatial frequency were measured at three orientations (horizontal, vertical, and oblique). The 132 images were first grouped into six groups according to the apparent subject matter of the images (single face, one whole person, two or more whole persons, indoor scenes, natural scenes, and miscellaneous). Then the amplitude spectra and slopes were analyzed statistically to show which groups were distinctive from other groups.

There were differences in amplitude and slope with respect to orientation. For most image groups, the amplitude is greater in the cardinal orientations than the oblique. Essock et al. (2003) suggested greater gains in the oblique vs. vertical vs. horizontal meridian. This is the reverse of the finding that in images there is greatest average amplitude for horizontal contours (vertical spatial frequency components) and least in the oblique orientation, which was found for almost all image types in this study. Thus, it would seem that the anisotropy of gains within the visual system tends towards

compensating for the anisotropy of real world images, resulting in a more equal perception of differently orientated contours.

For slopes, the current study found the same trend in all six groups of images: vertical > horizontal > oblique, i.e., shallower in the vertical. This implies that there is relatively more high-frequency content in the vertical meridian, i.e., for horizontal contours.

Single faces were found to be the most consistently distinctive image type (according to spatial frequency content) among all six groups. They had significantly lower average amplitudes than other groups of images. However, they are similar to other images in having the smallest slope in the vertical meridian, thus having relatively more high spatial frequency information in the vertical meridian (horizontal contours). The physical uniqueness of single-face images is consistent with the uniqueness of single face perception in the visual cortex (Farah et al., 1998; Wang et al., 1998, Hasson, et al., 2001; Ishai et al., 2000). Therefore, grouping images into single full faces and general scenes was considered to be reasonable in the later section of image visibility enhancement with digital filtering.

8.4 Measurement of perceived visibility improvement

This part was a continuation of the study of Leat et al. (2005). Due to the modified method, more filters were found effective. Both generic filters and custom-designed filters were tested. The custom-designed filters were derived from the supra-threshold contrast loss compared to the normal age-matched control data. Eight filters

were found to be effective in improving perceived visibility: contrast enhancement, Peli's adaptive enhancement, DoG convolution, high-pass/unsharp masking, Sobel edge enhancement, band-pass at 3.6% and 27.9%, and equi-emphasis band-pass filters. These filters are effective specifically for one or more combinations of maculopathy type (atrophic ARMD, exudative ARMD, and JMD) and image category (single full faces and general scenes). The combination of subjects with exudative ARMD viewing single faces did not give rise to any significantly effective filters.

The DoG filter in this study was applied in both spatial domain and frequency domain. There was some overlap in enhancement effects between these two domains. As shown in Figure 8-2, the effect of DoG convolution with a kernel of 7x7 and a gain of 1 is very close to the DoG FFT with a central spatial frequency of 4cpd and a gain of 4. This suggests that the convolution processing with a kernel of 7x7 has its primary effect at a central spatial frequency of 4cpd which is therefore the highest central spatial frequency that a convolution domain DoG filter would enhance in this study. Therefore, the DoG FFT filters used in this study enhanced spatial frequencies at a wider range of central spatial frequencies (from 0.5 to 8cpd) than the spatial domain DoGs.

DoG Convolution_7x7_gain1

DoG FFT_4cpd_gain4



Figure 8-2. The overlap effects of DoG convolution and DoG FFT.

The current findings regarding Peli’s adaptive enhancement filter are basically in agreement with Peli’s studies of this filter (Fullerton, & Peli, 2006; Peli et al., 1991; Peli, 1994a, 1994b). In Peli’s studies, the filter was effective for both single faces images and TV segments in improving visibility for people with visual impairment. In the current study, Peli’s adaptive enhancement was demonstrated to be effective mainly for the general scenes. For the single faces, only the atrophic ARMD group found this filter effective. The within-filter rankings showed that large kernel sizes (21 or 25) and smaller gains (2 or 4) were most often preferred by subjects. In the former study of Leat et al. (2005), Peli’s adaptive enhancement filter was found to be borderline effective for the image category of “faces” in perceived visibility improvement. However, this effect was not found for subjects with maculopathy (their Figure 4). The modified methodology may explain why more effective filters were found from the current study.

It is found that high-pass/unsharp mask had no effect for single faces but was effective for both the subjects with atrophic ARMD and JMD with general scenes. This is in agreement with Leat et al. (2005) regarding the unsharp masking filter.

Generally, for all preferred filters, the face images seem to be preferred with less gain/strength of filtering than the general scenes. This difference may be attributed to the spatial characteristics of single face images and general scene images. Chapter 5 has shown that single face images have lower amplitude spectra of spatial frequencies in three orientations (horizontal, vertical, and oblique) but have similar slopes (amplitude spectrum versus spatial frequency) compared to general scene images. This suggests that the single face images have less high-spatial frequency content than the general scenes. For people with maculopathy, the high spatial frequencies perception is more damaged than medium and lower spatial frequencies. Thus general scene viewing (with relatively more high spatial frequency information) should be more damaged than single face viewing (with relatively less high spatial frequency information) for people with maculopathy. Therefore, it is expected that the optimum digital filtering gains/strengths for single faces are smaller than those for general scenes.

The subjects with atrophic ARMD and JMD behaved more similarly. They preferred smaller gains and bigger kernels than the subjects with exudative ARMD. This is probably related to the severity of pathology. Usually, exudative ARMD is more severe than the other two maculopathies.

The custom-devised filters based on supra-threshold contrast perception loss were found to be effective. This supports the concept that supra-threshold contrast may be more important to everyday visual function than contrast sensitivity because most everyday scenes contain spatial information that is supra-threshold. However, the custom-devised filters were not found to be superior to the generic filters. Thus compensating for the lost contrast at each band of spatial frequency for each individual is not better for enhancing image visibility than filters which are similar between subjects such as Peli's adaptive enhancement and the contrast enhancement filters.

8.5 Measurement of quantitative visibility improvement

Digital filtered images do enhance the visibility of images for people with maculopathy. The question is how much improvement is generated. Peli et al. tried three methods to measure image visibility improvement quantitatively (Fine, Peli, & Brady, 1998; Peli, 1999; Peli & Fine, 1996, Peli 1994 a, b; Peli, 2005). For single faces, a method of recognizing celebrity or non-celebrity faces was applied. The application of this method depends on subjects' familiarity with those celebrities. For general scenes, a method of answering questions about the tested images was applied. The results from these developed questions were not effective because of the "ceiling effect". That is, the low vision subjects answered the questions quite accurately even with the un-enhanced images which renders many questions useless. There was no room for improvement. Therefore, Peli's methods have limitations. The current study reconsidered this question and demonstrated that visibility improvement can be measured quantitatively. The two

most preferred filters were evaluated for 9 subjects who took part in the qualitative measurements.

This section was done in two steps. The first step was to develop effective methods in a preliminary study. The second step was to apply these methods to the nine subjects to measure the improved visibility quantitatively.

For face images, the recognition of facial expression is important in daily life. This section adopted this idea to measure the enhanced visibility quantitatively after filtering. A CD of full face images with seven different expressions named JACFEE was used. All the expressions shown in the images had been previously tested by large numbers of subjects and shown to be accurately recognizable. The preliminary study testing subjects with normal vision was done to develop the effective methodology. Four emotions from the seven were chosen based on difficulty of recognition (for example, surprise and happiness were too easy to recognize) and the short memory of seniors (four emotions were easier for them to remember than 7 emotions). For general scenes, the measurement of the perception of image detail before and after filtering was found to be an effective measure. The preliminary study with subjects in normal vision was done to develop eight effective questions from each of the 7 images. This ensures the “quality” of the questions. Additionally, all the answers were a certain numbers varying from 0 to 11 or 12 which gave a wide span to measure change. Through the preliminary study, the developed methodology for single faces and general scenes avoided the “ceiling effect” that was demonstrated in Peli’s studies.

With the methods developed by the preliminary study, the image visibility enhancement with digital filtering was demonstrated in a quantitative way for the people with maculopathy. The results firstly showed that both face expression recognition and answering questions designed for the general scene images had good repeatability. This suggests that the two methods are reliable. It was also confirmed that, when subjects prefer an image, it does lead to improved performance, i.e., people do actually see more accurate information in an image. However the higher rated perceived visibility enhancement does not necessarily correspond to higher quantitative enhancement. The top two highly rated filters from the section of qualitative measurement were compared and the statistical analysis showed that there was a significant difference between the two perceived rating scores across the 9 subjects. But the quantitative measurement results did not show this same trend (7 out of 9 did not show significance, 2 showed opposite significance). This suggests that the quantitative measurement may be more reliable in demonstrating visibility enhancement than the qualitative measurement.

In general, the methodology developed in this section is repeatable, valid and sensitive. It could be applied in future studies.

8.6 Implementation in the future

From an application point of view, the generic filters allow images to be processed quicker than the custom-devised filters. Besides, the custom devised filters are individually based on the lost contrast perception due to maculopathy and require the prior measurement of contrast matching. If generic filters have a similar or better effect on image visibility compared to the custom-devised filters, it would not be worthwhile to

use custom-devised filters. The present results show that the custom-devised filters were not better at improving image visibility than the generic filters. The two most frequently effective filters for all three groups of maculopathy and the two categories of images were Peli's adaptive enhancement filter and the contrast enhancement filter.

8.7 Future work

Based on the findings from the current study, several questions still remain to be answered. 1) There is still no filter that was preferred for subjects with exudative ARMD for face images. 2) Would quantitative testing reduce the number of filters that are shown to be effective for the whole population of people with maculopathy? The qualitative results show that there are some filters which are commonly preferred between groups. 3) Are the same filters effective for static and moving images?

Three further studies could be done in the future.

Study one: Identification of potential filters for people with exudative ARMD viewing single face images. The results showed a larger variability in preferred filter ratings scores for the subjects with exudative ARMD. Therefore, one possibility is to test those borderline effective filters (such as the DoG convolution and the band-pass based on CM at 27.9%) quantitatively for a whole group of subjects with exudative ARMD for faces. It is possible that subjects with exudative ARMD did not rate the filters very highly as the image still looks poor to them, but they might gain improvement in performance. An alternative method would be to study the effects of phase in this population.

Study two: Identification of effective filters for the whole population of maculopathy.

If study one shows some effective filters for subjects with exudative ARMD viewing single face images and these filters are also preferred by subjects with atrophic ARMD and juvenile maculopathy, a commonly preferred group of filters would be tested using the quantitative method for all groups of maculopathy. This might simplify the implementation of effective filters in low vision devices by reducing the number of filters.

If the three groups of subjects with maculopathy do not show any common preferences, the three eye disorders still need to be tested separately. Again quantitative assessment could be applied but for each maculopathy group separately. The best filter(s) for each group could be identified.

Study three: Application of effective filters assessed from static images to video clips. Quantitative assessment could be applied to viewing video face clips and general scene video clips.

For the face clips, facial expression recognition could be investigated with and without filtering. For general scene clips, a series of questions could be generated similar to the current study. The subjects would be asked to answer these questions with and without filtering.

The ultimate aim of the project is to implement these beneficial image processing techniques into actual vision aid devices to help people with maculopathy. Ideally these filters would be effective for static images (as viewed through a closed-circuit TV or a computer) and for moving images such as video viewed with DVD or video clips viewed

with a computer. A specialized application would be real-time images viewed through a head-mounted electro-optical device which includes magnification.

Chapter 9

General Conclusions

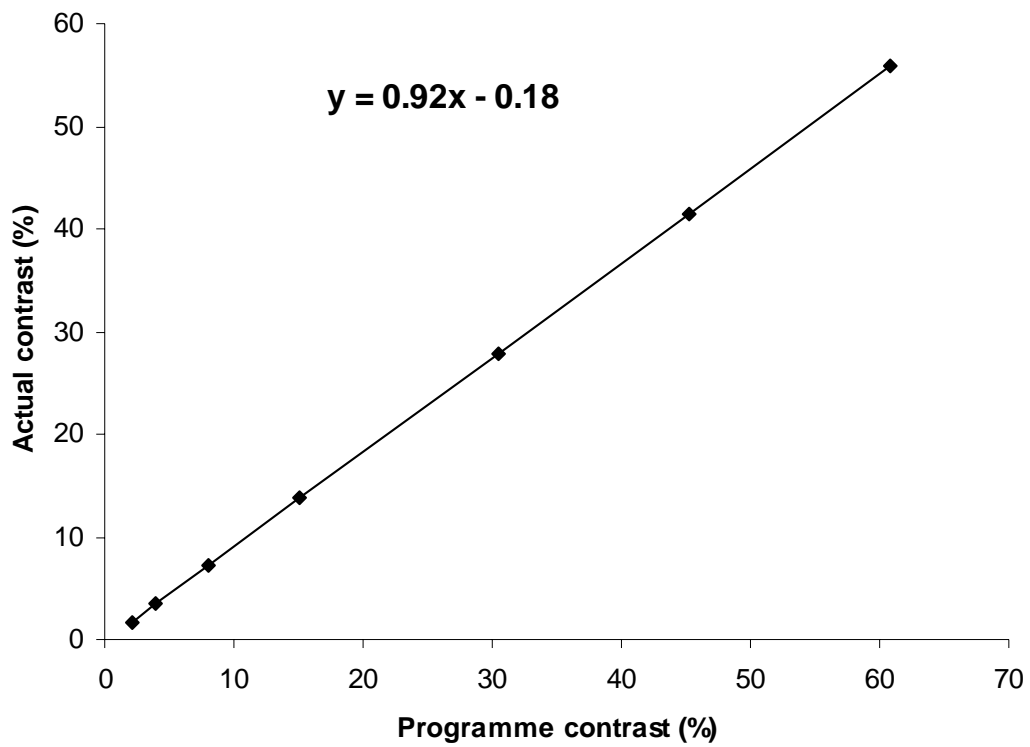
1. Contrast constancy was shown to exist in a larger group of naïve subjects of different ages, but did not perfectly compensate for the differences in contrast thresholds. The results are discussed in terms of the currently proposed models of contrast perception and are best explained by the model proposed by Näsänen et al (1998).
2. A degree of contrast constancy was shown in maculopathy, although there were still deficits compared to control subjects. This is discussed in terms of either the gain of the visual system adjusting to compensate for CS losses (although incompletely) or contrast overconstancy, which is present in normal peripheral vision, helping to compensate for the CS loss.
3. The amplitude spectra and slope in the three orientations can be used to describe the physical characteristics of images and to distinguish between different groups of images. Single faces were the most distinctive image group showing lower amplitude spectra in all three orientations. It was also shown that most everyday scenes have more spatial frequency power in the vertical and horizontal than oblique orientations.
4. Eight filters were found to be effective: contrast enhancement, Peli's adaptive enhancement, DoG convolution, high-pass/unsharp masking, Sobel edge enhancement, band-pass at 3.6% and 27.9%, and equi-emphasis band-pass filters.

Three filters were not effective: DoG FFT filter, the band-pass at contrast threshold, and peak-emphasis filter.

5. The custom-devised filters derived from the supra-threshold contrast loss were effective, but were not better than the generic filters in visibility enhancement.
6. The single full faces were preferred with smaller gains and bigger kernels than the general scenes. The subjects with atrophic ARMD and JMD preferred smaller gains and bigger kernels than the subjects with exudative ARMD.
7. The methodologies developed for performance assessment were found to be effective in measuring changes of image visibility with digital filtering for people with maculopathy. The results of objective measurement were not directly proportional to those of the qualitative measurements. The methodologies developed in the current study meet the criteria to be a standard method to be utilized in future studies of image enhancement.

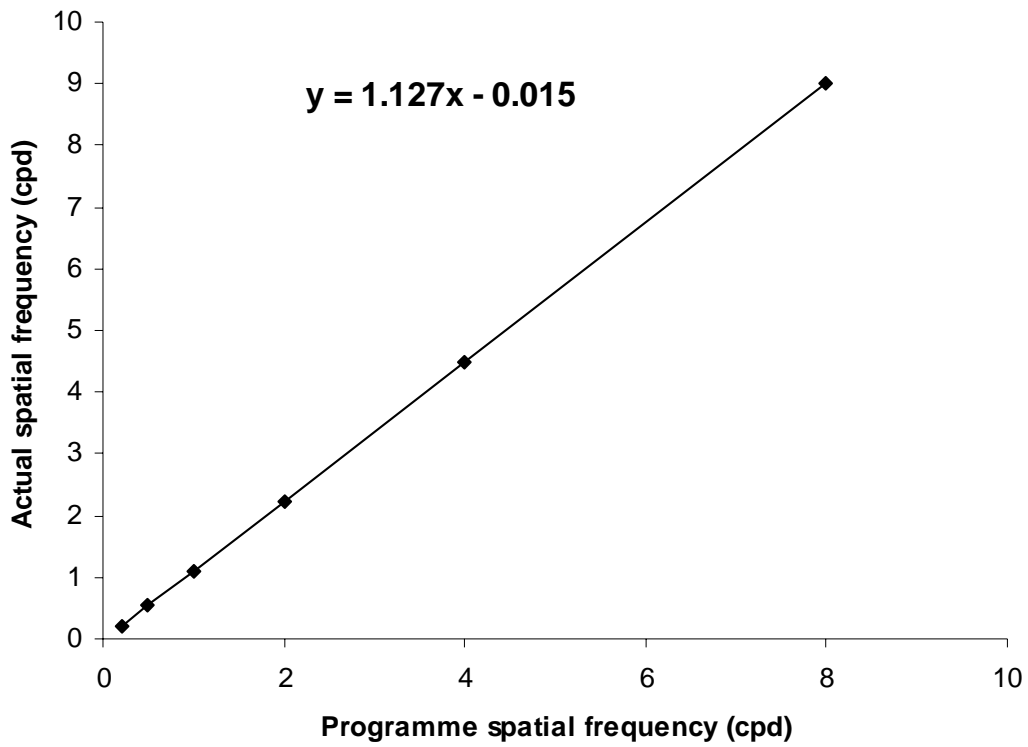
APPENDIX A

Contrast Calibration for Sony Trinitron Monitor and Morphonome Software, used for the Contrast Threshold and Contrast Matching Studies



APPENDIX B

Spatial Frequency Calibration for Trinitron Monitor and Morphonome Software, used for the Contrast Threshold and Contrast Matching Experiment



APPENDIX C

Examples of Filters

Original (low-passed)



High-pass/unsharp masking



Sobel edge enhancement



Contrast enhancement



DoG convolution



DoG FFT



Peli's adaptive enhancement



Band-pass - 3.6%



Band-pass - 27.9%



Band-pass - CS



Band-pass - Peak emphasis



Band-pass - Equi Emphasis



Original (low-passed)



High-pass/unsharp masking



Sobel edge enhancement



Contrast enhancement



DoG convolution



DoG FFT



Peli's adaptive enhancement



Band-pass - 3.6%



Band-pass - 27.9%



Band-pass - CTh



Band-pass - Peak emphasis



Band-pass - Equi Emphasis



APPENDIX D

Codes of the Generic Filters

The codes of the generic filters were written by Gorden Deng from the System Designs Department, University of Waterloo. According to the ImageLab manual, the purpose of the convolution here is to enhance certain information in the original image, so the enhanced image should be added back to the original image, that is

$$e = \lambda_1 \alpha + \lambda_2 c$$

where e denotes the overlaid enhanced image, and λ_1 and λ_2 are the weights for overlaying requiring $\lambda_1 + \lambda_2 = 1$.

The above two equations can be combined into one equation if changing the convolution kernel h :

$$e = \alpha \otimes h'$$

where $h' = \lambda h + E$, E has the same size of h and all its elements are zeros but the central element is one, and λ is a scale factor to determine how much the convoluted image is overlaid with the original image.

Appendix D. 1 3x3 Unsharp Masking

This functions by enhancing edge information in the original image. The convolution kernel h' is

$$h' = \begin{bmatrix} -1 & -1 & -1 \\ -1 & 12 & -1 \\ -1 & -1 & -1 \end{bmatrix} \times 2s/9 + E$$

Where E represents the original image. s is the scaling value in the parameter scroll bar in

Figure D-1. $s = 1, 2, 4,$ or 8 .

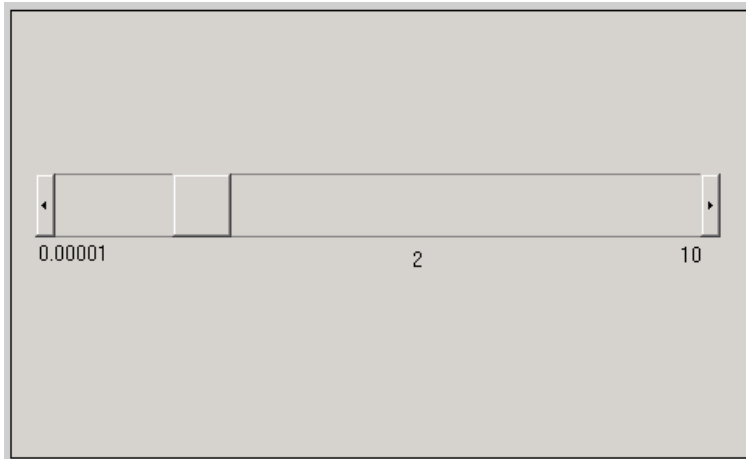


Figure D-1. The scroll bar for the high-pass/unsharp masking and Sobel edge enhancement.

Appendix D. 2 High-pass Convolution Filter

This functions to enhance high frequency information in the original image.

3x3 high-pass

The convolution kernel $(3 \times 3)h'$ is

$$h' = \begin{bmatrix} 0 & -1 & 0 \\ -1 & 4 & -1 \\ 0 & -1 & 0 \end{bmatrix} \times s/2 + E$$

Where E represents the original image. s is the scaling value in the parameter scroll bar in

Figure D-1. $s = 1, 2, 4,$ or 8 .

5x5 high-pass

The convolution kernel $(5 \times 5)h'$ is

$$h' = \begin{bmatrix} -1 & -1 & -1 & -1 & -1 \\ -1 & -1 & -2 & -1 & -1 \\ -1 & -2 & 28 & -2 & -1 \\ -1 & -1 & -2 & -1 & -1 \\ -1 & -1 & -1 & -1 & -1 \end{bmatrix} \times s/14 + E$$

Where E represents the original image. s is the scaling value in the parameter scroll bar in Figure D-1. $s = 1, 2, 4, \text{ or } 8$.

7x7 high-pass

The convolution kernel (7×7) h' is

$$h' = \begin{bmatrix} -1 & -1 & -1 & -1 & -1 & -1 & -1 \\ -1 & -1 & -1 & -2 & -1 & -1 & -1 \\ -1 & -1 & -2 & -3 & -2 & -1 & -1 \\ -1 & -2 & -3 & 64 & -3 & -2 & -1 \\ -1 & -1 & -2 & -3 & -2 & -1 & -1 \\ -1 & -1 & -1 & -2 & -1 & -1 & -1 \\ -1 & -1 & -1 & -1 & -1 & -1 & -1 \end{bmatrix} \times s/32 + E$$

Where E represents the original image. s is the scaling value in the parameter scroll bar in Figure D-1. $s = 1, 2, 4, \text{ or } 8$.

Appendix D. 3 3x3 Sobel Horizontal & Vertical Edge

Enhancement

This functions by enhancing edge information in the original image. The convolution kernel h' is

$$h' = \begin{bmatrix} 0 & 2 & 2 \\ -2 & 0 & 2 \\ -2 & -2 & 0 \end{bmatrix} \times s/3 + E$$

Where E represents the original image. s is the scaling value in the parameter scroll bar in Figure D-1. $s = 1, 2, 4, \text{ or } 8$.

There are two modes of this filter, RGB and HSB. $s = 1, 2, 4, \text{ or } 8$.

Appendix D. 4 Difference of Gaussians (DoG) Convolution Filter

This functions by enhancing high information in the original image.

7x7 DoG convolution

The convolution kernel h' is

$$h' = \begin{bmatrix} 0 & 0 & -1 & -1 & -1 & 0 & 0 \\ 0 & -2 & -3 & -3 & -3 & -2 & 0 \\ -1 & -3 & 5 & 5 & 5 & -3 & -1 \\ -1 & -3 & 5 & 16 & 5 & -3 & -1 \\ -1 & -3 & 5 & 5 & 5 & -3 & -1 \\ 0 & -2 & -3 & -3 & -3 & -2 & 0 \\ 0 & 0 & -1 & -1 & -1 & 0 & 0 \end{bmatrix} \times s/28 + E$$

Where E represents the original image. s is the scaling value in the parameter scroll bar in Figure D-1. $s = 1, 2, 4, \text{ or } 8$.

9x9 DoG convolution

The convolution kernel h' is

$$h' = \begin{bmatrix} 0 & 0 & 0 & -1 & -1 & -1 & 0 & 0 & 0 \\ 0 & -2 & -3 & -3 & -3 & -3 & -3 & -2 & 0 \\ 0 & -3 & -2 & -1 & -1 & -1 & -2 & -3 & 0 \\ -1 & -3 & -1 & 10 & 10 & 10 & -1 & -3 & -1 \\ -1 & -3 & -1 & 10 & 20 & 10 & -1 & -3 & -1 \\ -1 & -3 & -1 & 10 & 10 & 10 & -1 & -3 & -1 \\ 0 & -3 & -2 & -1 & -1 & -1 & -2 & -3 & 0 \\ 0 & -2 & -3 & -3 & -3 & -3 & -3 & -2 & 0 \\ 0 & 0 & 0 & -1 & -1 & -1 & 0 & 0 & 0 \end{bmatrix} \times s/50 + E$$

Where E represents the original image. s is the scaling value in the parameter scroll bar in Figure D-1. $s = 1, 2, 4,$ or 8 .

11x11 DoG convolution

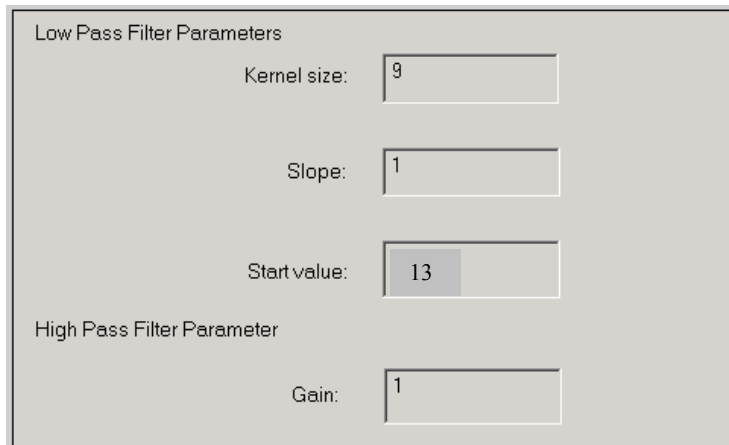
The convolution kernel h' is

$$h' = \begin{bmatrix} 0 & 0 & 0 & 0 & 0 & -1 & 0 & 0 & 0 & 0 & 0 \\ 0 & 0 & 0 & 0 & -1 & -1 & -1 & 0 & 0 & 0 & 0 \\ 0 & 0 & -2 & -3 & -3 & -3 & -3 & -3 & -2 & 0 & 0 \\ 0 & 0 & -3 & -2 & -1 & -1 & -1 & -2 & -3 & 0 & 0 \\ 0 & -1 & -3 & -1 & 10 & 10 & 10 & -1 & -3 & -1 & 0 \\ -1 & -1 & -3 & -1 & 10 & 24 & 10 & -1 & -3 & -1 & 0 \\ 0 & -1 & -3 & -1 & 10 & 10 & 10 & -1 & -3 & -1 & 0 \\ 0 & 0 & -3 & -2 & -1 & -1 & -1 & -2 & -3 & 0 & 0 \\ 0 & 0 & -2 & -3 & -3 & -3 & -3 & -3 & -2 & 0 & 0 \\ 0 & 0 & 0 & 0 & -1 & -1 & -1 & 0 & 0 & 0 & 0 \\ 0 & 0 & 0 & 0 & 0 & -1 & 0 & 0 & 0 & 0 & 0 \end{bmatrix} \times s/52 + E$$

Where E represents the original image. s is the scaling value in the parameter scroll bar in Figure D-1. $s = 1, 2, 4,$ or 8 .

Appendix D. 5 Peli's Adaptive Enhancement Filter

This filter is described by Peli et al. (1982, 1984). A set of parameters should be set in the parameter area shown in Figure D-2.



The image shows a software interface for setting filter parameters. It is divided into two sections: 'Low Pass Filter Parameters' and 'High Pass Filter Parameter'. Under 'Low Pass Filter Parameters', there are three input fields: 'Kernel size' with the value '9', 'Slope' with the value '1', and 'Start value' with the value '13'. Under 'High Pass Filter Parameter', there is one input field: 'Gain' with the value '1'. Each input field is a rectangular box with a scroll bar on the right side.

Figure D-2. Peli's adaptive enhancement filter processing parameters used in this study were kernel size (9,15, 21, or 25), slope (0.9), start Value (13), and gain (2, 4, 8, or 16).

Appendix D. 6. Contrast Enhancement Filter

This functions by enhancing contrast. The formula for contrast enhancement is as follows:

$$e = \alpha + \lambda[\alpha - \text{mean}(\alpha)]/100$$

where e is the enhanced image, α is the original image, $\text{mean}(\alpha)$ is the mean pixel values of the original image, and λ is the scale adjusted by the scroll bar in the parameter area (Figure D-3). The units are in percentage. The value of λ gives the power of the filter.

The bigger the λ value, the stronger the filtering is.

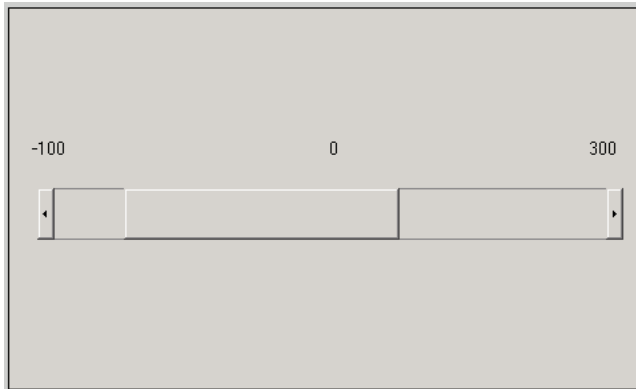


Figure D-3. The scroll bar for the contrast enhancement. The unit is in percentage.

There are two modes of this filter, RGB and HSB. $\lambda = 20, 40, 80, 160\%$ in this study.

Appendix D. 7 DOG FFT Filter

With this filter, certain spatial frequencies are enhanced. A set of parameters should be set in the parameter area shown in Figure D-4.

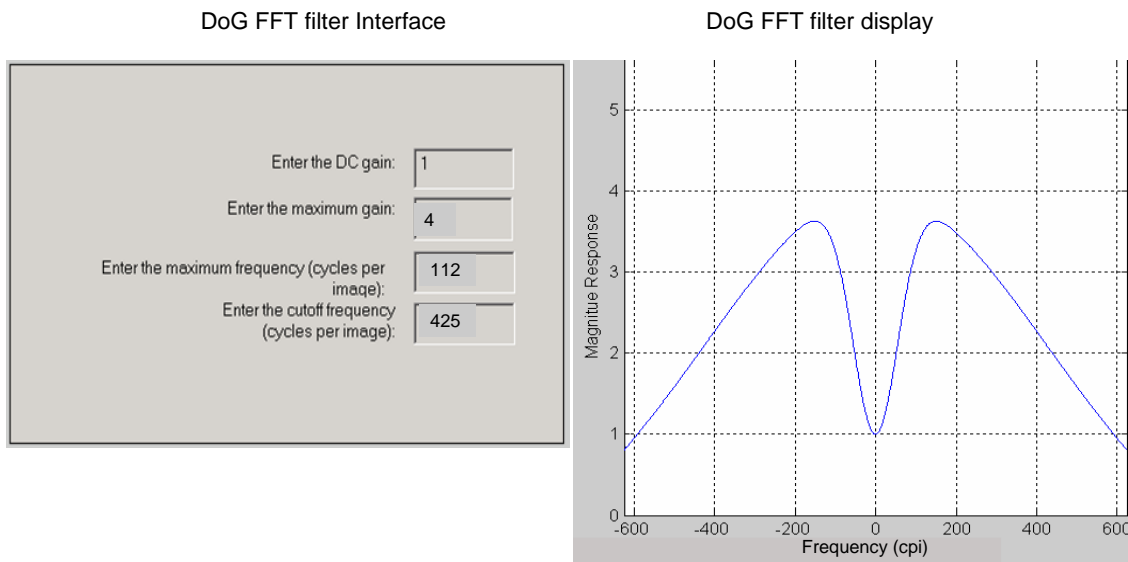


Figure D-4. Examples of DoG FFT filter parameters and filter profile.

Direct current (DC) gain = 1 (to maintain unchanged luminance)

Maximum gain = 2, 4, 8, 16

Maximum frequency = 0.5, 1, 2, 4, 8 cpd (7, 14, 28, 56, 112 cycles per image for half-sized image or 14, 28, 56, 112, 224 cycles per image for full-sized image)

Cutoff frequency = 15 cpd (210 cycles per image for half-sized image or 420 cycles per image for full-sized image). The cutoff frequency is the frequency at half-height.

Appendix D.8 Low-pass Filter

A Gaussian function with zero mean and standard deviation f is used to generate the low pass filter h_l . An example of a low pass filter with $f = 100\text{cpi}$ is shown in Figure D-5

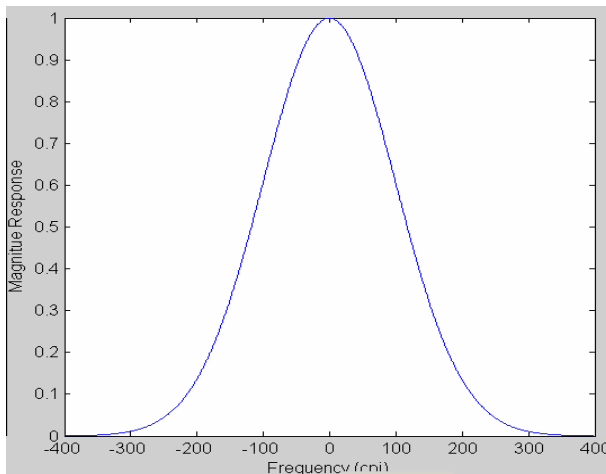


Figure D-5. Low pass filter with $f = 100\text{cpi}$ (image size is 600x800)

A cutoff frequency f should be set in the parameter area shown in Figure D-6.

Enter the cutoff frequency (cycles per image):

Figure D-6. Cutoff frequency of low-pass filter

Bibliography

- Aguirre, G. K., Zarahn, E., & D'Esposito, M. (1998). An area within human ventral cortex sensitive to "building" stimuli: Evidence and implications. *Neuron*, 21, 373-383.
- Anastasi, A., & Urbina, S. (1997). *Psychological testing* (7th ed.). Upper Saddle River, NJ: Simon & Schuster. 114.
- Albrecht, D. G., & Hamilton, D. B. (1982). Striate cortex of monkey and cat: Contrast response function. *Journal of Neurophysiology*, 48, 217-237.
- Allison, T., Ginter, H., McCarthy, G., Nobre, A. C., Puce, A., Luby, M., & Spencer, D. D. (1994). Face recognition in human extrastriate cortex. *Journal of Neurophysiology*, 71, 821-825.
- Allison, T., Puce, A., & McCarthy, G. (2000). Social perception from visual cues: Role of the STS region. *Trends in Cognitive Sciences*, 4, 267-278.
- Allison, T., Puce, A., Spencer, D. D., & McCarthy, G. (1999). Electrophysiological studies of human face perception. I: Potentials generated in occipitotemporal cortex by face and non-face stimuli. *Cerebral Cortex* (New York, N.Y. : 1991), 9, 415-430.
- Andrews, T. J., Schluppeck, D., Homfray, D., Matthews, P., & Blakemore, C. (2002). Activity in the fusiform gyrus predicts conscious perception of rubin's vase-face illusion. *NeuroImage*, 17, 890-901.

- Arundale, K. (1978). An investigation into the variation of human contrast sensitivity with age and ocular pathology. *The British Journal of Ophthalmology*, 62, 213-215.
- Attebo, K., Mitchell, P., & Smith, W. (1996). Visual acuity and the causes of visual loss in Australia. The Blue Mountains Eye Study. *Ophthalmology*, 103, 357-364.
- Baddeley, R. J., & Hancock, P. J. (1991). A statistical analysis of natural images matches psychophysically derived orientation tuning curves. *Proceedings of the Royal Society of London. Series B, Biological sciences*, 246, 219-223.
- Baker, C. I., Peli, E., Knouf, N., & Kanwisher, N. G. (2005). Reorganization of visual processing in macular degeneration. *The Journal of Neuroscience*, 25, 614-618.
- Baseler, H. A., Brewer, A. A., Sharpe, L. T., Morland, A. B., Jagle, H., & Wandell, B. A. (2002). Reorganization of human cortical maps caused by inherited photoreceptor abnormalities. *Nature Neuroscience*, 5, 364-370.
- Beard, B. L., Yager, D., & Neufeld, S. (1994). Contrast detection and discrimination in young and older adults. *Optometry and Vision Science*, 71, 783-791.
- Bellmann, C., Unnebrink, K., Rubin, G. S., Miller, D., & Holz, F. G. (2003). Visual acuity and contrast sensitivity in patients with neovascular age-related macular degeneration. Results from the radiation therapy for age-related macular degeneration (RAD-) study. *Graefe's Archive for Clinical and Experimental Ophthalmology = Albrecht Von Graefes Archiv Fur Klinische Und Experimentelle Ophthalmologie*, 241, 968-974.

Biehl, M., Matsumoto, D., Ekman, P., Hearn, V., Heider, K., Kudoh, T., & Ton, V. (1997). Matsumoto and Ekman's Japanese and Caucasian Facial Expressions of Emotion (JACFEE): Reliability data and cross-national differences. *Journal of Nonverbal Behavior*, 21, 2-21.

Billock, V. A., Cunningham, D. W., Havig, P. R., & Tsou, B. H. (2001). Perception of spatiotemporal random fractals: An extension of colorimetric methods to the study of dynamic texture. *Journal of the Optical Society of America. A, Optics, Image Science, and Vision*, 18, 2404-2413.

Bird, A. C., Bressler, N. M., Bressler, S. B., Chisholm, I. H., Coscas, G., Davis, M. D., de Jong, P. T., Klaver, C. C., Klein, B. E., & Klein, R. (1995). An international classification and grading system for age-related maculopathy and age-related macular degeneration. The International ARM Epidemiological Study Group. *Survey of Ophthalmology*, 39, 367-374.

Blakemore, C., Muncey, J. P., & Ridley, R. M. (1973). Stimulus specificity in the human visual system. *Vision Research*, 13, 1915-1931.

Blakemore, C., Muncey, J. P., & Ridley, R. M. (1971). Perceptual fading of a stabilized cortical image. *Nature*, 233, 204-205.

Bland, J.M., & Altman, D.G. (1986). Statistical methods for assessing agreement between two methods of clinical measurement. *Lancet*, 1, 307-310.

- Brady, N., & Field, D. J. (1995). What's constant in contrast constancy? The effects of scaling on the perceived contrast of bandpass patterns. *Vision Research*, 35, 739-756.
- Bressler, N. M., Bressler, S. B., & Fine, S. L. (1988). Age-related macular degeneration. *Survey of Ophthalmology*, 32, 375-413.
- Bressler, N. M., Silva, J. C., Bressler, S. B., Fine, S. L., & Green, W. R. (1994). Clinicopathologic correlation of drusen and retinal pigment epithelial abnormalities in age-related macular degeneration. *Retina (Philadelphia)*, 14, 130-142.
- Brown, B., & Lovie-Kitchin, J. E. (1989). Temporal summation in age-related maculopathy. *Optometry and Vision Science*, 66, 426-429.
- Brown, B., Zadnik, K., Bailey, I. L., & Colenbrander, A. (1984). Effect of luminance, contrast, and eccentricity on visual acuity in senile macular degeneration. *American Journal of Optometry and Physiological Optics*, 61, 265-270.
- Burgess, A. E., & Colborne, B. (1988). Visual signal detection. IV. observer inconsistency. *Journal of the Optical Society of America. A, Optics and Image Science*, 5, 617-627.
- Burton, G. J., Haig, N. D., & Moorhead, I. R. (1986). A self-similar stack model for human and machine vision. *Biological Cybernetics*, 53, 397-403.

- Calford, M. B., Wang, C., Taglianetti, V., Waleszczyk, W. J., Burke, W., & Dreher, B. (2000). Plasticity in adult cat visual cortex (area 17) following circumscribed monocular lesions of all retinal layers. *The Journal of Physiology*, 524 Pt 2, 587-602.
- Cannon, M. W., Jr. (1985). Perceived contrast in the fovea and periphery. *Journal of the Optical Society of America. A, Optics and Image Science*, 2, 1760-1768.
- Cannon, M. W., Jr. (1985). Perceived contrast in the fovea and periphery. *Journal of the Optical Society of America. A, Optics and Image Science*, 2, 1760-1768.
- Carandini, M., & Ferster, D. (1997). A tonic hyperpolarization underlying contrast adaptation in cat visual cortex. *Science*, 276, 949-952.
- Chao, L. L., Haxby, J. V., & Martin, A. (1999). Attribute-based neural substrates in temporal cortex for perceiving and knowing about objects. *Nature Neuroscience*, 2, 913-919.
- Chao, L. L., Martin, A., & Haxby, J. V. (1999). Are face-responsive regions selective only for faces? *Neuroreport*, 10, 2945-2950.
- Cheng, A. S., & Vingrys, A. J. (1993). Visual losses in early age-related maculopathy. *Optometry and Vision Science*, 70, 89-96.
- Cheong, A.M., Lovie-Kitchin, J.E., Bowers, A.R., Brown, B. (2005). Short-Term In-Office Practice Improves Reading Performance with Stand Magnifiers for People with AMD. *Optometry and Vision Science*, 82, 114-127.

- Collin, C. A., Liu, C. H., Troje, N. F., McMullen, P. A., & Chaudhuri, A. (2004). Face recognition is affected by similarity in spatial frequency range to a greater degree than within-category object recognition. *Journal of Experimental Psychology: Human Perception and Performance*, 30, 975-987.
- Collins, M. (1986). Pre-age related maculopathy and the desaturated D-15 colour vision test. *Clinical & Experimental Optometry*, 69, 223-227.
- Coppola, D. M., Purves, H. R., McCoy, A. N., & Purves, D. (1998). The distribution of oriented contours in the real world. *Proceedings of the National Academy of Sciences of the United States of America*, 95, 4002-4006.
- Cummings, R. W., Whittaker, S. G., Watson, G. R., & Budd, J. M. (1985). Scanning characters and reading with a central scotoma. *American Journal of Optometry and Physiological Optics*, 62, 833-843.
- Curcio, C. A., & Allen, K. A. (1990). Topography of ganglion cells in human retina. *The Journal of Comparative Neurology*, 300, 5-25.
- Curcio, C. A., Medeiros, N. E., & Millican, C. L. (1996). Photoreceptor loss in age-related macular degeneration. *Investigative Ophthalmology & Visual Science*, 37, 1236-1249.
- Curcio, C. A., Owsley, C., & Jackson, G. R. (2000). Spare the rods, save the cones in aging and age-related maculopathy. *Investigative Ophthalmology & Visual Science*, 41, 2015-2018.

- Darian-Smith, C., & Gilbert, C. D. (1994). Axonal sprouting accompanies functional reorganization in adult cat striate cortex. *Nature*, 368, 737-740.
- De Valois, R. L., Albrecht, D. G., & Thorell, L. G. (1982). Spatial frequency selectivity of cells in macaque visual cortex. *Vision Research*, 22, 545-559.
- Derefeldt, G., Lennerstrand, G., & Lundh, B. (1979). Age variations in normal human contrast sensitivity. *Acta Ophthalmologica*, 57, 679-690.
- Dickinson, C.M. & Abadi, R.V. (1992). Suprathreshold Contrast Perception in Congenital Nystagmus. *Clinical Vision Science*, 7, 31-37.
- Ditzinger, T., Billock, V. A., Kelso, J. A., & Holtz, J. (2000). The Leaning Tower of Pisa effect: An illusion mediated by colour, brightness, and motion. *Perception*, 29, 1269-1272.
- Dunaief, J. L., Dentchev, T., Ying, G. S., & Milam, A. H. (2002). The role of apoptosis in age-related macular degeneration. *Archives of Ophthalmology*, 120, 1435-1442.
- Eisner, A., Stoumbos, V. D., Klein, M. L., & Fleming, S. A. (1991). Relations between fundus appearance and function. Eyes whose fellow eye has exudative age-related macular degeneration. *Investigative Ophthalmology & Visual Science*, 32, 8-20.

- Elliott, D., Whitaker, D., & MacVeigh, D. (1990). Neural contribution to spatiotemporal contrast sensitivity decline in healthy ageing eyes. *Vision Research*, 30, 541-547.
- Elliott, D. B. (1987). Contrast sensitivity decline with ageing: A neural or optical phenomenon? *Ophthalmic & Physiological Optics*, 7, 415-419.
- Elliott, D. B., Glasser, A., & Rubin, G. S. (2001). Aging--preparing for the 21 st century. *Optometry and Vision Science*, 78, 361-363.
- Enoch, J. M. (1978). Quantitative layer-by-layer perimetry. *Investigative Ophthalmology & Visual Science*, 17, 208-257.
- Epstein, R., & Kanwisher, N. (1998). A cortical representation of the local visual environment. *Nature*, 392, 598-601.
- Essock, E. A., DeFord, J. K., Hansen, B. C., & Sinai, M. J. (2003). Oblique stimuli are seen best (not worst!) in naturalistic broad-band stimuli: A horizontal effect. *Vision Research*, 43, 1329-1335.
- Evans, D. W., & Ginsburg, A. P. (1985). Contrast sensitivity predicts age-related differences in highway-sign discriminability. *Human Factors*, 27, 637-642.
- Farah, M. J., Wilson, K. D., Drain, M., & Tanaka, J. N. (1998). What is "special" about face perception? *Psychological Review*, 105, 482-498.

- Field, D. J. (1987). Relations between the statistics of natural images and the response properties of cortical cells. *Journal of the Optical Society of America. A, Optics and Image Science*, 4, 2379-2394.
- Fine, E.M., & Peli, E. (1995). Enhancement of text for the visually impaired. *Journal of the Optical Society America*, 12, 2286-2292.
- Fine, I., Smallman, H. S., Doyle, P., & MacLeod, D. I. (2002). Visual function before and after the removal of bilateral congenital cataracts in adulthood. *Vision Research*, 42, 191-210.
- Fiorentini, A., Maffei, L., & Sandini, G. (1983). The role of high spatial frequencies in face perception. *Perception*, 12, 195-201.
- Fletcher, D. C., & Schuchard, R. A. (1997). Preferred retinal loci relationship to macular scotomas in a low-vision population. *Ophthalmology*, 104, 632-638.
- Folk, J. C. (1985). Aging macular degeneration. Clinical features of treatable disease. *Ophthalmology*, 92, 594-602.
- Fullerton, M., & Peli, E. (2006). Post transmission digital video enhancement for people with visual impairments. *Journal of Applied Physics*, 14, 15-24.
- Furmanski, C. S., & Engel, S. A. (2000). An oblique effect in human primary visual cortex. *Nature Neuroscience*, 3, 535-536.
- Ganel, T. (2006). The objects of face perception. *Neuron*, 50, 7-9.

Gardner, J. L., Sun, P., Waggoner, R. A., Ueno, K., Tanaka, K., & Cheng, K. (2005). Contrast adaptation and representation in human early visual cortex. *Neuron*, 47, 607-620.

Geisler, W. S., & Albrecht, D. G. (1992). Cortical neurons: Isolation of contrast gain control. *Vision Research*, 32, 1409-1410.

Georgeson, M. A. (1991). Contrast overconstancy. *Journal of the Optical Society of America. A, Optics and Image Science*, 8, 579-586.

Georgeson, M. A., & Sullivan, G. D. (1975). Contrast constancy: Deblurring in human vision by spatial frequency channels. *The Journal of Physiology*, 252, 627-656.

Gilbert, C. D., & Wiesel, T. N. (1992). Receptive field dynamics in adult primary visual cortex. *Nature*, 356, 150-152.

Ginsburg, A. P. (1980). Specifying relevant spatial information for image evaluation and display design: an explanation of how we see certain objects. *Proceeding Society for Information Display*, 21, 219-227.

Green, W. R. (1999). Histopathology of age-related macular degeneration. *Molecular Vision*, 5, 27.

Green, W. R., & Enger, C. (1993). Age-related macular degeneration histopathologic studies. The 1992 Lorenz E. Zimmerman Lecture. *Ophthalmology*, 100, 1519-1535.

- Greene, H. A., Beadles, R., & Pekar, J. (1992). Challenges in applying autofocus technology to low vision telescopes. *Optometry and Vision Science*, 69, 25-31.
- Grill-Spector, K., Kushnir, T., Edelman, S., Avidan, G., Itzhak, Y., & Malach, R. (1999). Differential processing of objects under various viewing conditions in the human lateral occipital complex. *Neuron*, 24, 187-203.
- Grill-Spector, K., & Malach, R. (2004). The human visual cortex. *Annual Review of Neuroscience*, 27, 649-677.
- Guyader, N., Chauvin, A., Peyrin, C., Herault, J., & Marendaz, C. (2004). Image phase or amplitude? Rapid scene categorization is an amplitude-based process. *Comptes Rendus Biologies*, 327, 313-318.
- Hasson, U., Hendler, T., Ben Bashat, D., & Malach, R. (2001). Vase or face? A neural correlate of shape-selective grouping processes in the human brain. *Journal of Cognitive Neuroscience*, 13, 744-753.
- Haxby, J. V., Gobbini, M. I., Furey, M. L., Ishai, A., Schouten, J. L., & Pietrini, P. (2001). Distributed and overlapping representations of faces and objects in ventral temporal cortex. *Science*, 293, 2425-2430.
- Haxby, J. V., Hoffman, E. A., & Gobbini, M. I. (2000). The distributed human neural system for face perception. *Trends in Cognitive Sciences*, 4, 223-233.

Haxby, J. V., Ungerleider, L. G., Clark, V. P., Schouten, J. L., Hoffman, E. A., & Martin, A. (1999). The effect of face inversion on activity in human neural systems for face and object perception. *Neuron*, 22, 189-199.

Haymes, S. A., Johnston, A. W., & Heyes, A. D. (2001). The development of the Melbourne low-vision ADL index: A measure of vision disability. *Investigative Ophthalmology & Visual Science*, 42, 1215-1225.

Hazel, C. A., Petre, K. L., Armstrong, R. A., Benson, M. T., & Frost, N. A. (2000). Visual function and subjective quality of life compared in subjects with acquired macular disease. *Investigative Ophthalmology & Visual Science*, 41, 1309-1315.

Hess, R. F. (1990). The Edridge-Green lecture vision at low light levels: Role of spatial, temporal and contrast filters. *Ophthalmic & Physiological*, 10, 351-359.

Hess, R. F., & Bradley, A. (1980). Contrast perception above threshold is only minimally impaired in human amblyopia. *Nature*, 287, 463-464.

Hier, R. G., Schmidt, G. W., Miller, R. S., & Deforest, S. E. (1993). Realtime locally adaptive contrast enhancement: a practical key to overcoming display and human-visual-system limitations. *SID Symposium Digest of Technical Papers*, 491-494.

Hoekstra, J., van der Goot, D. P., van den Brink, G., & Bilsen, F. A. (1974). The influence of the number of cycles upon the visual contrast threshold for spatial sine wave patterns. *Vision Research*, 14, 365-368.

- Howell, E. R. (1978). The functional area for summation to threshold for sinusoidal gratings. *Vision Research*, 18, 369-374.
- Hubner, M., Rentschler, I., Trempe, C., & Encke, W. (1989). Hidden face recognition: comparing foveal and extrafoveal performance. *Human Neurobiology*, 4, 1-7.
- Ishai, A., Ungerleider, L. G., Martin, A., & Haxby, J. V. (2000). The representation of objects in the human occipital and temporal cortex. *Journal of Cognitive Neuroscience*, 12 Suppl 2, 35-51.
- Jaccard J and Wan CK. (1996). LISREL approaches to interaction effects in multiple regressions; Sage Publications, CA: Thousand Oaks,.
- Kanwisher, N., McDermott, J., & Chun, M. M. (1997). The fusiform face area: A module in human extrastriate cortex specialized for face perception. *The Journal of Neuroscience*, 17, 4302-4311.
- Keil, M. S., & Cristobal, G. (2000). Separating the chaff from the wheat: Possible origins of the oblique effect. *Journal of the Optical Society of America. A, Optics, Image Science, and Vision*, 17, 697-710.
- Kennedy, A. J., Leat, S. J., & Jernigan, M. E. (1998). A generalized image processing application for the enhancement of images for the visually impaired. *Vision science and its application. Optical Society of American Technical Digest Series*, 1, 124-127.

Kim, S. Y., Sadda, S., Humayun, M. S., de Juan, E., Jr, Melia, B. M., & Green, W. R. (2002). Morphometric analysis of the macula in eyes with geographic atrophy due to age-related macular degeneration. *Retina (Philadelphia, Pa.)*, 22, 464-470.

Kirchner C. (1988). *Data on Blindness and Visual Impairment in the U.S.: A Resource Manual on Social Demographic Characteristics, Education, Employment and Income, and Service Delivery*. New York: American Foundation for the Blind.

Klaver, C. C., Wolfs, R. C., Vingerling, J. R., Hofman, A., & de Jong, P. T. (1998). Age-specific prevalence and causes of blindness and visual impairment in an older population: The Rotterdam study. *Archives of Ophthalmology*, 116, 653-658.

Kulikowski, J. J. (1976). Effective contrast constancy and linearity of contrast sensation. *Vision Research*, 16, 1419-1431.

Lawton, T. A., Sebag, J., Sadun, A. A., & Castleman, K. R. (1998). Image enhancement improves reading performance in age-related macular degeneration patients. *Vision Research*, 38, 153-162.

Lawton, T. B. (1992). Image enhancement filters significantly improve reading performance for low vision observers. *Ophthalmic & Physiological Optics*, 12, 193-200.

Lawton, T. B. (1989). Improved reading performance using individualized compensation filters for observers with losses in central vision. *Ophthalmology*, 96, 115-126.

Leat, S.J., Fryer, A., & Rumney, N.J. (1994). Outcome of Low Vision Aid Provision: The Effectiveness of a Low Vision Clinic. *Optometry and Vision Science*, 71, 199-206.

Leat, S. J., Legge, G. E., & Bullimore, M. A. (1999). What is low vision? A re-evaluation of definitions. *Optometry and Vision Science*, 76, 198-211.

Leat, S.J., Millodot, M. (1990) Contrast discrimination in normal and impaired human vision. *Clinical Vision Science*, 5, 37-43.

Leat, S. J., Omoruyi, G., Kennedy, A., & Jernigan, E. (2005). Generic and customized digital image enhancement filters for the visually impaired. *Vision Research*, 45, 1991-2007.

Leat, S. J., & Woodhouse, J. M. (1993). Reading performance with low vision aids: Relationship with contrast sensitivity. *Ophthalmic & Physiological Optics*, 13, 9-16.

Legge, G. E. (1978). Sustained and transient mechanisms in human vision: Temporal and spatial properties. *Vision Research*, 18, 69-81.

Legge, G. E., & Foley, J. M. (1980). Contrast masking in human vision. *Journal of the Optical Society of America*, 70, 1458-1471.

Legge, G.E., Rubin, G.S., Pelli, D.G., & Schleske, M.M. (1985). Psychophysics of reading. II. Low Vision. *Vision Research*, 25, 253-256.

- Leibowitz, H. W., Post, R. B., Rodemer, C. S., Wadlington, W. L., & Lundy, R. M. (1980). Roll vection analysis of suggestion-induced visual field narrowing. *Perception & Psychophysics*, 28, 173-176.
- Li, B., Peterson, M. R., & Freeman, R. D. (2003). Oblique effect: A neural basis in the visual cortex. *Journal of Neurophysiology*, 90, 204-217.
- Li, J., Tso, M. O., & Lam, T. T. (2001). Reduced amplitude and delayed latency in foveal response of multifocal electroretinogram in early age related macular degeneration. *The British Journal of Ophthalmology*, 85, 287-290.
- Loffler, G., Gordon, G. E., Wilkinson, F., Goren, D., & Wilson, H. R. (2005). Configural masking of faces: Evidence for high-level interactions in face perception. *Vision Research*, 45, 2287-2297.
- Loshin, D. S., & White, J. (1984). Contrast sensitivity. The visual rehabilitation of the patient with macular degeneration. *Archives of Ophthalmology*, 102, 1303-1306.
- Lund, R., & Watson, G. R. (1997). *The CCTV book, habilitation and rehabilitation with closed circuit television systems*. LUV Reading Series. Synsforum ans, Fordlund, Norway, 13-15.
- Luntinen, O., Rovamo, J., & Nasanen, R. (1995). Modelling the increase of contrast sensitivity with grating area and exposure time. *Vision Research*, 35, 2339-2346.
- Macular photocoagulation study (MPS) Group (1994). Visual outcome after laser photocoagulation for subfoveal choroidal neovascularization secondary to age-related

- macular degeneration. The influence of initial lesion size and initial visual acuity. *Archives of Ophthalmology*, 112, 480-488.
- Malach, R., Reppas, J. B., Benson, R. R., Kwong, K. K., Jiang, H., Kennedy, W. A., Ledden, P. J., Brady, T. J., Rosen, B. R., & Tootell, R. B. (1995). Object-related activity revealed by functional magnetic resonance imaging in human occipital cortex. *Proceedings of the National Academy of Sciences of the United States of America*, 92, 8135-8139.
- Mansfield, R. J., & Ronner, S. F. (1978). Orientation anisotropy in monkey visual cortex. *Brain Research*, 149, 229-234.
- Markowitz, M. (2006). Occupational therapy interventions in low vision rehabilitation. *Canadian Journal of Ophthalmology. Journal Canadien d'Ophtalmologie*, 41, 340-347.
- Martin, A., Wiggs, C. L., Ungerleider, L. G., & Haxby, J. V. (1996). Neural correlates of category-specific knowledge. *Nature*, 379, 649-652.
- Mayer, M. J., Ward, B., Klein, R., Talcott, J. B., Dougherty, R. F., & Glucks, A. (1994). Flicker sensitivity and fundus appearance in pre-exudative age-related maculopathy. *Investigative Ophthalmology & Visual Science*, 35, 1138-1149.
- Medjbeur, S., & Tulunay-Keesey, U. (1986). Supra-threshold responses of the visual system in normals and in demyelinating diseases. *Investigative Ophthalmology & Visual Science*, 27, 1368-1378. *Clinical & Experimental Optometry*, 4, 272-281.

Mei, M., & Leat S.J. (2007). Supra-threshold contrast matching and effect of contrast threshold and age. *Clinical & Experimental Optometry*, 4, 272-281.

Mei, M., & Leat S.J. (2007). Supra-threshold contrast matching in maculopathy. *Investigative Ophthalmology & Visual Science*, in press.

Mitchell, P., Smith, W., Attebo, K., & Wang, J. J. (1995). Prevalence of age-related maculopathy in Australia. The Blue Mountains Eye Study. *Ophthalmology*, 102, 1450-1460.

Morland, A. B., Baseler, H. A., Hoffmann, M. B., Sharpe, L. T., & Wandell, B. A. (2001). Abnormal retinotopic representations in human visual cortex revealed by fMRI. *Acta Psychologica*, 107, 229-247.

Nasanen, R., Tiippana, K., & Rovamo, J. (1998). Contrast restoration model for contrast matching of cosine gratings of various spatial frequencies and areas. *Ophthalmic & Physiological Optics*, 18, 269-278.

Nomura, H., Ando, F., Niino, N., Shimokata, H., & Miyake, Y. (2003). Age-related change in contrast sensitivity among Japanese adults. *Japanese Journal of Ophthalmology*, 47, 299-303.

Olshansky, S. J., Carnes, B. A., & Cassel, C. K. (1993). The aging of the human species. *Scientific American*, 268, 46-52.

Owsley, C., Ball, K., & Keeton, D. M. (1995). Relationship between visual sensitivity and target localization in older adults. *Vision Research*, 35, 579-587.

Owsley, C., Gardner, T., Sekuler, R., & Lieberman, H. (1985). Role of the crystalline lens in the spatial vision loss of the elderly. *Investigative Ophthalmology & Visual Science*, 26, 1165-1170.

Owsley, C., Jackson, G. R., Cideciyan, A. V., Huang, Y., Fine, S. L., Ho, A. C., Maguire, M. G., Lolley, V., & Jacobson, S. G. (2000). Psychophysical evidence for rod vulnerability in age-related macular degeneration. *Investigative Ophthalmology & Visual Science*, 41, 267-273.

Owsley, C., Jackson, G. R., White, M., Feist, R., & Edwards, D. (2001). Delays in rod-mediated dark adaptation in early age-related maculopathy. *Ophthalmology*, 108, 1196-1202.

Owsley, C., Sekuler, R., & Siemsen, D. (1983). Contrast sensitivity throughout adulthood. *Vision Research*, 23, 689-699.

Patel, A. S. (1966). Spatial resolution by the human visual system. The effect of mean retinal illuminance. *Journal of the Optical Society of America*, 56, 689-694.

Peli, E. (2005). Recognition performance and perceived quality of video enhanced for the visually impaired. *Ophthalmic & Physiological*, 25, 543-555.

Peli, E. (1999). Perceived quality of video enhanced for the visually impaired. *Vision science and its application*. Optical Society of America, Technical Digest Series, FC3, 46-49.

- Peli, E. (1997). In search of a contrast metric: Matching the perceived contrast of Gabor patches at different phases and bandwidths. *Vision Research*, 37, 3217-3224.
- Peli, E. (1992b). Limitations of image enhancement for the visually impaired. *Optometry and Vision Science*, 69, 15-24.
- Peli, E., Arend, L., & Labianca, A. T. (1996). Contrast perception across changes in luminance and spatial frequency. *Journal of the Optical Society of America. A, Optics, Image Science, and Vision*, 13, 1953-1959.
- Peli, E., & Fine, E. M. (1996). Evaluating information provided by audio description. *Journal of Visual Impairment and Blindness*, 90, 378-384.
- Peli, E., Fine, E.M., & Pisano, K., (1994a). Video enhancement of text and movies for the visually impaired. In A.C. Kooijman (Ed.), *Low vision: Research and ne developments in rehabilitation* (pp. 191-198). Amsterdam: IOS Press.
- Peli, E., Goldstein, R. B., Young, G. M., Trempe, C. L., & Buzney, S. M. (1991). Image enhancement for the visually impaired. Simulations and experimental results. *Investigative Ophthalmology & Visual Science*, 32, 2337-2350.
- Peli, E., Kim, J., Yitzhaky, Y., Goldstein, R. B., & Woods, R. L. (2004). Wideband enhancement of television images for people with visual impairments. *Journal of the Optical Society of America.A, Optics, Image Science, and Vision*, 21, 937-950.

Peli, E., Lee, E., Trempe, C. L., & Buzney, S. (1994). Image enhancement for the visually impaired: The effects of enhancement on face recognition. *Journal of the Optical Society of America. A, Optics, Image Science, and Vision*, 11, 1929-1939.

Peli, T., & Lim, T. S. (1982). Adaptive filtering for image enhancement. *Optical Engineering*, 21, 108-112.

Peli, E., Peli, T. (1984) Image enhancement for the visually impaired. *Optical Engineering*, 23, 47-51.

Peli, E., Yang, J. A., Goldstein, R., & Reeves, A. (1991). Effect of luminance on supra-threshold contrast perception. *Journal of the Optical Society of America. A, Optics and Image Science*, 8, 1352-1359.

Phipps, J. A., Guymer, R. H., & Vingrys, A. J. (2003). Loss of cone function in age-related maculopathy. *Investigative Ophthalmology & Visual Science*, 44, 2277-2283.

Pointer, J. S., & Hess, R. F. (1989). The contrast sensitivity gradient across the human visual field: With emphasis on the low spatial frequency range. *Vision Research*, 29, 1133-1151.

Polk, T. A., & Farah, M. J. (1998). The neural development and organization of letter recognition: Evidence from functional neuroimaging, computational modeling, and behavioral studies. *Proceedings of the National Academy of Sciences of the United States of America*, 95, 847-852.

- Prevent Blindness America (1994). Vision problems in the U.S. Schaumburg, IL: Prevent Blindness America, 1-20.
- Przybylski, A. W., Gaska, J. P., Foote, W., & Pollen, D. A. (2000). Striate cortex increases contrast gain of macaque LGN neurons. *Visual Neuroscience*, 17, 485-494.
- Puce, A., Allison, T., Asgari, M., Gore, J. C., & McCarthy, G. (1996). Differential sensitivity of human visual cortex to faces, letterstrings, and textures: A functional magnetic resonance imaging study. *The Journal of Neuroscience*, 16, 5205-5215.
- Puce, A., Allison, T., Gore, J. C., & McCarthy, G. (1995). Face-sensitive regions in human extrastriate cortex studied by functional MRI. *Journal of Neurophysiology*, 74, 1192-1199.
- Puce, A., Allison, T., & McCarthy, G. (1999). Electrophysiological studies of human face perception. III: Effects of top-down processing on face-specific potentials. *Cerebral Cortex*, 9, 445-458.
- Rempt, F., Hoogerheide, J., & Hoogenboom, W. P. (1976). Influence of correction of peripheral refractive errors on peripheral static vision. *Ophthalmologica. Journal International d'Ophthalmologie. International Journal of Ophthalmology. Zeitschrift Fur Augenheilkunde*, 173, 128-135.
- Ross, J. E., Clarke, D. D., & Bron, A. J. (1985). Effect of age on contrast sensitivity function: Unocular and binocular findings. *The British Journal of Ophthalmology*, 69, 51-56.

- Rovamo, J., Luntinen, O., & Nasanen, R. (1993). Modelling the dependence of contrast sensitivity on grating area and spatial frequency. *Vision Research*, 33, 2773-2788.
- Rubin, G. S., & Legge, G. E. (1989). Psychophysics of reading. VI-- The role of contrast in low vision. *Vision Research*, 29, 79-91.
- Rubin, G. S., Munoz, B., Bandeen-Roche, K., & West, S. K. (2000). Monocular versus binocular visual acuity as measures of vision impairment and predictors of visual disability. *Investigative Ophthalmology & Visual Science*, 41, 3327-3334.
- Rubin, G. S., & Siegel, K. (1984). Recognition of low pass filtered faces and letters. *Investigative Ophthalmology & Visual Science Supplement*, 25, 28.
- Ruderman, D. L., & Bialek, W. (1994). Statistics of natural images: Scaling in the woods. *Physical Review Letters*, 73, 814-817.
- Sarks, J. P., Sarks, S. H., & Killingsworth, M. C. (1994). Evolution of soft drusen in age-related macular degeneration. *Eye*, 8 (Pt 3), 269-283.
- Savoy, R. L., & McCann, J. J. (1975). Visibility of low-spatial-frequency sine-wave targets: Dependence on number of cycles. *Journal of the Optical Society of America*, 65, 343-350.
- Schneider, S., Greven, C. M., & Green, W. R. (1998). Photocoagulation of well-defined choroidal neovascularization in age-related macular degeneration: Clinicopathologic correlation. *Retina (Philadelphia)*, 18, 242-250.

- Seddon, J. M., Ajani, U. A., Sperduto, R. D., Hiller, R., Blair, N., Burton, T. C., Farber, M. D., Gragoudas, E. S., Haller, J., & Miller, D. T. (1994). Dietary carotenoids, vitamins A, C, and E, and advanced age-related macular degeneration. eye disease case-control study group. *The Journal of the American Medical Association*, 272, 1413-1420.
- Sekuler, R., Hutman, L. P., & Owsley, C. J. (1980). Human aging and spatial vision. *Science*, 209, 1255-1256.
- Sergent, J. (1986) Microgenesis of face perception. *Aspects of Face Processing*, 17-33.
- Sergent, J., Ohta, S., & MacDonald, B. (1992). Functional neuroanatomy of face and object processing. A positron emission tomography study. *Brain; a Journal of Neurology*, 115 Pt 1, 15-36.
- Sjostrand, J., & Frisen, L. (1977). Contrast sensitivity in macular disease. A preliminary report. *Acta Ophthalmologica*, 55, 507-514.
- Skalka, H. W. (1980). Effect of age on Arden grating acuity. *The British Journal of Ophthalmology*, 64, 21-23.
- Sloane, M. E., Owsley, C., & Alvarez, S. L. (1988). Aging, senile miosis and spatial contrast sensitivity at low luminance. *Vision Research*, 28, 1235-1246.
- Steinmetz, R. L., Haimovici, R., Jubb, C., Fitzke, F. W., & Bird, A. C. (1993). Symptomatic abnormalities of dark adaptation in patients with age-related Bruch's membrane change. *The British Journal of Ophthalmology*, 77, 549-554.

- Stelmack, J., Reda, D., Ahlers, S., Bainbridge, L., & McCray, J. (1991). Reading performance of geriatric patients post exudative maculopathy. *Journal of the American Optometric Association*, 62, 53-57.
- Strong, G., & Woo, G. C. (1985). A distance visual acuity chart incorporating some new design features. *Archives of Ophthalmology*, 103, 44-46.
- Sultan M.B., Meehan R.H., & Castor C. (1997). The impact of ocular disease on the instrumental activities of daily living. *Investigative Ophthalmology & Visual Science*, 38, S710.
- Sunness, J. S., Liu, T., & Yantis, S. (2004). Retinotopic mapping of the visual cortex using functional magnetic resonance imaging in a patient with central scotomas from atrophic macular degeneration. *Ophthalmology*, 111, 1595-1598.
- Sunness, J. S., Massof, R. W., Johnson, M. A., Finkelstein, D., & Fine, S. L. (1985). Peripheral retinal function in age-related macular degeneration. *Archives of Ophthalmology*, 103, 811-816.
- Swanson, W. H., & Wilson, H. R. (1985). Eccentricity dependence of contrast matching and oblique masking. *Vision Research*, 25, 1285-1295.
- Swanson, W. H., Wilson, H. R., & Giese, S. C. (1984). Contrast matching data predicted from contrast increment thresholds. *Vision Research*, 24, 63-75.

Switkes, E., Mayer, M. J., & Sloan, J. A. (1978). Spatial frequency analysis of the visual environment: Anisotropy and the carpentered environment hypothesis. *Vision Research*, 18, 1393-1399.

Tang, J., Kim, J., & Peli, E. (2004). Image enhancement in the JPEG domain for people with vision impairment. *IEEE Transactions on Bio-Medical Engineering*, 51, 2013-2023.

Tolhurst, D. J. (1975). Reaction times in the detection of gratings by human observers: A probabilistic mechanism. *Vision Research*, 15, 1143-1149.

Tolhurst, D. J., Tadmor, Y., & Chao, T. (1992). Amplitude spectra of natural images. *Ophthalmic & Physiological Optics*, 12, 229-232.

Torralba, A., & Oliva, A. (2003). Statistics of natural image categories. *Network: Computation in Neural Systems*, 14, 391- 412.

Truchard, A. M., Ohzawa, I., & Freeman, R. D. (2000). Contrast gain control in the visual cortex: Monocular versus binocular mechanisms. *The Journal of Neuroscience*, 20, 3017-3032.

Tulunay-Keesey, U., Ver Hoeve, J. N., & Terkla-McGrane, C. (1988). Threshold and supra-threshold spatiotemporal response throughout adulthood. *Journal of the Optical Society of America. A, Optics and Image Science*, 5, 2191-2200.

Tyler, C. W., & McBride, B. (1997). The Morphonome image psychophysics software and a calibrator for MacIntosh systems. *Spatial Vision*, 10, 479-484.

- van der Schaaf, A., & van Hateren, J. H. (1996). Modelling the power spectra of natural images: Statistics and information. *Vision Research*, 36, 2759-2770.
- van Hateren, J. H., & van der Schaaf, A. (1998). Independent component filters of natural images compared with simple cells in primary visual cortex. *Proceedings. Biological sciences*, 265, 359-366.
- Wang, G., Tanifuji, M., & Tanaka, K. (1998). Functional architecture in monkey inferotemporal cortex revealed by in vivo optical imaging. *Neuroscience Research*, 32, 33-46.
- Watson, A. B. (1987). Estimation of local spatial scale. *Journal of the Optical Society of America. A, Optics and Image Science*, 4, 1579-1582.
- Webb, B. S., Tinsley, C. J., Barraclough, N. E., Easton, A., Parker, A., & Derrington, A. M. (2002). Feedback from V1 and inhibition from beyond the classical receptive field modulates the responses of neurons in the primate lateral geniculate nucleus. *Visual Neuroscience*, 19, 583-592.
- Webb, B. S., Tinsley, C. J., Barraclough, N. E., Parker, A., & Derrington, A. M. (2003). Gain control from beyond the classical receptive field in primate primary visual cortex. *Visual Neuroscience*, 20, 221-230.
- West, S. K., Rubin, G. S., Broman, A. T., Munoz, B., Bandeen-Roche, K., & Turano, K. (2002). How does visual impairment affect performance on tasks of everyday life?

The SEE project. Salisbury Eye Evaluation. *Archives of Ophthalmology*, 120, 774-780.

Whittaker, S.G., Lovie-Kitchin, J.E. (1993). Visual requirements for reading. *Optometry and Vision Science*, 70, 54-65.

Winer B.J. (1962). Chapter 4: Single-factor experiments having repeated measurements on the same elements. *Statistical principles in experimental design*. McGraw-hill Book Company, Inc., 105-138.

Winer B.J. (1962). Chapter 7: Multifactor experiments having repeated measures on the same elements. *Statistical principles in experimental design*. McGraw-hill Book Company, Inc., 298-374.

Wolkstein, M., Atkin, A., & Bodis-Wollner, I. (1980). Contrast sensitivity in retinal disease. *Ophthalmology*, 87, 1140-1149.

World Health Organization (1980). *International Classification of Impairments, Disabilities and Handicaps: A Manual of Classification Relating to the Consequences of Disease*. Geneva: World Health Organization.

Zarbin, M. A. (1998). Age-related macular degeneration: Review of pathogenesis. *European Journal of Ophthalmology*, 8, 199-206.

Zhang, X., Hargitai, J., Tammur, J., Hutchinson, A., Allikmets, R., Chang, S., & Gouras, P. (2002). Macular pigment and visual acuity in stargardt macular dystrophy. *Graefe's Archive for Clinical and Experimental Ophthalmology = Albrecht Von Graefes Archiv Fur Klinische Und Experimentelle Ophthalmologie*, 240, 802-809.